



Overview of the Caucasian *Perla* Geoffroy, 1762 (Plecoptera: Perlidae) based on morphological and molecular data with description of two new species


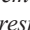
VALENTINA A. TESLENKO^{1*}, DMITRY M. PALATOV² & ALEXANDER A. SEMENCHENKO^{1,3}

¹Federal Scientific Center of the East Asia Terrestrial Biodiversity, Far Eastern Branch, Russian Academy of Sciences (FSC EATB FEB RAS), 690022, Vladivostok, Russia.

²Severtsov A.N. Institute of Ecology and Evolution of RAS, 33 Leninsky prospect, 119071 Moscow, Russia.

 triops@yandex.ru;  <https://orcid.org/0000-0002-8826-9316>

³ semenchenko_alexander@mail.ru;  <https://orcid.org/0000-0001-7207-9529>

*Corresponding author  teslenko@biosoil.ru;  <https://orcid.org/0000-0002-0649-8028>

Abstract

Six species of Caucasian *Perla* are reviewed, and diagnostic morphological characteristics of all stages of development (where possible) are described, supplemented, and illustrated in detail with comparative light microscope and scanning electron microscopy images. The DNA barcoding of five species is presented. Two new morphologically and genetically distinct species, *Perla schapsugica* **sp. nov.** and *Perla palatovi* **sp. nov.**, are described for both sexes and all life stages in the North Caucasus, Russia, Krasnodar Kray. Reinstatement of *Perla persica* Zwick, 1975, as a valid species distinct from *P. caucasica* Guérin-Méneville, 1843, is proposed. A new record of *P. persica* is reported for the Greater Caucasus, Russia, North-Ossetia-Alania for the first time. Morphologically, these two latter species can be separated in male adults by the shape of the hemitergal hook on terga X, an additional ventral brush on the penis of *P. caucasica*, wing length, and color.

Key words: *Perla*, morphology, redescription, DNA barcoding, new species, Caucasus

Introduction

The genus *Perla* Geoffroy, 1762 (Plecoptera: Perlidae) is known from the West Palaearctic and is considered an endemic genus for this region (Zwick 2004). The recent *sensu stricto* generic concept of *Perla* was introduced by Zwick (1977), who reinstated *Kamimuria* Klapálek, 1907a as a valid genus and subsequently it is treated as the Asian sister group of *Perla* in the East Palaearctic. The number of currently recognized species is very problematic, in spite of 47 valid *Perla* counted in the Neotropical, Nearctic, East and West Palaearctic (DeWalt *et al.* 2023). Among them, several Neotropical species are actually either members of other families or are considered nomen dubium and cannot even be assigned to a suborder (Murányi *et al.* 2016). On the other hand, three new species and the reinstated *Perla carlukiana* Klapálek, 1907b, recognized by Reding (2023) as a result of a revision of the West Palaearctic *Perla bipunctata* Pictet, 1833 complex, remain unaccounted for.

Four *Perla* species (*P. caucasica* Guérin-Méneville, 1843, *P. pallida* Guérin-Méneville, 1843, *P. kiritshenkoi* Zhiltzova, 1961, and *P. persica* Zwick, 1975) were originally described from the streams and rivers of the Caucasus Mountain system, including the Greater Caucasus, the Lesser Caucasus, and the neighboring Alborz Mountain range. *Perla abdominalis* Burmeister, 1839, and *P. marginata* Panzer, 1799 were also reported by Kasymov (1972) from the Caucasus, but their presence is considered improbable (Sivec & Stark 2002, Murányi *et al.* 2021). The taxonomy of *Perla* is unresolved and poses a major challenge. Diagnosis of *Perla* species relies on male penial setae patterns, details of the ovum chorion, and larval dorsal maculations. Several species are morphologically cryptic in one or more life stages. The most recent revision (Sivec & Stark 2002) showed convincingly that there seem to be many more species than presently recognized. To solve this problem, along with morphological characteristics, genomic data has begun to be used. DNA barcoding by means of the standardized 658-bp region of the mitochondrial cytochrome c oxidase subunit I (COI) has proved to be a great tool to assist stonefly identification, for associating

different life stages, and to identify cryptic species (Hebert *et al.* 2003a, 2003b; Morinière *et al.* 2017, Hlebec *et al.* 2022). COI sequences of *Perla* have been generated in complex faunal studies of Europe (Morinière *et al.* 2017; Ferreira *et al.* 2020; Hlebec *et al.* 2022), metabarcoding analyses using high-throughput sequencing (Corse *et al.* 2017), or the spatial distribution of stoneflies across river habitats (Gamboa *et al.* 2023). Each study contributed to the accumulation of *Perla* DNA barcodes. To date, more than 150 barcodes from 10 described and two undescribed *Perla* species (1/3 of known species) are available in the Barcode of Life Data System (BOLD; <http://www.boldsystems.org/>, accessed on January 2, 2024); some of them are probably misidentified. *Perla pallida*, *P. marginata* (Panzer, 1799), and *P. grandis* Rambur, 1842, exhibit deep intraspecific divergence that led their specimens to be assigned to two or more Barcode Index Numbers (BIN)s available in BOLD. Other species (for example, *P. carantana* Sivec & Graf, 2003, and *P. abdominalis*), on the contrary, have extremely low interspecific distances and belong to the same BIN.

The main aims of the present study were to provide an overview of Caucasian *Perla* species based on morphological and molecular data and discuss their inconsistencies. In order to better define the morphological concepts of Caucasian species, in particular, (a) to make available the DNA barcodes of already known *P. pallida*, *P. caucasica*, and *P. persica* and compare the obtained sequences of *P. pallida* with data from other European populations; (b) to make a morphological description with the DNA barcoding of new *P. palatovi* **sp. nov.** and *P. schapsugica* **sp. nov.**; (c) to reconstruct a phylogeny, quantify inter- and intraspecific genetic distances, and delimit species of all available DNA barcodes of *Perla* to disentangle the taxonomical issues.

Material and methods

Adults and larvae were collected by hand during daylight and nighttime hours and preserved in 96% ethanol for DNA analyses or 75% ethanol for morphological studies. The association of mature larvae with adults was established from pre-emergent male larvae collected together with adults, taking into account the results of DNA barcoding. Specimens were examined with the aid of a compound microscope in transmitted light. Illustrations were produced using digital cameras (Nikon Coolpix 995 and ToupView 3.7), stereo microscope Olympus SZX1 6, digital camera Olympus DP74, and stacked using Helicon Focus software. The final illustrations were postprocessed for contrast and brightness using Adobe® Photoshop® software. Eggs were investigated in the Center of Collective Use of FSC EATB FEB RAS using Zeiss EVO and Merlin scanning electron microscopes (SEM). Terminology follows Sivec *et al.* (1988), Sivec & Stark (2002), Stewart & Stark (2002), and Zwick (1975, 2004).

The holotypes and paratypes are deposited in the collection of the Federal Scientific Center of the East Asia Terrestrial Biodiversity Far Eastern Branch, Russian Academy of Sciences, Vladivostok, Russia.

Total genomic DNA was extracted using DNeasy Blood and Tissue Kit (Qiagen, Hilden, Germany) or ExtractDNA Blood & Cells (Evrogen, Moscow, Russia) following the manufacturer's instructions. We amplified mitochondrial protein coding gene cytochrome *c* oxidase I (COI) using the polymerase chain reaction (PCR). For primers, see Teslenko & Semchenko (2022) for reaction protocols, cycle programs used for amplification, purification of PCR products, and sequencing. The obtained sequences have been deposited in GenBank under accession numbers PP216454–PP216469 and PP236723–PP236724 (Table 1).

Evolutionary divergence was estimated using uncorrected pairwise genetic distances (p-distances) in MEGA7 (Kumar *et al.* 2016). A Bayesian Inference (BI) phylogenetic analysis was performed using MrBayes v.3.2.7 (Ronquist *et al.* 2012), which was preceded by the selection of the best-fit partitioning scheme and models separately for each codon position of COI using PartitionFinder 2.1.1 (Lanfear *et al.* 2012). The best models for the first, second, and third codon positions of COI were SYM+I (Zharkikh 1994), F81+I (Felsenstein 1981), and GTR+G (Tavaré 1986), respectively. For the BI, two separate runs with four Markov chain Monte Carlo (MCMC) simulations were performed for 10 million generations, sampling every 500 generations and discarding the first 25% of trees as burn-in. Trace files were visually inspected in Tracer v.1.7 (Rambaut *et al.* 2018). Phylogenetic trees were visualized using FigTree v.1.4.4. *Kamimuria coreana* Ra, Kim, Kang, & Ham, 1994 (BOLD process ID GBMNB60521-20) was selected as the outgroup species.

Molecular species delineation was achieved through two distance-based and two tree-based methods. Distance-based approaches used BINs (Ratnasingham & Hebert 2013) and Assemble Species by Automatic Partitioning (ASAP) (Puillandre *et al.* 2021, web site <https://bioinfo.mnhn.fr/abi/public/asap>) using simple p-distances as the

substitution model. The tree-based approaches Multi-rate Poisson tree processes (mPTP, Kapli *et al.* 2017) and general mixed Yule-coalescent (GMYC, Fujisawa & Barraclough 2013) were run on the web servers <https://mptp.h-its.org/> and <https://species.h-its.org/gmyc/>, respectively, using default parameters. An input ultrametric gene tree was constructed in BEAST v.1.10.4 (Suchard *et al.* 2018) with a strict clock, TN93 substitution model, Yule speciation model, and MCMC chain using 100 million generations. The results were summarized with the Tree Annotator in BEAST package.

Three different alignments were generated for analysis of DNA barcodes of *Perla*. The first dataset included sequences obtained in this study. In addition to our own data, a second alignment contained whole COI *Perla* sequences with BINs from BOLD systems (141 sequences, accessed January 26, 2024), which were used for inter- and intraspecific p-distances. Finally, the third dataset was used for phylogeny reconstruction and includes our sequences and three specimens (if available) from each BIN. If one BIN included several morphospecies, we used three specimens from each morphospecies. The highest priority was given to specimens with the imaginal development stage and the longest sequence length.

Results

Perla caucasica Guérin-Méneville, 1843

Figs. 1–23

Guérin-Méneville, 1843:394;
Pictet, 1841:206–207;
Klapálek, 1923: 49–50;
Zhiltzova, 1961:873 (distribution in the Caucasus);
Zhiltzova, 1964:43 (list of species);
Zwick, 1978:236 (synonymy proposed);
Sivec & Stark, 2002:13, figs. 22–24 (egg illustration, assignation to *P. caucasica* group, *Perla abbreviata* Klapálek, 1921 syn. nov., *Perla persica* Zwick, 1975 syn. nov.);
Zhiltzova & Cherchesova, 2003:321, figs. 1–2, 5–6 (nymph description and illustration);
Kazanci, 2008:43 (new records for Turkey);
Teslenko & Zhiltzova, 2009:126 (key with illustrations copied from Zhiltzova 1961);
Cherchesova & Zhiltzova, 2013:11, 42, 82, fig. 302 (key imago and larva, with larva illustrations copied from Zhiltzova & Cherchesova, 2003, phenology and distribution);
Darilmaz *et al.*, 2016:52 (distribution map in Turkey);
Murányi *et al.*, 2021:74 (new records for Azerbaijan);
Cherchesova *et al.*, 2023:85 (distribution in North Ossetia).

Diagnosis. The male is distinguished by a long mesal field on tergum 9 (Fig. 2). The field expands anteriorly, with lateral longitudinal serrated ridges that are longer than the central ridges of teeth and an anterior part and posterior margin of the mesal field devoid of serrated ridges (Figs. 2, 5). The hemitergal hook is triangular, without projections, narrowed towards the top, apex rounded (Figs. 2, 5–6). The sac of the penis bears a narrow apical brush, ending in triangles ventrally and dorsally (Figs. 9–10, C). Ventrally, on the sac, there is an additional barely noticeable ventral brush in the form of a short and narrow stripe, consisting of tiny spines (Figs. 10, D). The female is recognized by the distinctive subgenital plate, with a small rectangular projection with rounded corners posteriorly (Fig. 4). The egg is oval-elongated; collar short, with irregular ribs; rim apex smooth with very slight irregular incisions; chorion is rough with numerous funnel-shaped punctations throughout; micropylar orifices with thin raised rims set in pits (Figs. 11–15). The larva is distinguished by a wide, V-shaped pale spot on the head without serrations laterally, reaching the clypeus; by the narrow semi-oval pale bands on the pronotum; and by the pilosity of the cerci (Figs. 16–17, 21–23).

Complimentary description. The color pattern of the head, abdomen, legs, and wings generally corresponds to the original description of Guérin-Méneville (1843), supplemented by Pictet (1841) and Klapálek (1923).

Adult habitus. The general body color is brownish-yellow (Fig. 1). The M-line on the head is slightly darkened and clearly defined (Fig. 3). A pair of thin, longitudinal, narrow light spots parallel to the lateral clypeal edges reach the anterior edge of the clypeus; the clypeus has dark lateral margins. The anterior and lateral ocelli are outlined by a black band; lateral margins of the head darkened. The interocellar area is yellow-orange, extending to M-line

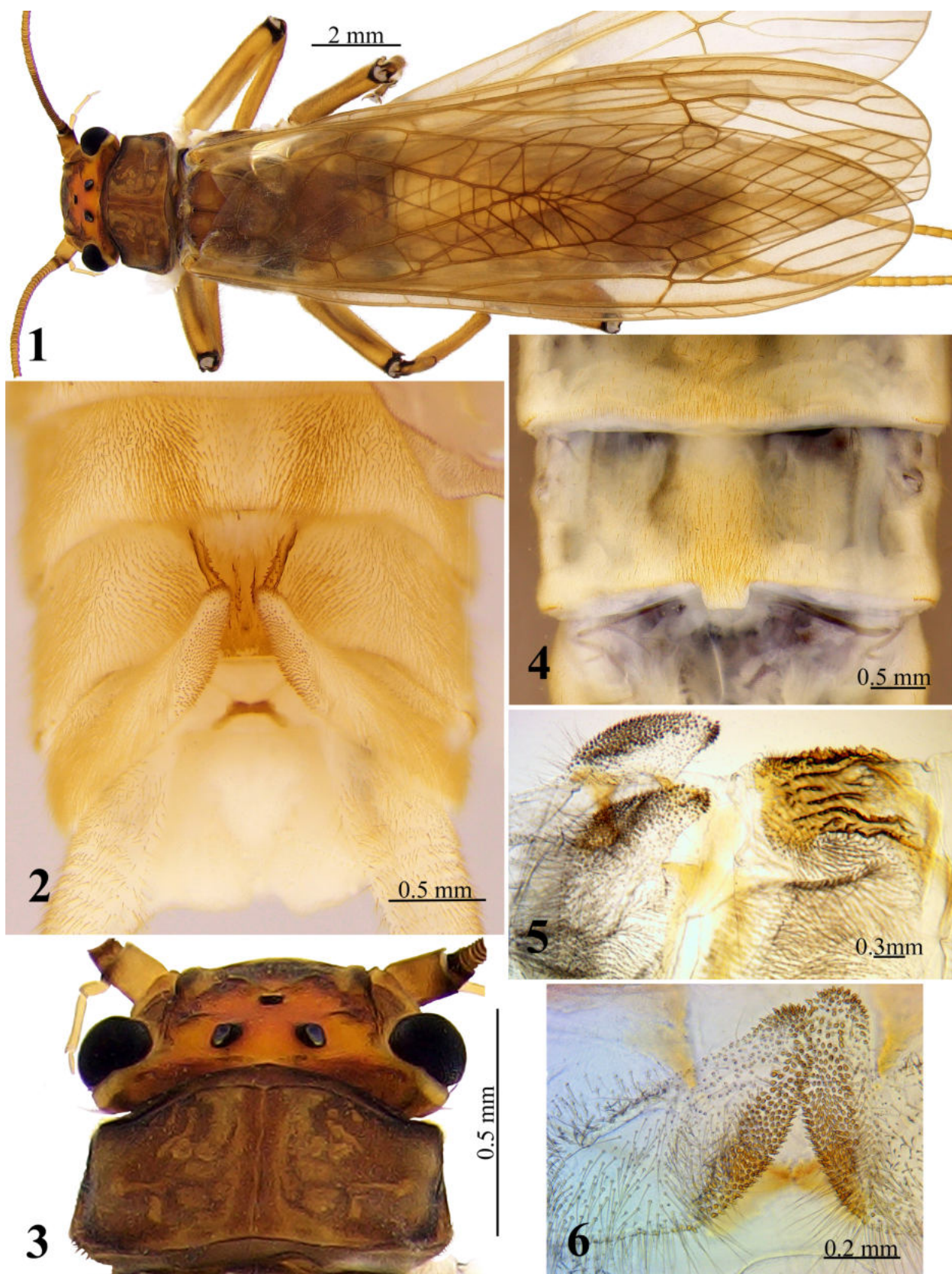
and compound eyes; the tentorial pits dorsal to the lateral ocelli are light brown; the occiput is darkened (Figs. 1, 3). Pronotum brown; rugosities are pale-grayish, forming an X-shaped pattern (Figs. 1, 3); anterolateral and posterolateral margins darkened; medial stripe brownish, widened to anterior and posterior margins; lateral margins of pronotum bordered by brown stripe, widening posterolaterally; sometimes the lateral edges are bent down and not visible dorsally. The legs and cerci are yellow-brown (Fig. 1). The femur bears a narrow, darkish band close to the outer edge and a black band distally. Tibia darkened basally with an additional narrow brownish band at the base (Fig. 1); tarsi also darkened. Anal gills small and visible only in newly molted females. Each cercal segment slightly darkened distally (Fig. 1).

Male. Tergum 8 medially has a membranous furrow and posterolateral humps covered with dense and thick setae (Fig. 2). Tergum 9 with a depressed sclerotized mesal field reaching the end of the posterior margin; the length of the field exceeds its width, expanded anteriorly, covered with longitudinal ridges (10–11) of sclerotized pointed teeth; lateral longitudinal serrated ridges longer than central rows of teeth; devoid of serrated ridges in the anterior part and posterior margin (Figs. 2, 5). Tergum 10 bears hemitergites; the paired triangular hooks narrowed towards the tip, apices rounded, the base of the hook distended, and covered with long setae (Figs. 2, 5–6). Hemitergites without projections, with an inner edge covered with sensilla basiconica, which is extended at the tip to the front and outer edges (Figs. 2, 5–6). The artificially everted penis has a tube that is 1.8 times the length of the sac (Fig. 7); the base of the tube is membranous with patches of rounded spine bases laterally; the dorsal tube is covered with densely arranged longitudinal rows of heavy sclerotized serrate sclerites, sometimes changed into scales with small spines (Figs. 7, 9, A–B); ventrally, the tube at the basal half is weakly sclerotized; in the distal 1/3 there are longitudinal rows of leaf-shaped scales with small spines (Figs. 8, 10). The sac is bulbous, membranous, at the base with lobes (Figs. 7–8); thin pointed brown spines, forming a relatively narrow apical brush, noticeable in the form of a triangle ventrally and dorsally (Figs. 9–10, D). Ventrally between membranous lobes, closer to the sac base, there is also a barely noticeable ventral brush in the form of a short and narrow stripe consisting of tiny spines; the spine size in the ventral brush is half the size of the apical brush spines (Figs. 10, C).

Female. Color and pigmentation are similar for males. The lateral margins of the subgenital plate are weakly pronounced. The subgenital plate has medially a small rectangular projection with rounded corners (Fig. 4).

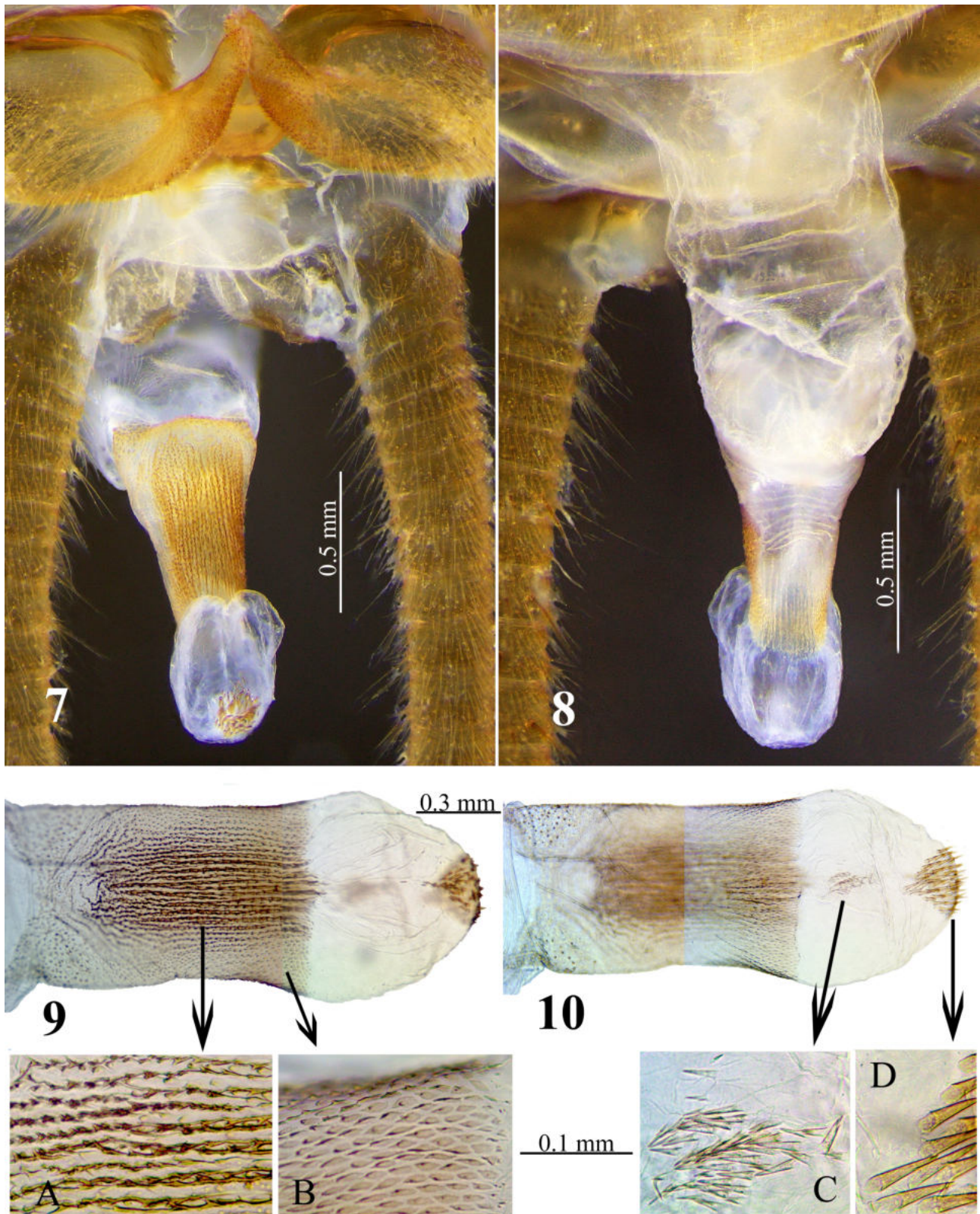
Egg. Oval-elongate, with mean dimensions of 509 x 270 μm ($n = 3$), and a mushroom-shaped anchor (Fig. 11). Collar short, with irregular ribs extending from rim to shoulders; rim apex smooth with very slight irregular incisions (Figs. 12–13). The chorion is pitted, with numerous funnel-shaped punctations throughout (Fig. 14). Micropylar row is approximately 1/3 length from the anterior pole; orifices with thin raised rims are set in pits (Figs. 12, 15). The shape and the chorion structure agree well with the original description (Sivec & Stark 2002).

Larva. Mature larvae were associated with adults and corroborated the results of DNA barcoding. GenBank accession numbers are PP216466 and PP216467 (Table 1). In appearance and color, our specimens generally correspond to the original description of the *P. caucasica* larva by Zhiltzova & Cherchesova (2003), except for the predominance of brown color and the pattern of the abdomen. Color yellow-brown (Figs. 16–17) with a distinct dark pattern on the head, pronotum, mesonotum, metanotum, and abdomen. Body covered with numerous short dark clothing hairs; bands of erect silky white hairs upward of the epicranial suture on the head and along the median body line, sometimes well pronounced (Fig. 16). Antennae and cerci are yellow-brown. M-line is pale, a wide V-shaped spot expanding to the clypeus is also pale, and the lateral clypeal margins are brown (Figs. 16–17). Head with a large transverse brown band, bounded above by the M-line and below by pale posterior tentorial pits and branches of the epicranial suture; a small triangular spot between the ocelli is pale; epicranial stem and base of the occiput brownish (Figs. 16–17). The transverse occipital fold and the fold running around the eye merge in a regularly curved line. Setation along the occipital fold extends only to behind the eye but not forward along the edge of the flat, expanded side of the head. Mesothoracic supracoxal gills with double trunks. Mandibles (Fig. 18) are heavily sclerotized along a rounded outer margin. The number of teeth and the form of the molar region are asymmetrical between the right and left mandibles. Left mandible ventrally with five pointed heavy sclerotized teeth; bearing three rows of setae; the marginal brush extends from the base of the 4th tooth to the basal third of the mandible; the submarginal setal row stretches from the base of the 3rd tooth to the mandible basal third; the last submarginal setal row prolongs from the base of the first tooth to the mandible base (Fig. 18). Right mandible ventrally with six teeth, the last tooth being small, obtuse-angled, sometimes not developed or poorly visible; marginal brush extending from the base of the 4th tooth to the basal 1/3 of the mandible; the submarginal setal row prolongs from the base of the first tooth to the mandible base (Fig. 18). Lacinia bidentate (Fig. 19) has a large, curved, and strongly sclerotized apical tooth;

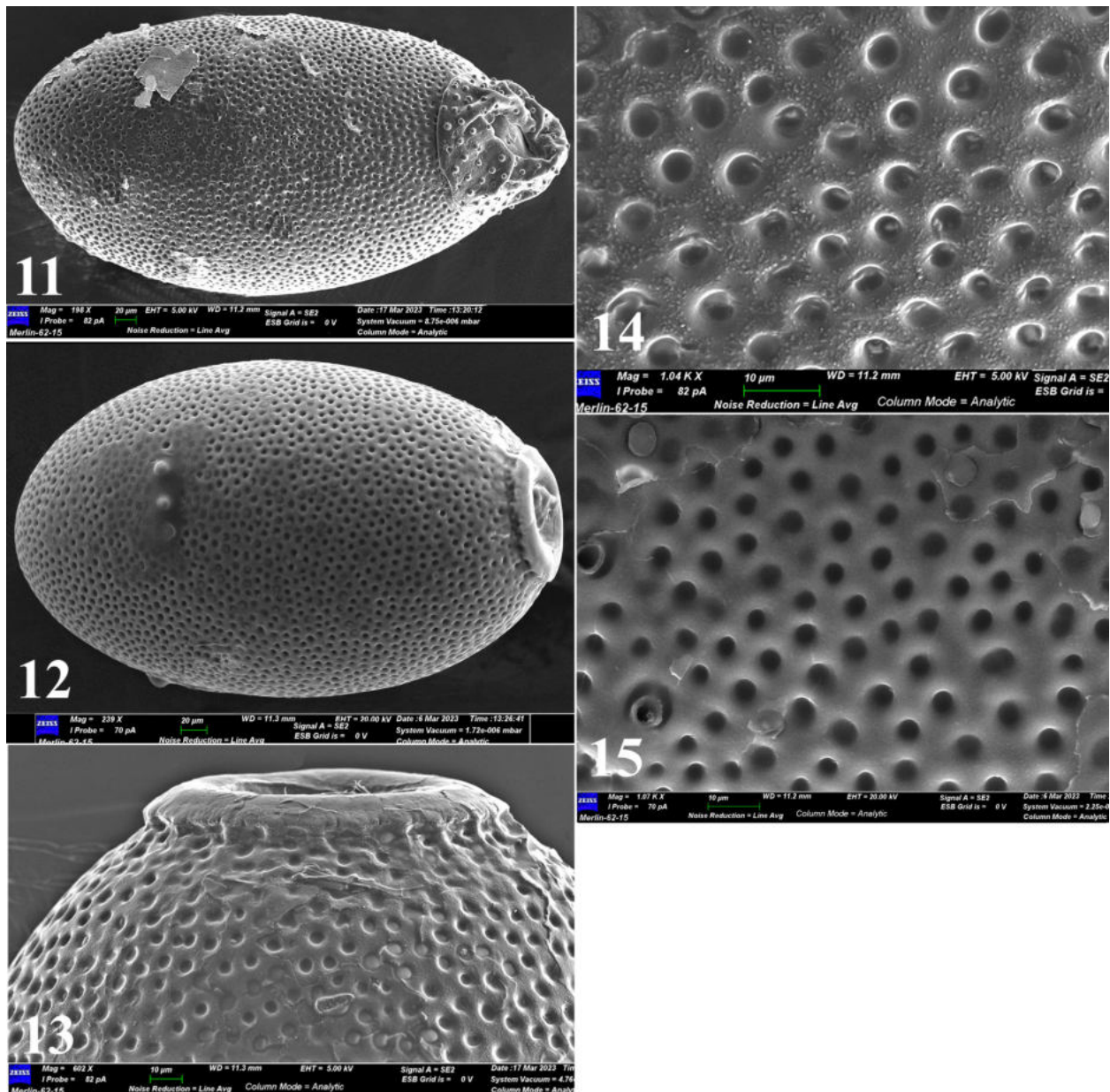


FIGURES 1–6. *Perla caucasica* Guérin-Ménéville, 1843. Caucasus: Russia, Adygea, Belaya River; Republic of North Ossetia-Alania, Mairamadag River. Georgia, Sukhum District, Kelasuri River. 1. Habitus, male, dorsal. 2. Male abdominal tip, dorsal. 3. Head and pronotum, male, dorsal. 4. Female subgenital plate, ventral. 5. Mesal field with longitudinal serrated ridges, dorsolateral, and hemitergal hooks covered with sensilla basiconica, lateral, cleared. 6. Hemitergal hooks covered with sensilla basiconica, caudal, cleared.

the subapical tooth is shorter, extending 2/3 of the apical tooth length. The marginal fringe of setae along the inner margin is complete; short median setae are present in a sparse patch; basal setae are sporadic. Galea length reaches half of apical tooth length (Fig. 19).



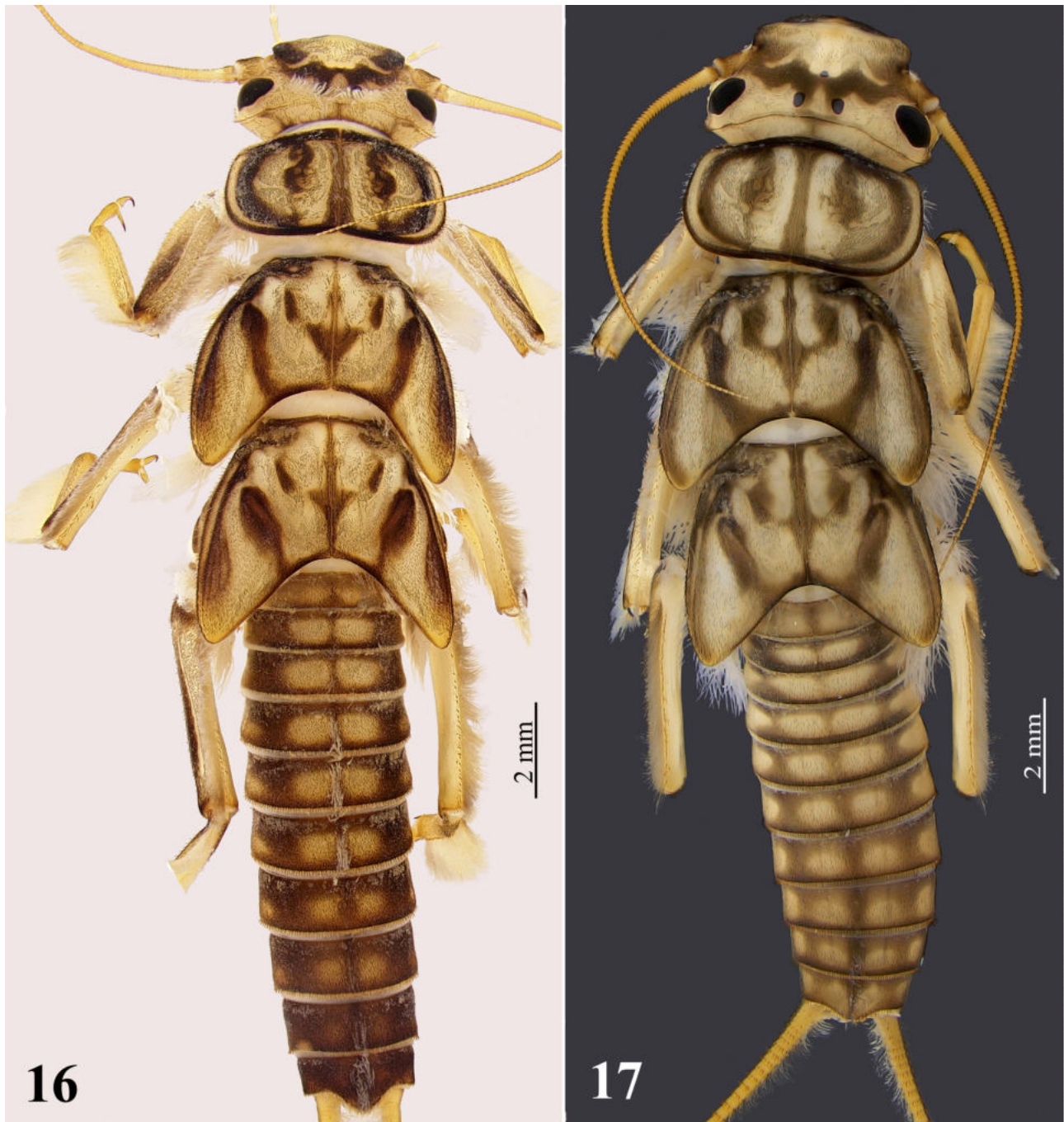
FIGURES 7–10. *Perla caucasica* Guérin-Ménéville, 1843. Caucasus, Russia, Adygea, Belaya River. 7. Hemitergal hooks and artificially everted penis, dorsal. 8. Penis, ventral. 9. Chaetotaxy of artificially everted penis, dorsal. A. Densely arranged longitudinal rows of heavy sclerotized serrate sclerites on the tube of the penis. B. Scales with small spines. 10. Same, ventral. C. Tiny spines in the ventral brush. D. Pointed brown spines in the apical brush.



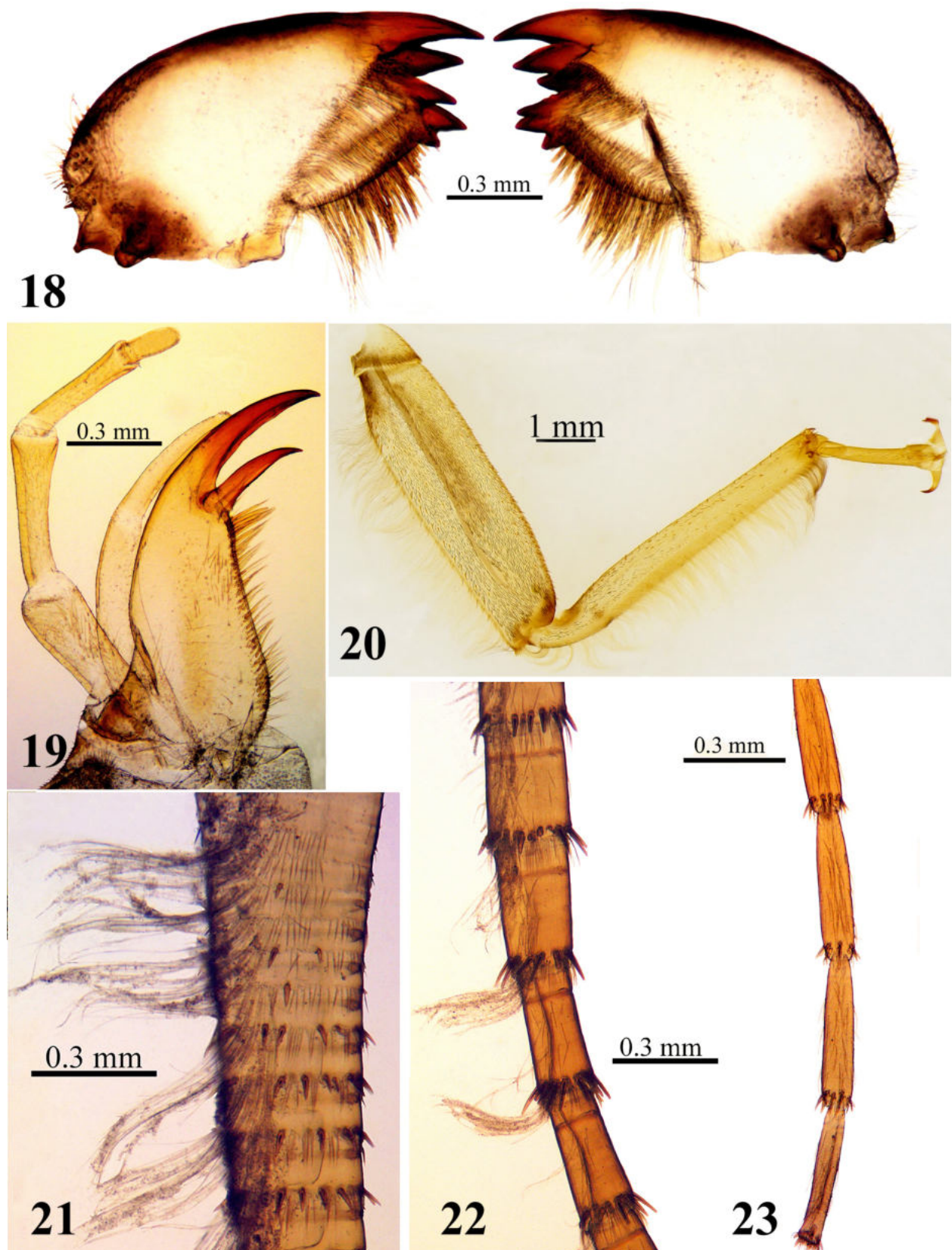
FIGURES 11–15. *Perla caucasica* Guérin-Ménéville, 1843. Caucasus, Georgia, Sukhum District, Kelasuri River. Egg. 11. Appearance with a mushroom-shaped anchor plate, lateral. 12. Same, without the anchor plate. 13. Collar, lateral. 14. Chorion structure with funnel-shaped punctations. 15. Micropyles, orifices with thin raised rims.

Pronotum transverse, approximately the same width as the head, with obtusely rounded anterior corners; lateral margins and posterior angles are evenly rounded (Figs. 16–17). The pronotal fringe is complete with mixed short and relatively long setae. Pronotum with a thin brown stripe along the edges; paired narrow semi-oval pale bands from the anterior corners to the middle of the posterior margin outline an oval brown band; lateral pronotal fields pale (Figs. 16–17). Medial pronotal band brown, widening anteriorly and posteriorly; band surrounded by pale rugosities of an X-shaped pattern; a paired vague S-shaped dark spot extends from the anterior margin to the middle of the pronotum (Figs. 16–17). Mesonotum and metanotum with identical Ψ-shaped brown pattern medially; posteriorly darkly margined; two wide brown bands limiting the wing pad bases; a brown stripe runs along the lateral edge of the wing pads (Figs. 16–17). Legs are yellow; the femur and tibia bear stout, short, acute bristles along the inner and outer edges, and a very dense fringe of long, silky hairs along the outer margins. Hind femur ca. 3.5–3.9 times as long as wide. The femur surface is covered with sparse, short, and irregular red bristles; there is a diffuse brownish spot in the distal half closer to the outer edge, and the distal edge of the femur is also darkened (Figs. 16–17, 20).

Tibia with a diffuse, narrow brownish band basally (Figs. 20). Abdomen brown, each tergum with two median and two lateral oval pale spots forming longitudinal rows (Figs. 16–17). The two last terga of the female larvae are somewhat darker than the previous ones (Fig. 16), the posterior margin of sternum 7 is incomplete for female larvae. Anal gills are small. Cerci brown; each cercal cirlet with rings of stout brown spines and fine pilosity between spines, tightly pressed to the segment surface (Figs. 21–23); short fine hairs are the same length as the basal cercal segment length (Fig. 21); towards the middle of the cerci, fine pilosity length decreases (Fig. 22), and on the apical cercal segments, the length of the fine pilosity is about a quarter of the apical segment length (Fig. 23). Long silky colorless hairs are included in the cirlet in tufts and form a dorsal longitudinal swimming fringe, well visible especially on the basal cercal segments (Fig. 21); the length and density of long silky hairs also decrease towards the apex (Fig. 21–23). Additionally, a few fine intercalary setae are present on each cercal segment, and their density and length increase from the basal to apical cercal segments (Figs. 21–23).



FIGURES 16–17. *Perla caucasica* Guérin-Ménéville, 1843. Caucasus, Georgia, Sukhum District, Kelasuri River; Russia, Adygea, Belaya River. Larvae, habitus, dorsal. 16. Female larva. 17. Male larva.



FIGURES 18–23. *Perla caucasica* Guérin-Méneville, 1843. Caucasus, Georgia, Sukhum District, Kelasuri River; Russia, Adygea, Belaya River. 18. Left and right mandibles, ventral. 19. Left lacinia, galea, maxillary palpus, ventral. 20. Right middle leg, dorsal. 21–23. Chaetotaxy of the right cercus, lateral. 21. Basal cercal segments. 22. Middle cercal segments. 23. Apical cercal segments.

Material examined. Caucasus. Russia: Republic North Ossetia-Alania: 1♂, 3♀, 1 larva, Prigorodny District, Mairamadag River, Terek R. Basin, altitude 703 m above sea level, 42.993308 N, 44.498150 E, 17.VII.2021, coll. D. Palatov; Krasnodar Krai, 1 larva, District of the City of Sochi, Estosadok, Mzymta River, altitude 622 m above sea level, 43.670007 N, 40.319902 E, 22.VIII.2020, coll. A. Semenchenko; 11♂, 2 larvae, Republic Adygea, Maikop District, Belaya River, vicinities of Guzeripl village, altitude 677 m above sea level, 43.995139 N, 40.135472 E, 7.VII.2023, coll. D. Palatov. Georgia: 3♂, 2♀, 7 larvae, Sukhum District, Kelasuri River, altitude 10 m above sea level, 42.972042 N, 41.067392 E, coll. D. Palatov.

DNA barcoding. GenBank accession numbers are PP216462, PP216465–PP216467, and PP504704.

Distribution. Northern slopes of the Greater Caucasus: Adygea, Caucasus Nature Reserve, Karachay-Cherkessia (Teberda River), North Ossetia-Alania (Terek River Basin); the Black Sea coast and the southern slopes of the Greater Caucasus (the Shakhe, Sochi, Mzymta, Bzyb, Avadhara, and Rioni Rivers); Georgia, Lagodekhi River (Zhiltzova 1964) (Fig. 159). Abkhazia, Kalasuri River. The question of whether *P. caucasica* is distributed in Turkey, Iran, and Cyprus or whether its range is limited to the watercourses of the Caucasus remains open.

Comments. *Perla caucasica* was originally described by Guérin-Méneville (1843) from the Caucasus without indicating the type locality, data, or sex. The original description was soon supplemented by Pictet (1841). Later, the species was redescribed by Klapálek (1923) from Krasnaya Polyana on the Caucasus, collected in July, which belonged to the German Entomological Museum. The holotype of *P. caucasica* is lost (Sivec & Stark 2002), but the concept of the species was corrected by Zhiltzova (1964). This species is thought to be widely distributed throughout the Caucasian region, the whole of Anatolia, Cyprus, and the Alborz of Iran (Sivec & Stark 2002; Darilmaz *et al.* 2016). This is contrary to Teslenko & Zhiltzova (2009) and Cherkhova & Zhiltzova (2013), who considered it an endemic of the Greater Caucasus. This disagreement stems from the contentious synonymy of *P. persica* and *Perla abbreviata*. Because of their similar eggs, these species were synonymized under *P. caucasica* (Sivec & Stark 2002). However, the external and internal male genitalia of *P. caucasica* and *P. persica* are distinct (see below).

Perla persica Zwick, 1975

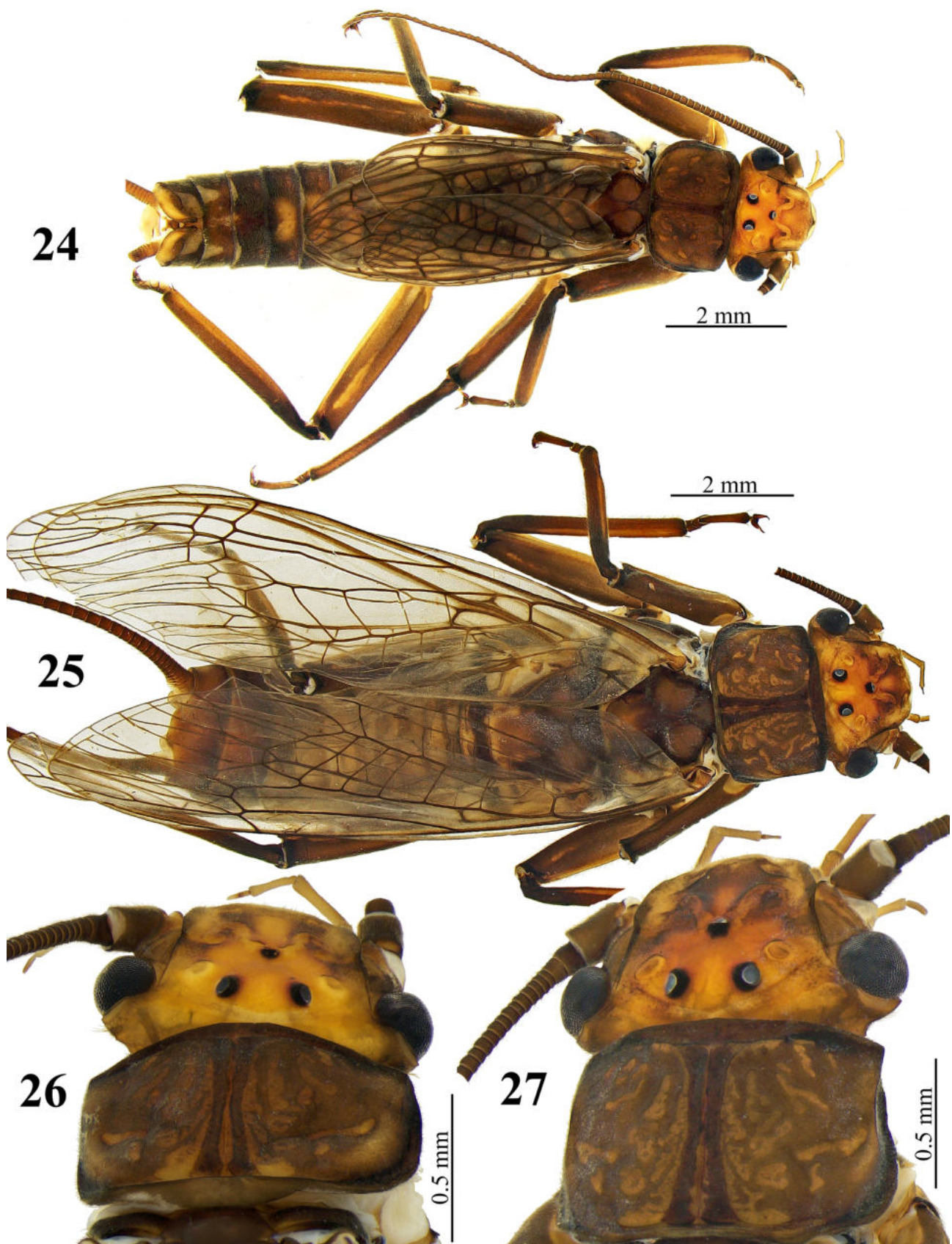
Figs. 24–49

Zwick, 1975: 392–394, figs. 19–23 (original description);

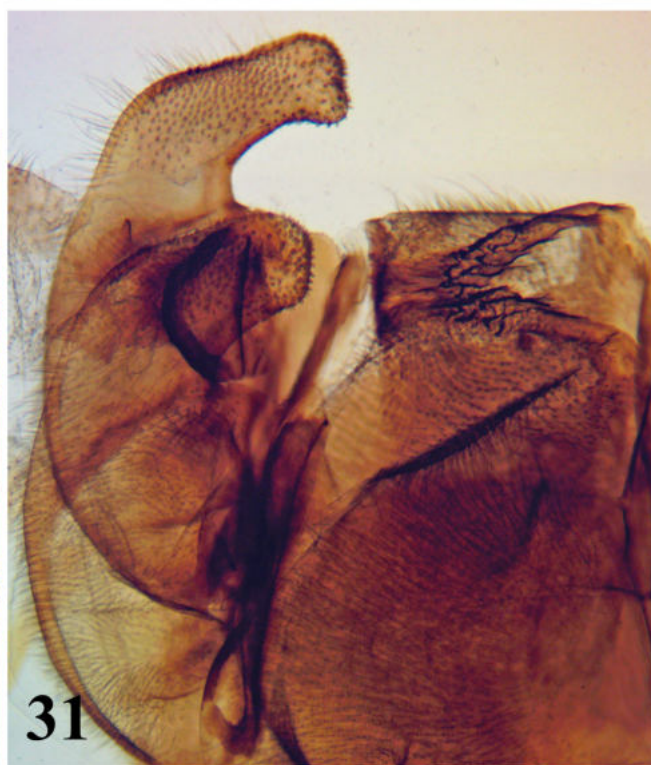
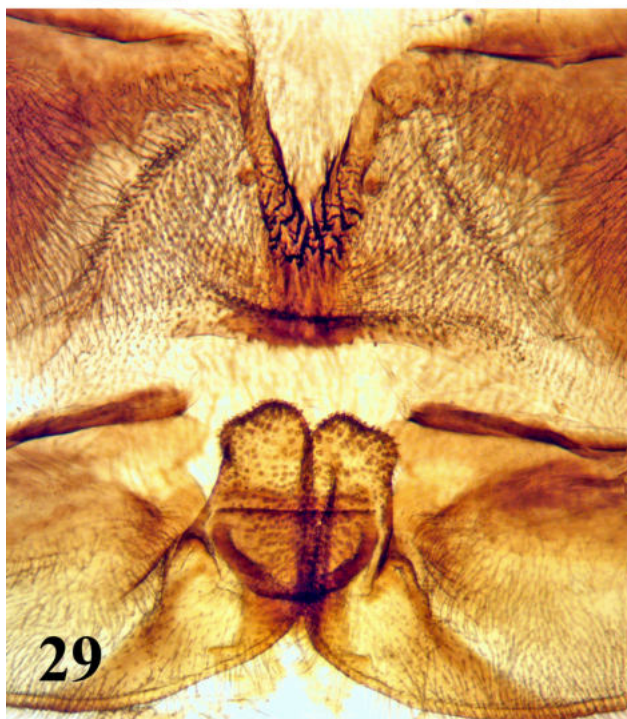
Zwick, 1978: 236 (synonymy proposed);

Sivec & Stark, 2002: 13 (as *Perla caucasica*).

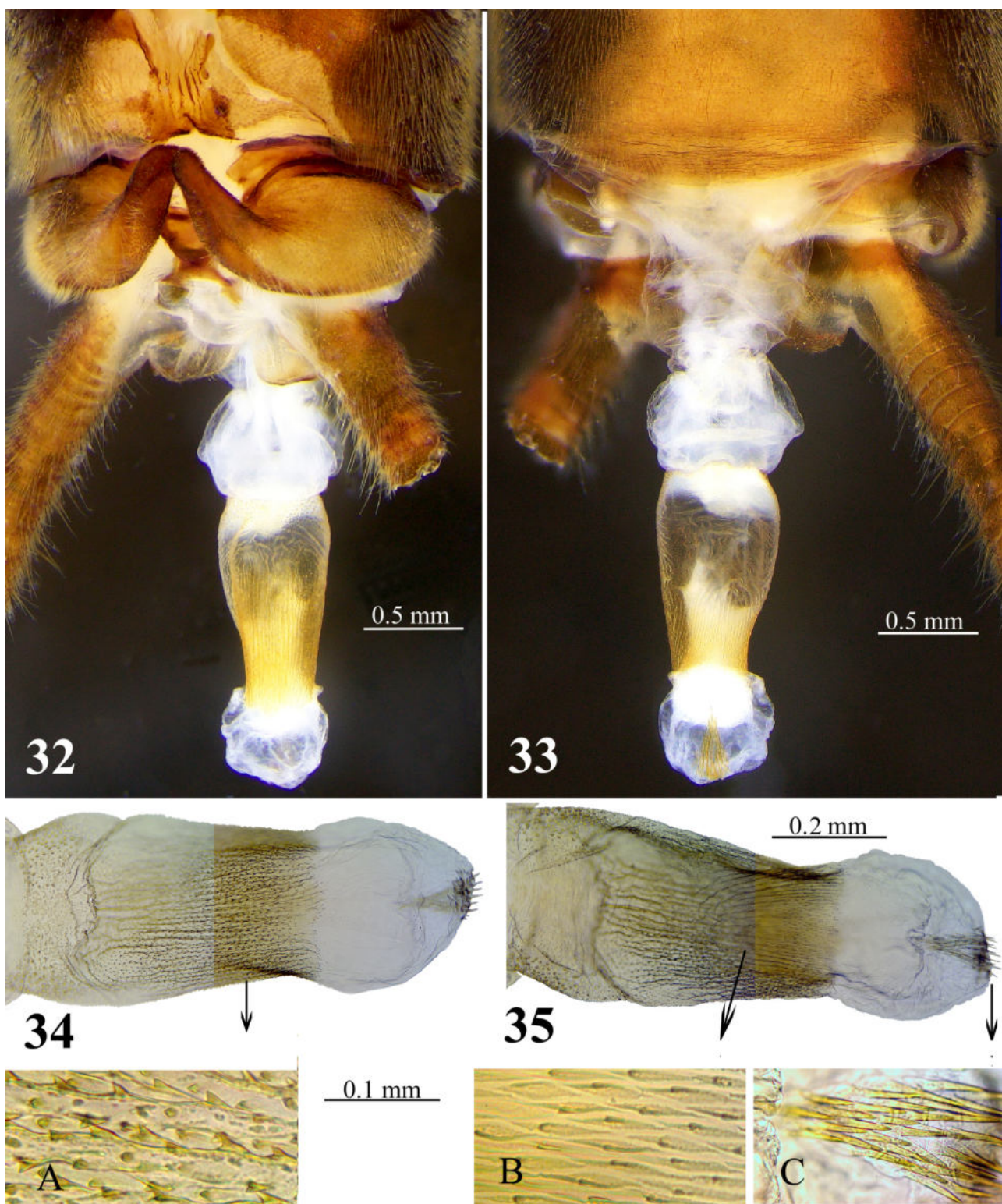
Remarks. In our collections, a few specimens from Iran and North Ossetia-Alania correspond to the original description of *P. persica* in Zwick (1975). Zwick (1978) considered the possibility of a synonymy between *P. persica* and *P. abbreviata*, but without studying the holotype of *P. abbreviata*, this question remained unresolved. Nevertheless, both species were proposed to be considered synonyms of *P. caucasica* based on a comparison of the eggs of topotype specimens from Alborz with the eggs of *P. caucasica* from the Caucasus (Sivec & Stark 2002). Notably, the female subgenital plate of the *P. persica* (Fig. 30) and *P. caucasica* specimens, as well as the chorion structures (Figs. 36–41) and larvae appearance (Figs. 42–49), are very similar, except for the body color of *P. persica* adults, which is much darker and more contrasting (Figs. 24–27) than that of *P. caucasica*. Additionally, males of *P. persica* are brachypterous (Fig. 24), whereas the wing length of *P. caucasica* males is usual. Upon closer examination of the male genitalia of *P. persica*, several morphological differences were discovered that are important and diagnostic. *Perla persica* and *P. caucasica* can be clearly distinguished by the male hemitergal structure and chaetotaxy of the penis. The shape of the hemitergal hook of *P. caucasica* is tapered towards its rounded apex (Figs. 2, 5, 7). The hemitergal hook of *P. persica* is distinguished by a plump, rounded rectangular tip in profile and, at the same time, an almost spatula-like flat shape in dorsal view (Figs. 28–29, 31–32). The penis of *P. caucasica* is armed with two brushes of setae: a typical apical brush and an additional small ventral brush of tiny setae (Figs. 10, C–D). In contrast, the penis of *P. persica* bears a single apical brush of setae at the apex (Figs. 32–35). In our opinion, these significant morphological differences indicate that *P. persica* should be considered a valid species rather than a synonym of *P. caucasica*. Reinstating the original name of *Perla persica* from synonymy on external and internal morphological features of males is proposed.



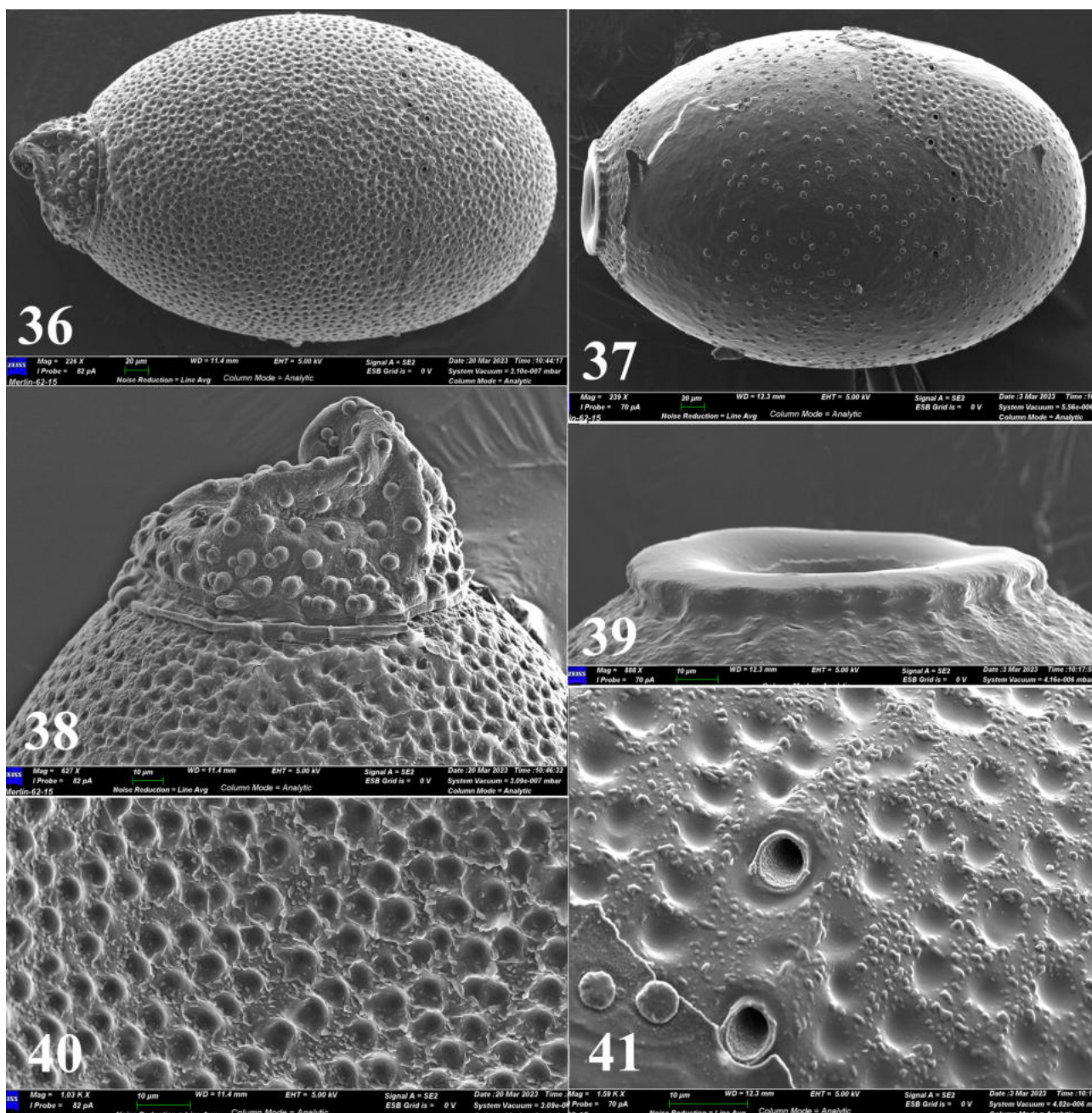
FIGURES 24–27. *Perla persica* Zwick, 1975. Central Alborz, Iran, Mazandaran province, Zarrin Kamar village, Nurrud (Noor?) River, Haraz River Basin. 24. Habitus, male, dorsal. 25. Habitus, female, dorsal. 26. Head and pronotum, male, dorsal. 27. Head and pronotum, female, dorsal.



FIGURES 28–31. *Perla persica* Zwick, 1975. Central Alborz, Iran, Mazandaran province, Zarrin Kamar village, Nurrud (Noor?) River, Haraz River Basin. 28. Male abdominal tip, dorsal. 29. Mesal field with longitudinal serrated ridges and hemitergal hooks covered with sensilla basiconica, dorsal, cleared. 30. Female abdominal tip, dorsal. 31. Mesal field with longitudinal serrated ridges and hemitergal hooks covered with sensilla basiconica, lateral, cleared.



FIGURES 32–35. *Perla persica* Zwick, 1975. Central Alborz, Iran, Mazandaran province, Zarrin Kamar village, Nurrud (Noor?) River, Haraz River Basin. 32. Mesal plate, hemitergal hooks, and artificially everted penis, cleared, dorsal. 33. Penis, ventral. 34. Chaetotaxy of the penis, dorsal. 35. Chaetotaxy of the penis, ventral. A. Densely arranged longitudinal rows of heavy sclerotized serrate sclerites. B. The longitudinal rows of leaf-shaped scales with small spines. C. Pointed brown spines in the apical brush.



FIGURES 36–41. *Perla persica* Zwick, 1975. Central Alborz, Iran, Mazandaran province, Zarrin Kamar village, Nurrud (Noor?) River, Haraz River Basin. Egg. 36. Appearance with mushroom-shaped anchor plate and micropylar row, lateral. 37. Appearance without anchor, with micropylar row, lateral. 38. Mushroom-shaped anchor plate covered with globular bodies, lateral. 39. Collar, lateral. 40. Chorion structure. 41. Micropyles, orifices with thin raised rims.

DNA barcoding. GenBank accession numbers are PP216463–PP216464 and PP216468–PP216469. According to phylogenetic relationships, *P. persica* and *P. caucasica* would be monophyletic if not for the specimen *P. caucasica* TVA364 from Adygea, which fell into the clade of *P. persica*. The DNA barcode of this specimen was identical to *P. persica* TVA199 therefore the minimum interspecies distances were zero (Table 2). Four methods of species delimitation united both species into a single mOTU (Fig. 160). This indicates that *P. persica* and *P. caucasica* are closely related species and have a recent common ancestor. Further molecular study with nuclear markers is needed to resolve the discrepancy between morphological and molecular characters.

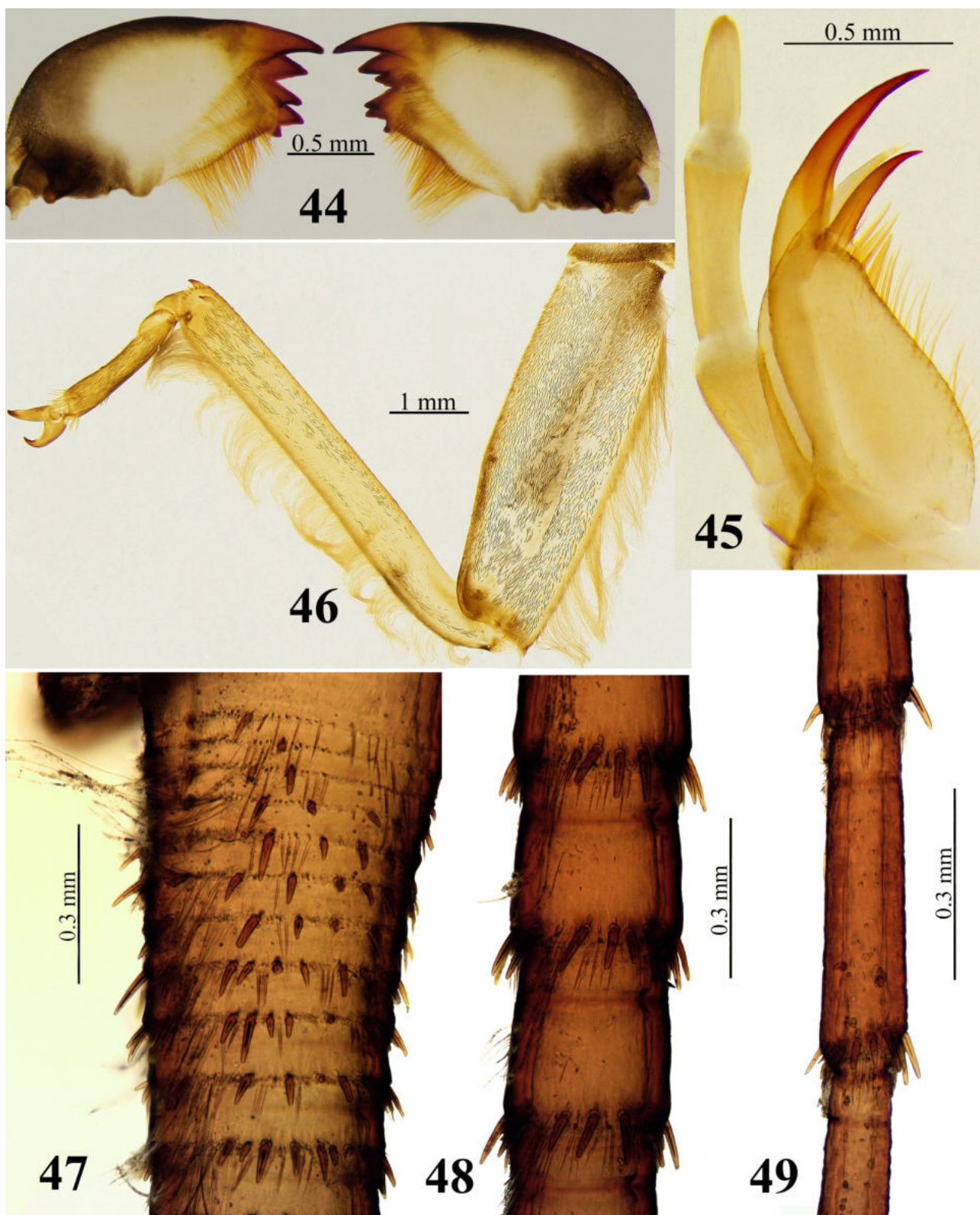
Material examined. Iran: 3♂, 4♀, 5 larval ♂, 2 larval ♀, 2 exuvia, Central Alborz, Mazandaran province, Zarrin Kamar village, Nurrud River, Haraz River Basin, altitude 1900 m above sea level, 36.205033 N, 51.82055

E, 25.VI. 2019, coll. D. Palatov. Russia, Republic of North Ossetia-Alania: 2♂, 2♀, 3 exuvia, Alagirsky District, Komdon River, in the area of the Tsey Gorge, Tseydon River Basin, Terek River Basin, altitude 1832 M above sea level, 42.803514 N, 43.933395 E; 25.07.2021, coll. D. Palatov; 1 larva, Prigorodny District, Mairamadag River, Terek River Basin, altitude 690 m above sea level, 42.993308 N, 44.49815 E, coll. D. Palatov.



FIGURES 42–43. *Perla persica* Zwick, 1975. Central Alborz, Iran, Mazandaran province, Zarrin Kamar village, Nurrud (Noor?) River, Haraz River Basin. Larvae, males, habitus, dorsal. Variation of the pattern.

Distribution. Iran: Alborz Mountains, Fars, Teheran, and Mazandaran Provinces. *Perla persica* was found in the streams and rivers of the northern slopes of the Greater Caucasus, Russia, and North-Ossetia-Alania for the first time (Fig. 159). The species was found in the Komdon River, which flowed down steeply by waterfalls on the dry slope of the Tsey Gorge in a narrow bushy ravine. The river has a width of 3–4 m, a bottom with pebbles and stones without fouling, water current of 0.3–0.7 m/s, and an altitude of 1700–1900 m above sea level.



FIGURES 44–49. *Perla persica* Zwick, 1975. Central Alborz, Iran, Mazandaran province, Zarrin Kamar village, Nurrud (Noor?) River, Haraz River Basin. Larva. 44. Left and right mandibles, ventral. 45. Left lacinia, galea, maxillary palpus, ventral. 46. Left hind leg, dorsal. 47–49. Chaetotaxy of the left cercus, lateral. 47. Basal cercal segments. 48. Middle cercal segments. 49. Apical cercal segments.

The ecological differences between *P. persica* and *P. caucasica* are currently difficult to assess due to the scarcity of information about their environments. In our collections, both species were found together in the Mairamadag River (Table 1). However, according to our collections and the original description (Zwick 1975), *P. persica* inhabits mainly an altitude of 1770–1900 m above sea level. *Perla caucasica*, as we assume, is a relatively low-mountain and warm-water species and has been recorded at altitudes of up to 700 m.

Perla kiritshenkoi Zhiltzova, 1961

Figs. 50–68

Zhiltzova, 1961: 874–876, figs. 1–5 (originally description);

Zwick, 1975: 392 (first record for Iran);

Kazanci, 1983: 90 (first record for Turkey);

Sivec & Stark, 2002: 16, figs. 28–30 (egg illustration);

Teslenko & Zhiltzova, 2009: 56, figs. 306–310 (key with illustrations copied from Zhiltzova 1961);

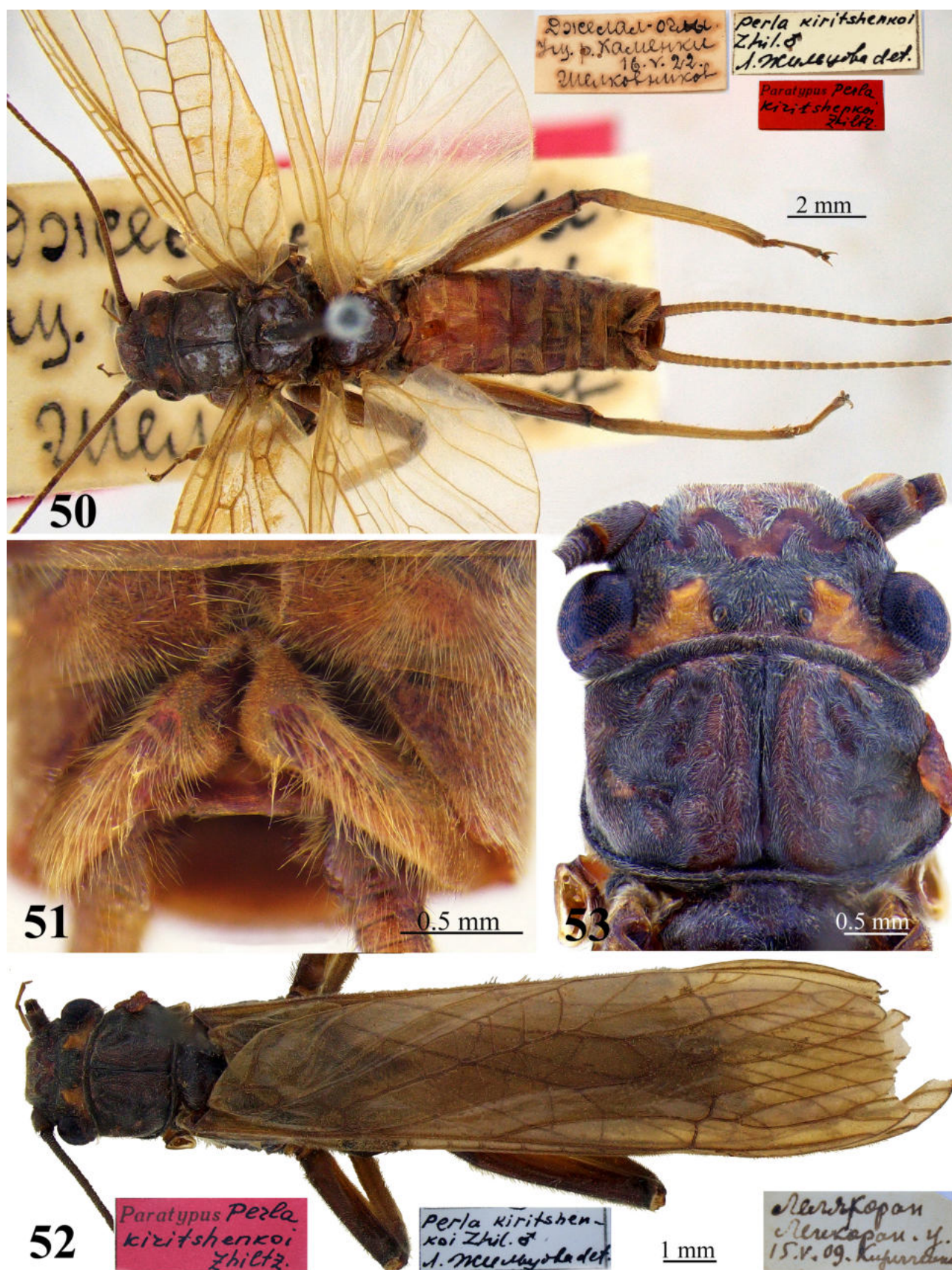
Darilmaz *et al.*, 2016: 52 (distribution, Turkey, map);

Murányi *et al.*, 2021: 74 (distribution, Azerbaijan).

Diagnosis. *Perla kiritshenkoi* is one of the darkest-colored species of Caucasian *Perla*. The male is distinguished by the long mesal field, which is widened and rounded posteriorly; the length does not exceed its width; and the longitudinal serrated ridges (7–8) are concentrated in the middle (Figs. 55, 57). The hemitergal hooks are strongly swollen in the place of the bend, forming a noticeable rounded protrusion, and the apexes are bluntly rounded (Figs. 54–57). An artificially everted penis bears the bulbous, membranous sac with a narrow apical brush ending in triangles of spines ventrally and dorsally; the membranous sac is rough, covered with dense tiny setae, clearly visible near the folds of the lobes (Figs. 58, D). The egg is spindle-shaped, tapering evenly to each pole (Fig. 62). The collar is short, but the rim is thick and rough (Fig. 64). The chorion is rough and punctate throughout; punctations are mostly uniform, but small punctations are also present near the micropylar row located near the equator; micropylar orifices with a raised thin edge are placed laterally on the pit wall; inside the pit there may be additional 1–2 small orifices (Figs. 62, 65–68).

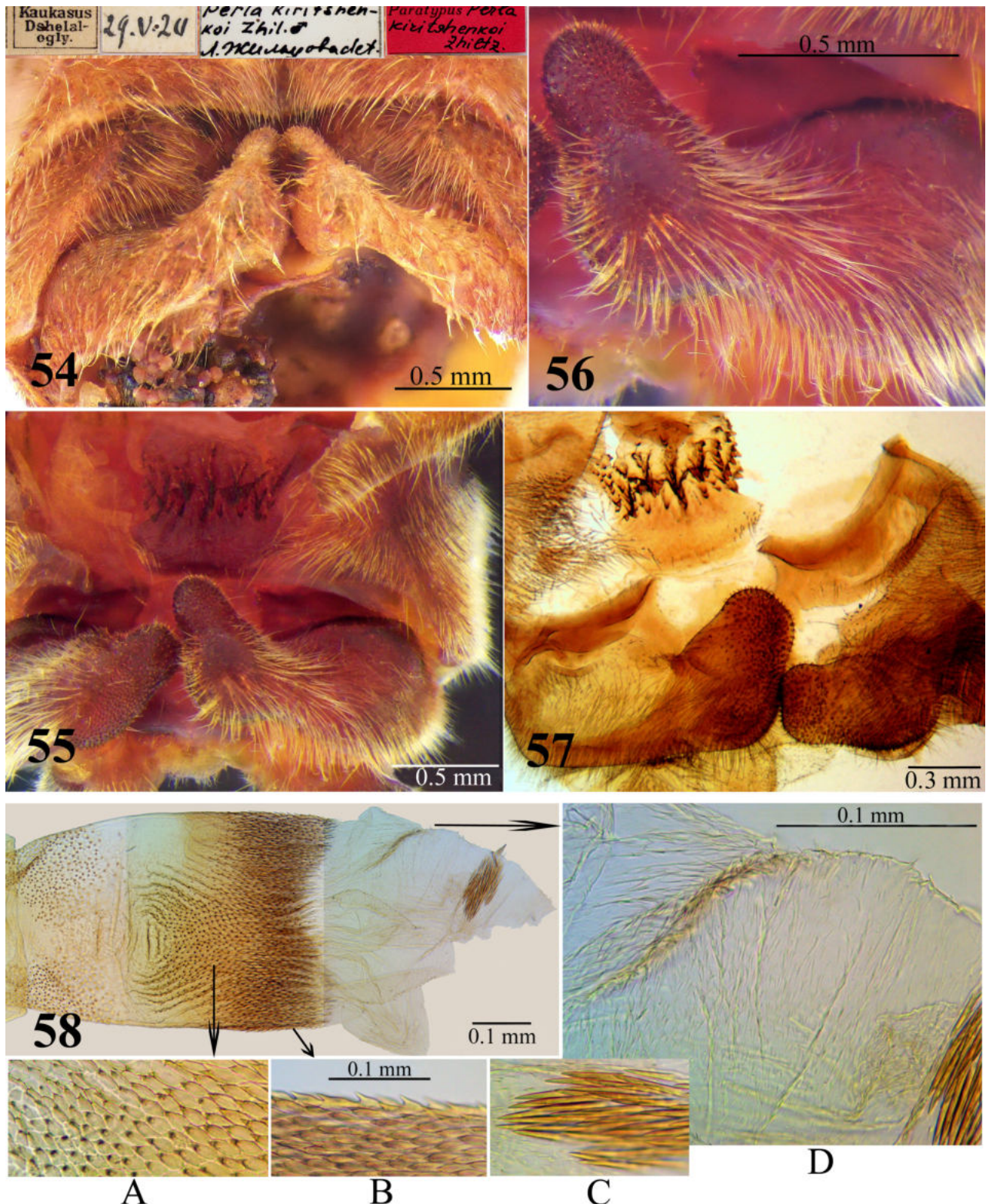
Complimentary description—adult habitus. Males and females are macropterous (Figs. 50, 59). The M-line on the head is rufous, smooth, and clearly defined (Fig. 53). The interocellar area has a dark brown spot extending upward to the M-line and down to the lateral ocelli, with the lateral branches of this spot reaching the lateral edges of the head above tentorial pits; the lateral edges of the clypeus are also dark brown; and paired rufous spots are located behind the compound eyes (Figs. 53, 59–60). Along the anterior margin of the clypeus, paired patches between the lateral ocelli and compound eyes, as well as paired patches on the occiput, are yellow (Figs. 53, 59–60). Tentorial pits above lateral ocelli are clearly defined, bean-shaped, yellow, and have a small, dark spot inside (Figs. 53, 60). Pronotum with a dark medial band noticeably widening towards the anterior margin; band surrounded by pale rugosities of an X-shaped pattern; lateral fields the same color as the medial band (Figs. 53, 59–60). Legs are brown (Figs. 50, 52). Femur darkened distally with a thin yellow band along the outer edge (Fig. 59); dark closing hairs and scattered brown bristles along the inner and outer edges; a medial band without hairs and bristles with a small oval pale spot distally. Tibia has a thin yellow band along the outer edge; the base darkened (Figs. 50, 59); there is a small dark band distally.

Male. Tergum 8 medially has a membranous furrow and posterolateral humps covered with dense, thick, and long setae. Tergum 9 has a depressed, sclerotized mesal field slightly widened posteriorly, and the length does not exceed its width. On the mesal plate, the longitudinal serrated ridges (7–8) are heavily sclerotized and concentrated mesally and do not reach the posterior edge, which is smooth and rounded with a weak notch in the middle (Figs. 55, 57). Tergum 10 has hemitergites that are curved at an obtuse angle and directed obliquely upward; each hook is strongly swollen in place of the bend on the outer and dorsal sides, forming a noticeable rounded protrusion covered with long setae; the same setae cover the outer edge of the hook (Figs. 54–57). The apex of the hook is rounded (on a cleared specimen, the hook apex is rectangular-rounded) and covered with sensilla basiconica, which is extended at the tip to the front and outer edges (Figs. 56–57). An artificially everted penis has a tube covered dorsally with densely arranged longitudinal rows of serrate sclerites, turning into scales sometimes with small spines; the shape of sclerites and rows in different parts of the tube is different; the tube is membranous basally with paired patches of



FIGURES 50–53. *Perla kiritshenkoi* Zhiltzova, 1961. Caucasus: Armenia, Stepanavan, Kamenka River; Azerbaijan, Lelyakoran. Paratypes. Males. 50. Habitus, dorsal. 51. Abdominal tip, dorsal. 52. Habitus, dorsal. 53. Head and pronotum, dorsal.

rounded spine bases laterally (Figs. 58, A–B). The sac is bulbous and membranous, with thin pointed brown spines, forming a narrow apical brush ending in triangles of spines ventrally and dorsally (Figs. 58, C). The membranous sac is rough, covered with dense, tiny setae, clearly visible near the folds of the lobes (Figs. 58, D).



FIGURES 54–58. *Perla kiritshenkoi* Zhiltzova, 1961. Caucasus, Armenia. Male. 54. Paratype male, abdominal tip, dorsal. 55. Mesal plate and hemitergites, dorsal, alcohol. 56. Hemitergal hook swollen in the place of the bend, dorsocaudally, alcohol. 57. Mesal plate, dorsal, and hemitergites, lateral, cleared. 58. Chaetotaxy of artificially everted penis, dorsal, cleared. A. Leaf-shaped scales with small spines. B. Densely arranged longitudinal rows of heavy sclerotized serrate sclerites. C. Pointed brown spines in the apical brush. D. Tiny setae covered the sac lobes.

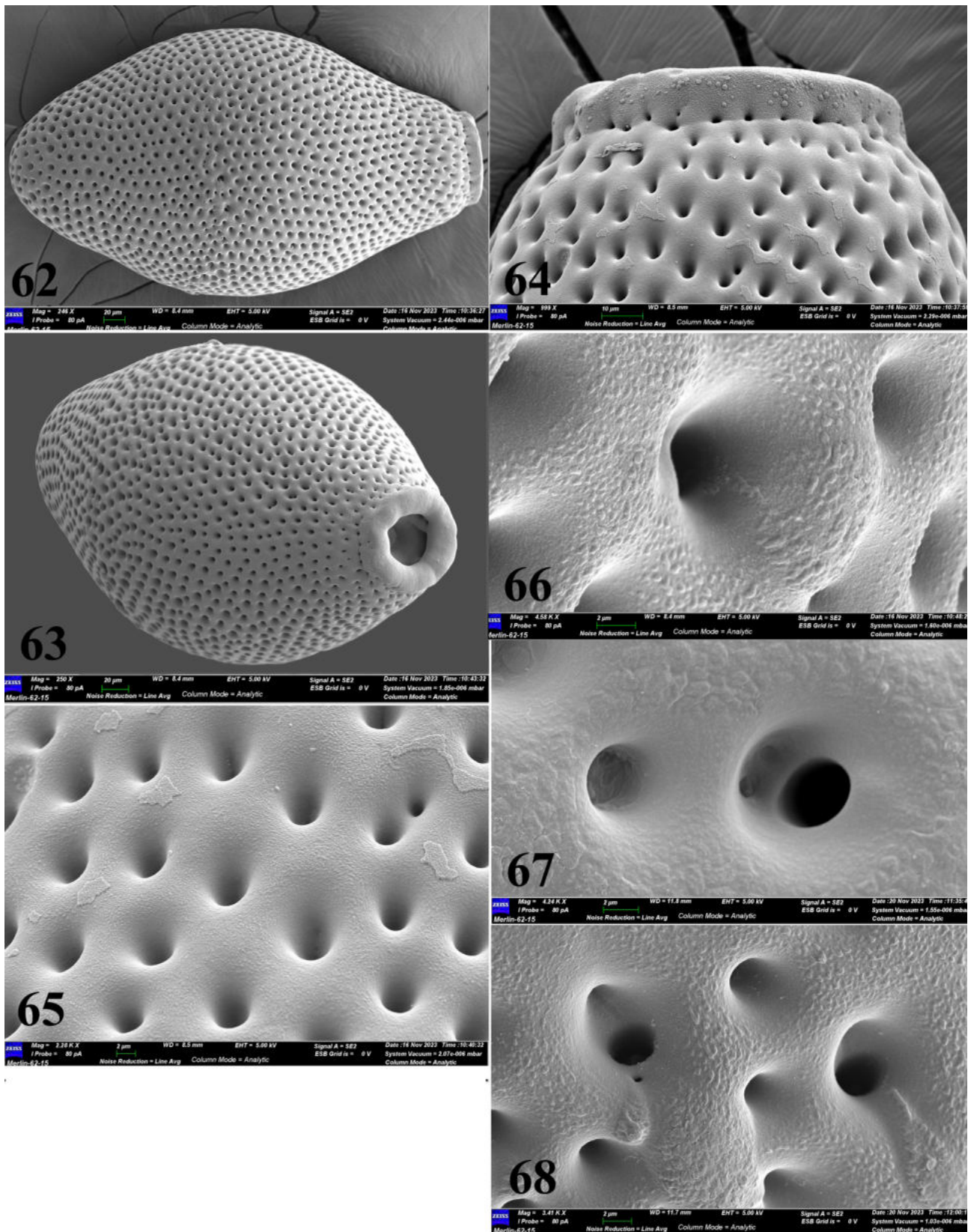


FIGURES 59–61. *Perla kiritshenkoi* Zhiltzova, 1961. Caucasus, Armenia, Stepanavan, Kamenka River. Female. 59. Habitus, dorsal. 60. Head and pronotum, dorsal. 61. Abdominal tip, ventral.

Female. Subgenital plate occupies $\frac{2}{3}$ of the width of sternum 8 with bilobed projection posteromedially (Fig. 61); lobes are small, narrow, pointed, and covered with small, reddish setae (Fig. 61). The cerci are long, projecting far beyond the end of the wings; the basal cercal segments are brown; and the distal cercal segments are bicolored, yellowish at the base and brown distally (Fig. 59).

Egg. The type material egg is spindle-shaped, tapering evenly to each pole (Figs. 62–63), with mean dimensions of $428 \times 242 \mu\text{m}$ ($n = 3$; length without anchor). The collar is short, and the rim is thick and rough, with a series of small pits around the base (Figs. 63–64). Chorion is rough and punctate throughout (Figs. 62, 65–68); punctations are large, deep, and mostly uniform, but small punctations are also present, especially near the micropylar row, which is located almost at the equator (Fig. 62); micropylar orifices with a slightly raised thin edge are located not on the bottom but laterally on the pit wall (Fig. 67); inside the pit there may be an additional 1–2 small orifices (Fig. 68).

Larva. Unknown.



FIGURES 62–68. *Perla kiritshenkoi* Zhiltzova, 1961. Caucasus: Armenia, Kamenka River. Egg. 62. Appearance with micropylar row, lateral. 63. Same, dorsolateral. 64. Collar rim, and small pits around the base, lateral. 65–66. Chorion structure with deep punctations. 67. Micropyle with a slightly raised, thin edge. 68. Micropyle on the pit wall with the addition of small orifices.

Material examined. Paratypes: male, Azerbaijan, Lelyakoran, Lenkoran. u. (u.=uezd, is an administrative unit of the Russian Empire, author's note) 15.V.1909, Kirichenko; 1♂, Armenia, Dshelal-ogly, Kamenka River Gorge, 16.V.22, Shelkovnikov; 1♂, Armenia, Kaukasus, Dshelal-ogly (now Stepanavan), 29.V.1924, collector unknown.

Additional material. 1♀, Armenia, st. 439, coll. 574, Kamenka River, vicinity of Stepanovan, 27.VI.1956, coll. Zhiltzova LA; 2♀ (damaged), Jalal-ogly (now Stepanavan), the Kamenka River Gorge, 16.V.1922, coll. Shelkovnikov; 1♂ (alcohol), Azerbaijan, River Divachach, Tsasharuchey; 5.V.1933, F. Lukyanovich.

Distribution. Caucasus: Armenia, Azerbaijan (Talysh). Iran (Alborz), Turkey (eastern Pontius) (Zhiltzova 1961; Zwick 1975; Kazanci 1983; Sivec & Stark 2002; Darilmaz *et al.* 2016) (Fig. 159). Adults emerge from the second half of May through the first half of July. Adults were found in Armenia at altitudes of 1440–1850 m along the banks of fast streams and small mountain rivers in the forest zone on cereals and other herbaceous plants. In the Talysh, *P. kirischenkoi* was found at approximately 1500 m above sea level at the upper border of the forest zone and higher in small, fast-flowing forested streams (Zhiltzova 1961) and mountain rivers (Muranyi *et al.* 2021).

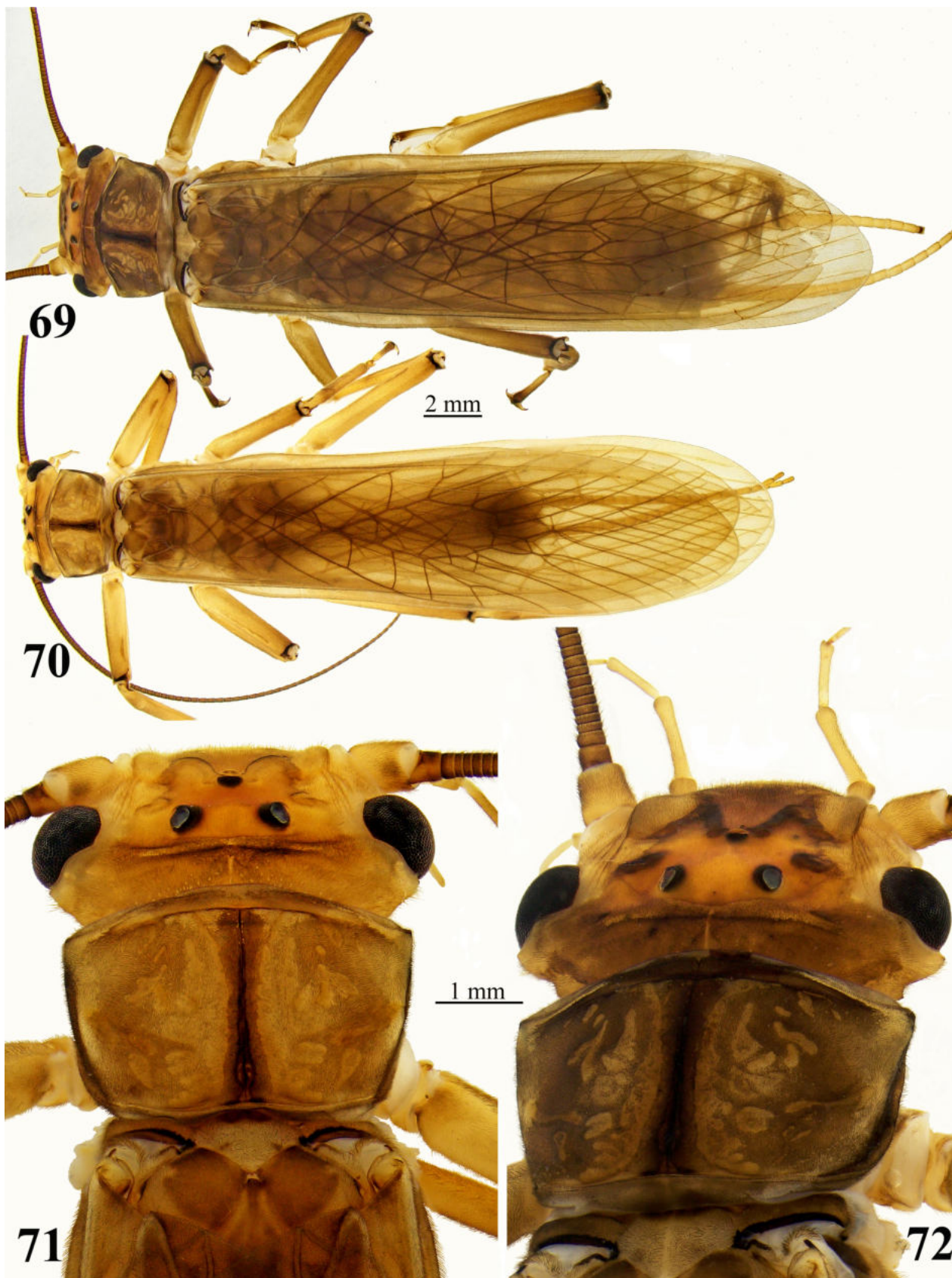
Perla schapsugica sp. nov. Teslenko & Palatov

Figs. 69–98

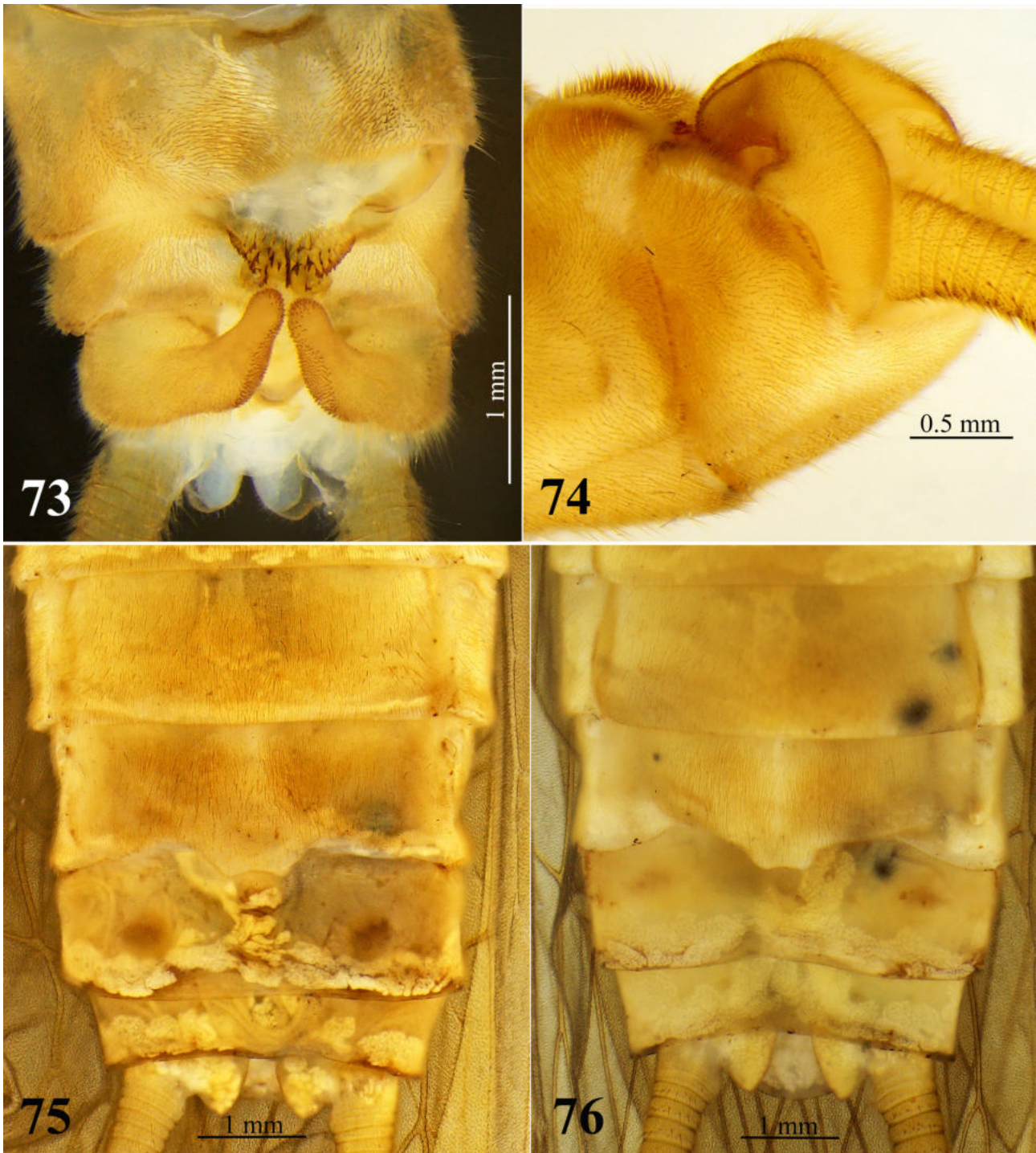
Diagnosis. Tergum 9 of males is distinguished by a butterfly-shaped mesal field; the width is greater than the length (Fig. 73); the longitudinal serrated ridges are short at the lateral margins, the long serrated ridges are located in the middle of the mesal field (Fig. 73). The hemitergal hook is rounded at the apex (Figs. 73, 77). The tube of the penis is ca. 2.3 times longer than the sac. The membranous sac is smooth, with a pair of rounded lateral lobes dorsally and ventrally and a tongue-shaped medial lobe dorsally; ventrally, the sac is deeply depressed, and the lobes are almost indistinguishable except for a pair of lateral lobes (Figs. 77–81). The apical brush is long, widened dorsally, and slightly pointed ventrally (Figs. 79–81). The egg is round-oval, anchor small, and covers only the collar rim (Fig. 82, 84–85). Collar wide, with barely noticeable discernable ribs; rim smooth, with weak incisions (Figs. 83, 85–86). Chorion is coarsely pitted; pits are round, large, and deep; the chorion surface between pits is rough (Figs. 84, 88). Micropyles in the pits are set not on flows but on the walls of the pits; orifices are raised with thin rims (Fig. 89). The larvae are distinctive by the color pattern of the head, pronotum, and cercal segment pilosity (Figs. 90–91, 96–98). **Adult habitus.** Body length: males 20.6–22.8 mm (n=5), females 21.2–28.5 mm (n=5); macropterous forewings are long, equal to body length, reaching males 21.3–23.0 mm and females 21.2–28.7 mm (Figs. 69–70); wingspan: males 44.9–49.0 mm and females 45.2–49.7 mm.

Head and pronotum are dorsally yellow-brown with dark brown and pale spots (Figs. 71–72). The wings are yellowish with dark brown veins (Figs. 69–70). Antennae are dark brown, palpi yellow. The M-line is dark brown with sharp projections, between which there is a small yellow spot connected to a brownish spot on the clypeus; the lateral edges of the clypeus are light brown (Figs. 71–72). Frontal tentorial pits are darkened. The interocellar area is yellow and the tentorial pits are dark brown (Figs. 71–72). The posterior occipital fold looks like a thin, dark brown stripe (Fig. 72). A pair of transversely oblique dark bands extends from the base of the occiput to the posterior occipital fold. Pronotum brown, as wide as the head with eyes, slightly narrowing posteriorly; anterolateral margins obtuse, posterolateral margins rounded; medial stripe dark brown, widened to anterior and posterior margins; anterior pronotal margin darkened medially; lateral pronotal margins bordered by a dark brown stripe, widening posterolaterally; sometimes the lateral edges are bent down and not visible dorsally (Figs. 71–72). Pronotal rugosities are grayish-yellow, darkly contoured, and form an X-shaped pattern; in the posterior 1/3, pale rugosities in the form of narrow paired transverse short stripes almost reach the lateral pronotal margins (Figs. 71–72). The legs and cerci are yellow-brown. Femur is yellow-brown with a narrow, dark brown stripe along the distal edge. Tibia is darker than the femur, with a narrow dark brown stripe along the inner edge and a short oblique dark stripe along the outer edge at the base; the distal edge of the tibia has a thin dark brown stripe (Figs. 69–70). Anal gills are absent. The cerci are yellowish in the basal third of their length and brownish apically (Figs. 69–70).

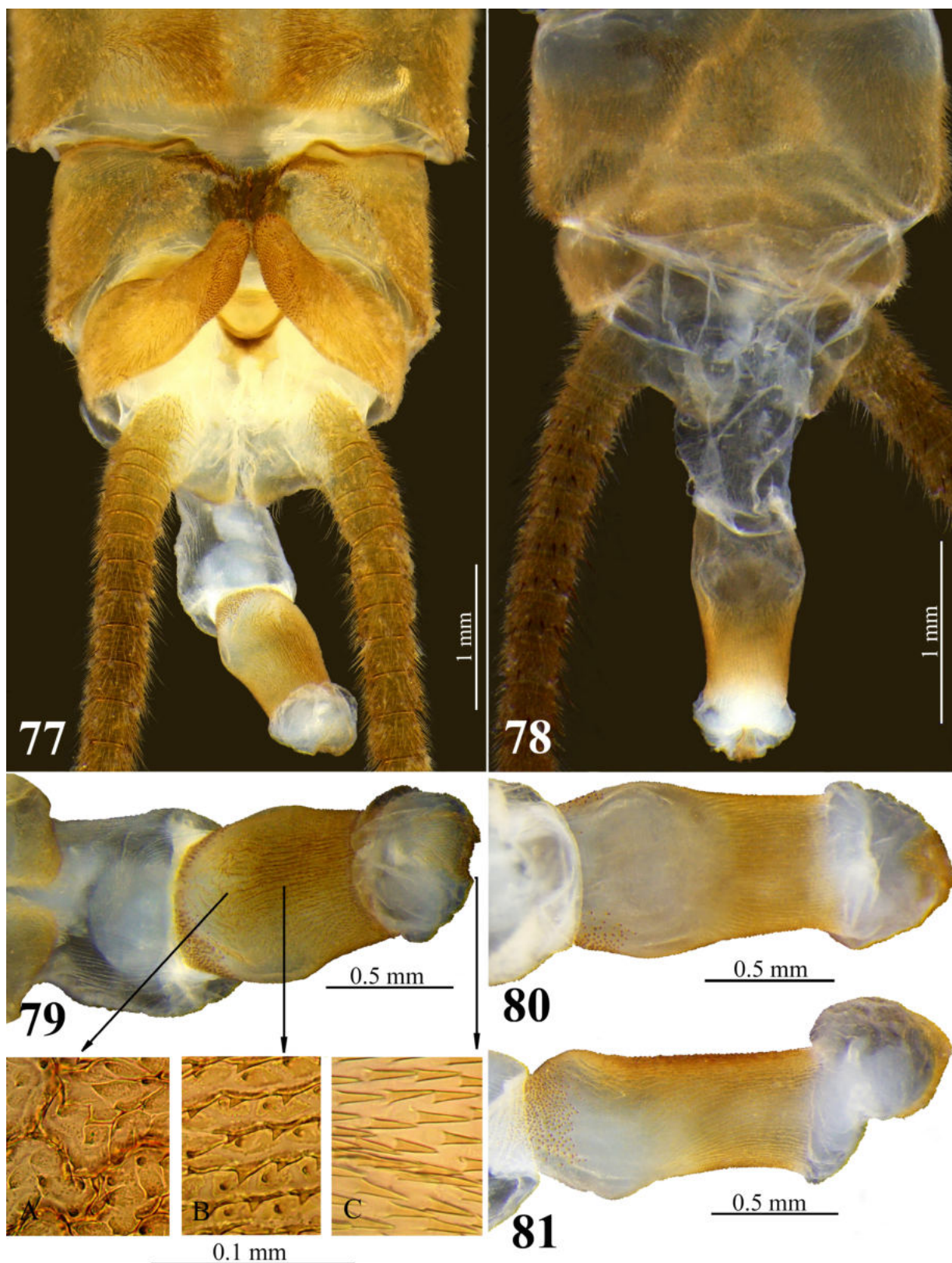
Male. Tergum 8 is medially depressed with a central membranous furrow; posterolateral humps are covered with dense and thick setae (Fig. 73). Tergum 9 has a sclerotized mesal field that is butterfly-shaped; the width is greater than the length (Fig. 73). The mesal field bears sharp, heavy sclerotized teeth that merge into long and short longitudinal serrated ridges; the long serrated ridges are located in the middle of the mesal field (Fig. 73). Tergum 10 has finger-shaped hemitergal hooks (cleared) with a weak notch in the distal third (Fig. 73); apex is rounded.



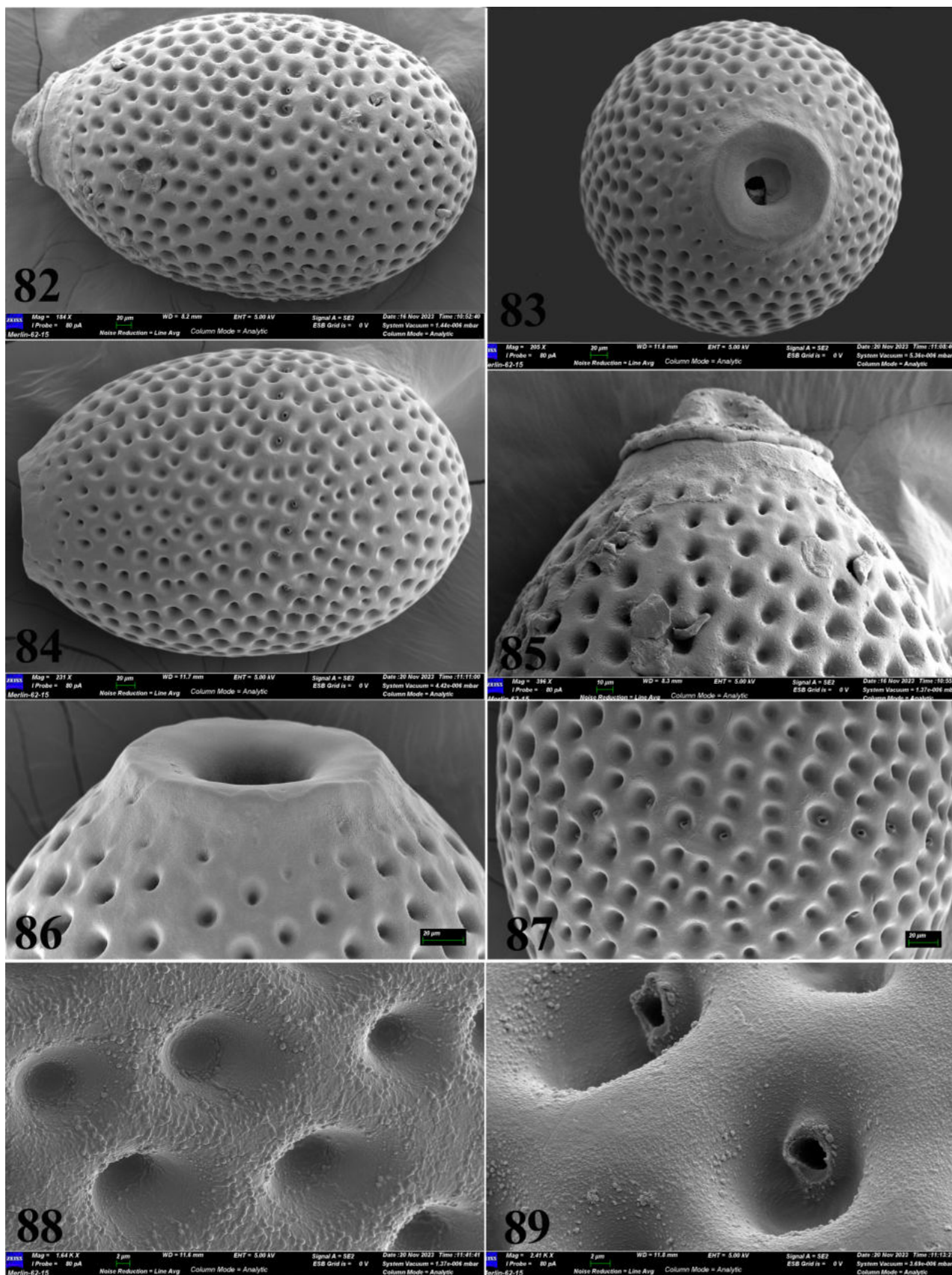
FIGURES 69–72. *Perla schapsugica* **sp. nov.** Caucasus, Russia, Krasnodar Kray, urban District of Sochi, Lazarevsky District, nameless small stream, right tributary of the Kuapse River opposite Verkhnyaya Mamedka village. 69. Paratype. Female habitus, dorsal. 70. Holotype. Male, habitus, dorsal. 71. Holotype, male, head and pronotum, dorsal. 72. Paratype, female, head and pronotum, dorsal.



FIGURES 73–76. *Perla schapsugica* **sp. nov.** Caucasus, Russia, Krasnodar Kray, urban District of Sochi, Lazarevsky District, nameless small stream, the right tributary of the Kuapse River opposite Verkhnyaya Mamedka village. 73. Paratype. Male. Abdominal tip, mesal plate, hemitergal hooks, dorsal, cleared. 74. Abdominal tip, hemitergal hooks, lateral, cleared. 75–76. Female abdominal tip, the subgenital plate, variations.



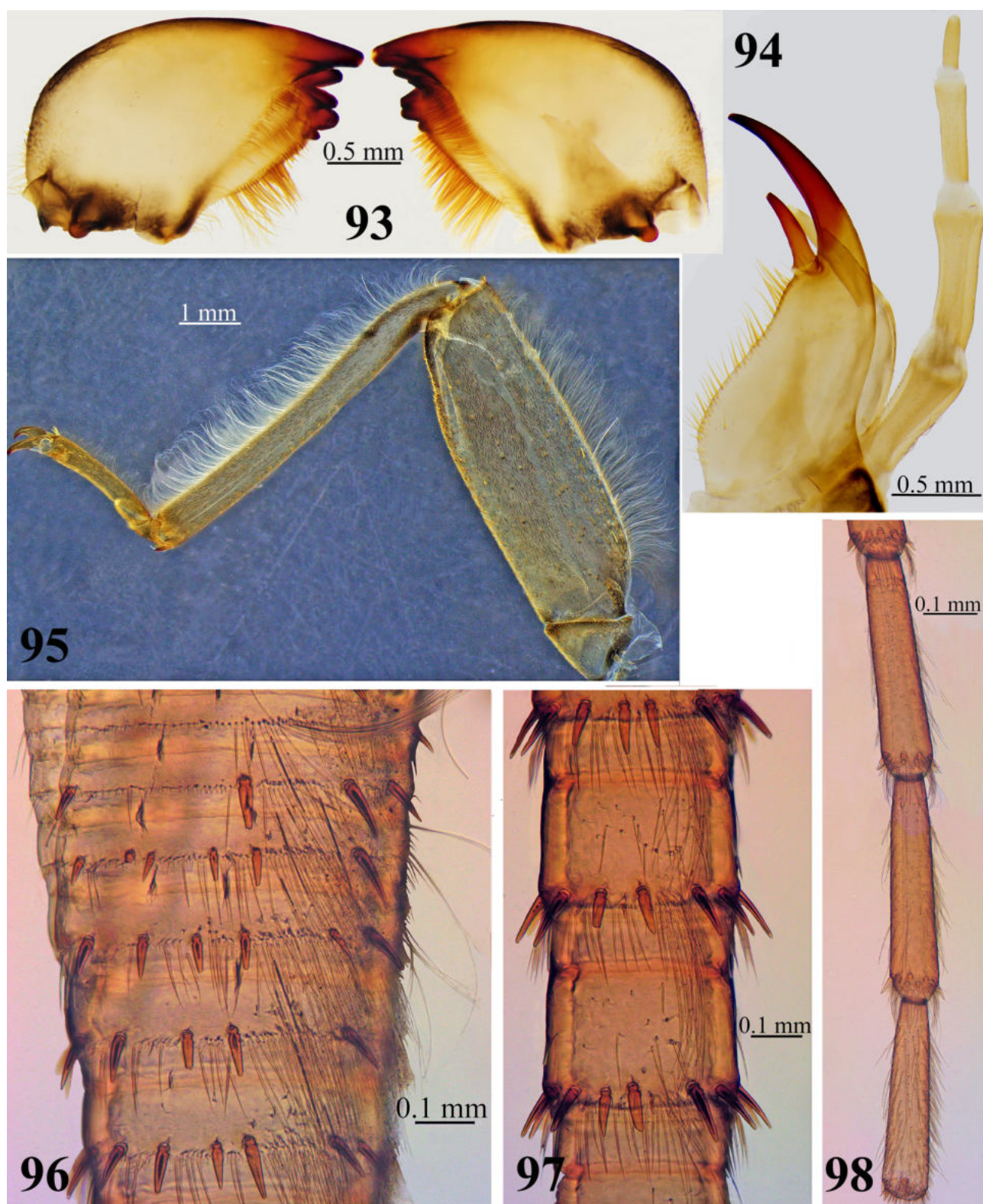
FIGURES 77–81. *Perla schapsugica* **sp. nov.** Caucasus, Russia, Krasnodar Kray, urban District of Sochi, Lazarevsky District, nameless small stream, the right tributary of the Kuapse River opposite Verkhnyaya Mamedka village. 77. Male. Abdominal tip, mesal plate, hemitergal hooks, and artificially everted penis, dorsal, cleared. 78. Abdominal tip, artificially everted penis, ventral, cleared. 79. Chaetotaxy of the penis, dorsal. A. Polygonal scales with small spines. B. Densely arranged longitudinal rows of heavy sclerotized serrate sclerites on the tube of the penis. D. Pointed brown spines in the apical brush. 80. Penis, ventral. 81. Penis, lateral.



FIGURES 82–89. *Perla schapsugica* sp. nov. Caucasus, Russia, Krasnodar Kray, urban District of Sochi, Lazarevsky District, the unnamed stream in the Krasnoaleksandrovskaya cave. Egg. 82. Appearance with mushroom anchor and micropylar row, lateral. 83. Collar, dorsal. 84. Appearance without anchor, lateral. 85. Posterior pole with anchor and collar, lateral. 86. Collar, dorsolateral. 87. Micropylar row. 88. Chorion structure. 89. Micropyles set on the walls of the pits; orifices raised with rims.



FIGURES 90–92. *Perla schapsugica* **sp. nov.** Caucasus, Russia, Krasnodar Kray, urban District of Sochi, Lazarevsky District, unnamed stream in the Krasnoaleksandrovskaya cave. Larva. 90. Female, habitus, dorsal. 91. Male, habitus, dorsal. 92. Head and pronotum, dorsal.



FIGURES 93–98. *Perla schapsugica* **sp. nov.** Caucasus, Russia, Krasnodar Kray, urban District of Sochi, Lazarevsky District, unnamed stream in the Krasnoaleksandrovskaya cave. Larva. 93. Left and right mandibles, ventral. 94. Left lacinia, galea, maxillary palpus, ventral. 95. Right hind leg, dorsal. 96–98. Chaetotaxy of the right cercus, lateral: 96. Basal cercal segments. 97. Middle cercal segments. 98. Apical cercal segments.

Sensilla basiconica are concentrated into an oval patch covering the inner side and top of the hook; the base of the hook is slightly rounded and covered with long setae (Figs. 73, 77). In lateral view, the hemitergites are bent almost at a right angle and directed obliquely forward and downward towards the mesal field (Fig. 74). The artificially everted penis has a tube that is ca. 2.3 times the length of the sac. The tube is widened in basal half; dorsally and ventrally covered with densely arranged longitudinal rows of serrate sclerites, sometimes with small spines; the shape of sclerites changes from serrated and oval elongated to polygonal pattern in different parts of the tube (Figs. 79, A–C, 81); the tube basally with paired lateral patches of rounded spine bases (Figs. 79–81); ventrally tube membranous in basal half. The sac is membranous and smooth, and at the base there is a pair of rounded lateral lobes dorsally and ventrally (Figs. 77, 79). On the dorsal side, the sac has a tongue-shaped medial lobe, tapering towards the base of the sac; ventrally, the sac is deeply depressed, and the lobes are almost indistinguishable (Figs. 77, 79). The apical brush of pointed brown spines is relatively long, widened dorsally, and slightly pointed ventrally (Figs. 79–81).

Female. Sternum 8 has a subgenital plate occupying $>1/2$ of the sternum width and is slightly convergent in the medial plane. The subgenital plate has a small bilobed projection posteromedially; the lobes are small, rounded or slightly pointed, covered with rufous setae, and project onto sternum 9, covering $1/4$ of its length. (Figs. 75–76).

Egg. Round-oval, $488 \times 322 \mu\text{m}$ ($n=7$), length with anchor (Figs. 82, 84). Anchor is small, mushroom-shaped, and covers only the collar rim (Figs. 82, 85). Collar wide, circumference with barely noticeable discernable ribs; rim smooth, with weak incisions (Figs. 82–86). Chorion is coarsely pitted; pits are regularly round in shape or oval (in micropylar row), relatively large and deep; and the chorion surface between pits is rough (Figs. 84, 87–88). Micropylar row in the form of a broken line located close to the equator (Figs. 82, 87). Micropyles in the pits are set not on flows but on the walls of the pits; orifices are raised with thin rims (Fig. 89).

Larvae. Female larva length 28.0–37.0 mm, length of antennae 11.5–13.0 mm, and cerci 14.5–17.0 mm ($n=9$); male larva length 17.0 mm, antennae 11.5 mm, and cerci 13.0 mm ($n=1$). The main color is olive-brown, with contrasting lighter patterns on the head, pronotum, mesonotum, and metanotum, and a less distinct pattern on the abdomen (Figs. 90–91). Body covered with dark clothing hairs; a dorsomesal band of erect silky setae is faintly visible (Figs. 90, 92). Antennae, cerci, and sterna are pale. The head is large, and its width along the posterior edge does not exceed the width of the pronotum (Fig. 92). Clypeus olive-brownish until M-line, with pale tentorial pits; lateral clypeal margins darkened. M-line pale, a large transverse brown spot below M-line extending from the anterior ocellus to the posterior ocelli and lateral margins of the head; a triangular spot between the posterior ocelli and small triangular spots near the posterior ocelli laterally are pale; the posterior tentorial pits are internally light brown (Fig. 92). A short, relatively wide brown stripe with rectangular lateral edges below the epicranial suture does not reach the lateral edges of the head; the epicranial stem and occiput edge are brownish (Fig. 92). The transverse occipital fold and the fold running around the eye merge into a regularly curved line. Setation along the occipital fold extends only to behind the eye but not forward along the edge of the flat, expanded side of the head. No wavy section of the occipital fold is near the inner corner of the eye. The labrum is brownish with a small pale spot medially. Mandibles are heavily sclerotized (Fig. 93), with a rounded, dark outer margin. Left mandible with five sclerotized, bluntly pointed teeth; the apical tooth is elongated; the next three teeth are distinctly shorter; the last tooth is small and obtuse; the molar area bears two rows of short setae and a marginal row of long setae; the first row of short setae extends from the base of the first tooth, the second from the base of the third (Fig. 93). Right mandible with six bluntly pointed teeth; the last tooth is small, sometimes hidden by a marginal row of setae; the molar area bears a marginal row of long setae and one medial row of small setae stretching from the base of the first tooth to the mandibular base (Fig. 93). Lacinia bidentate has a large, darkly curved apical tooth and a much shorter subapical tooth (Fig. 94). The marginal fringe of setae along the inner lacinial margin is complete; one strong seta is visible near the subapical tooth. Galea length reaches almost half of the apical tooth length (Fig. 94).

Pronotum transverse, not wider than the head posteriorly, with obtusely rounded anterior corners; lateral margins and posterior angles are evenly rounded (Figs. 90–92). The pronotal fringe is complete with mostly short setae; a few relatively long setae are present on the posterolateral angles. Pronotum with thin brown stripes along lateral margins; paired semi-oval pale bands outline semi-oval dark brown bands within the lateral pronotal fields; brown bands are wider than pale bands (Fig. 92). The central pronotal field is pale with a light brown median band widened anteriorly and posteriorly; the band is surrounded by pale rugosities of an X-shaped pattern; paired vague S-shaped brown bands extend from the anterior to posterior pronotal margin; and the lateral fields are the same pale as the X-shaped medial pattern (Fig. 92). Mesonotum and metanotum with similar Ψ -shaped brown pattern medially;

paired wide dark brown bands limiting the wing pad bases; a narrow dark stripe runs along the lateral edge of the wing pads (Figs. 90–91). The legs are light yellow-brown. The femur has a diffuse brownish spot in the distal half closer to the outer edge; the basal and distal edges are also brownish; the stout, hind femur is 3.2–3.5 times as long as wide (Figs. 91, 95). The femur and tibia are densely covered with dark clothing hairs bearing stout, short, acute red bristles along the inner and outer edges and a fringe of very dense, long, silky hairs along the outer margins (Fig. 95). Sparse red bristles also covered their surface irregularly. Tibia have diffuse, narrow, dark brown bands on the inner and outer edges basally.



FIGURES 99–101. *Perla schapsugica* sp. nov. Habitat. Caucasus, Russia, Krasnodar Kray, urban District of Sochi, Lazarevsky District, unnamed stream in the Krasnoaleksandrovskaya cave. 99. The Krasnoaleksandrovskaya cave, exit. 100. Outlet of a small stream from Krasnoaleksandrovskaya cave. 101. A shallow beech ravine.

The abdomen is dark brown, with variation in banding between female and male larvae (Figs. 90–91). On each abdominal tergum of the male larva are two pale transverse spots on the sides of the medial brown line; along the lateral tergal margins, there is another paired pale spot, not always clear (Fig. 91). On the last tergum of the male larva, the pale spots merge with each other (Fig. 91). The posterior terga margins bear acute bristles that are mostly short, with one or two relatively long, thin setae. Anal gills are very small (Fig. 90). Cerci are uncolored, yellowish, and have about 39 segments with striking rings of dark spines (Fig. 90). Fine pilosity is present between dark spines, tightly pressed to the segment surface; their length is 1/2 the length of the basal and middle cercal segments; on the apical cercal segments, the length of the thin hairs is slightly $>1/3$ of the length of the segment (Figs. 96–98). Long silky colorless hairs are present in the circlet in tufts (at least 15 in each on the basal and middle cercal segments), forming a dorsal longitudinal fringe, tightly pressed to the segments; the length and density of long silky hairs decrease towards the cercal apex (Figs. 96–98). On the middle and apical cercal segments, short and thin intercalary setae are visible; their length does not exceed the length of fine circlet hairs (Figs. 97–98).

Material examined. Holotype male (FSC EATB FEB RAS). Caucasus. Russia, Krasnodar Kray, urban District of Sochi, Lazarevsky District: a nameless small forest stream, right tributary of the Kuapse River opposite Verkhnyaya Mamedka village, altitude 113 m above sea level, 43.574294 N, 39.191197 E, 04.06.2024, coll. D. Palatov; paratypes: 5♂, 2♀, 6 larvae, (FSC EATB FEB RAS), same place and data; 6 larvae of females, 1 immature larva of male, 1 exuvium, unnamed stream in the Krasnoaleksandrovskaya cave (known as the “Witches Cave”) at the exit, altitude 160 m above sea level, 44.015361 N, 39.363833 E, 21.06.2023, coll. D. Palatov; 2♀, 2 larvae, 7 exuvia, the same place, 44.005558 N, 39.215108 E, 5.06.2024, coll. D. Palatov; 1♂, 2♀, 1 larva, stream on the right side of the road at the entrance to Maryino village, altitude 208 m above sea level, 43.562794 N, 39.284126 E, 3.06.2024, coll. D. Palatov; Tuapse District: 2 larvae, unnamed large and the last stream before the Agoi Ridge on the coast in the Tuapse District (Kiselev rock), altitude 60 m above sea level, 44.122083 N, 39.03300 E, 19.04.2006, coll. D. Palatov; 13♂, 8♀, 3 exuvia, the second stream north of the Kiseleva rock on the cape between Tuapse and Agoy village, altitude 50 m above sea level, 44.071981 N, 39.020388 E, 6.06.2024, coll. D. Palatov; 1 larva, Shepsi River (Tuapse River), 2 km above Shepsi village, near the last summer cottages, altitude 86 m above sea level, 44.015361 N, 39.363833 E, 13.05.2019, coll. D. Palatov.

DNA barcoding. GenBank accession number is PP236724. Both molecular and morphologic characters support the statement that *Perla schapsugica* **sp. nov.** is a valid species distinct from other Caucasian *Perla*. Genetic distances between *Perla schapsugica* **sp. nov.** and the different populations of the *Perla* species are approximately 17.0% (Table 2). Phylogenetic relationships show that this species is sister to *P. caucasica* and *P. persica* (Fig. 160).

Etymology. The species is named after the ancient subethnic group of Schapsugs, the indigenous population from the Black Sea coast of the Caucasus, living in the cities of Sochi, Lazarevsky, and Tuapse Districts of the Krasnodar Kray, where the type habitat of this species is located.

Distribution. *Perla schapsugica* **sp. nov.** occurs in the small karst streams of the Black Sea coast of the Caucasus from Tuapse to Sochi in the Krasnodar Kray, Russia (Fig. 159). The material was collected at the outlet of a small stream from a cave, quickly falling into a karst, 100–150 m long and 2.0–2.5 m wide, with a current ≤ 0.6 m/s. The bottom was enclosed with large stones covered with moss (Figs. 99–101). This species was also found in small rivers and streams on the Black Sea coast of the Tuapse District, flowing in low-mountain beech forest valleys up to 200 m above sea level. The stream has a width of 1.5–3.0 m, a depth varying from 0.1–0.5 m, a water current of 0.1–0.5 m/s, and a bottom with pebbles and small stones that rarely leave litter, detritus, and silt.

Perla pallida Guérin-Méneville, 1843

Figs. 102–127

Guérin-Méneville, 1843: 393–394;

Pictet, 1841: 192, pl. XIII, fig. 13;

Klapálek, 1923: 46–48, fig. 22;

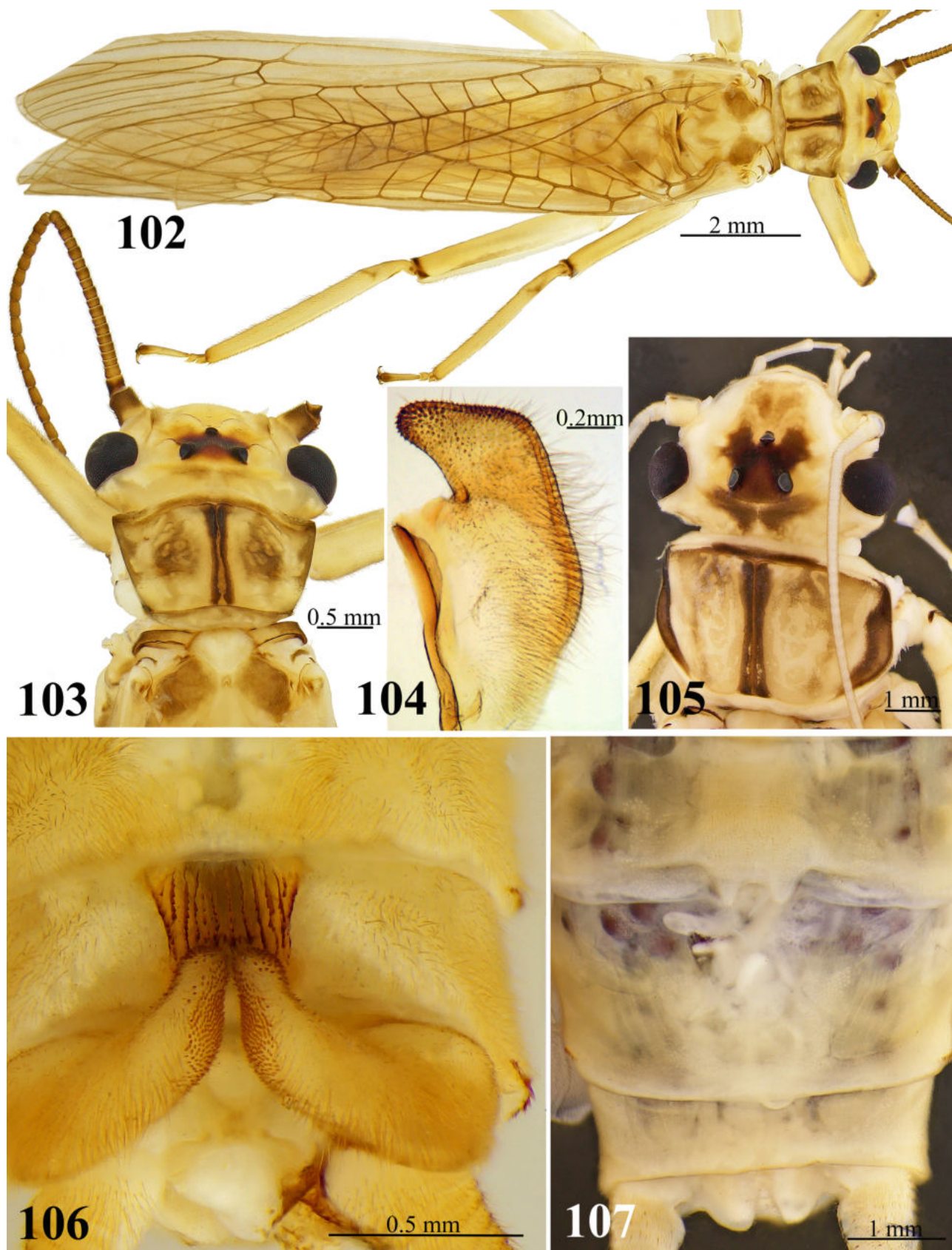
Zhiltzova, 1956: p. 660 (distribution in the Kura R. Basin, Trialetsky Range);

Sivec & Stark, 2002: 23, figs. 43–45, “Type 1”;

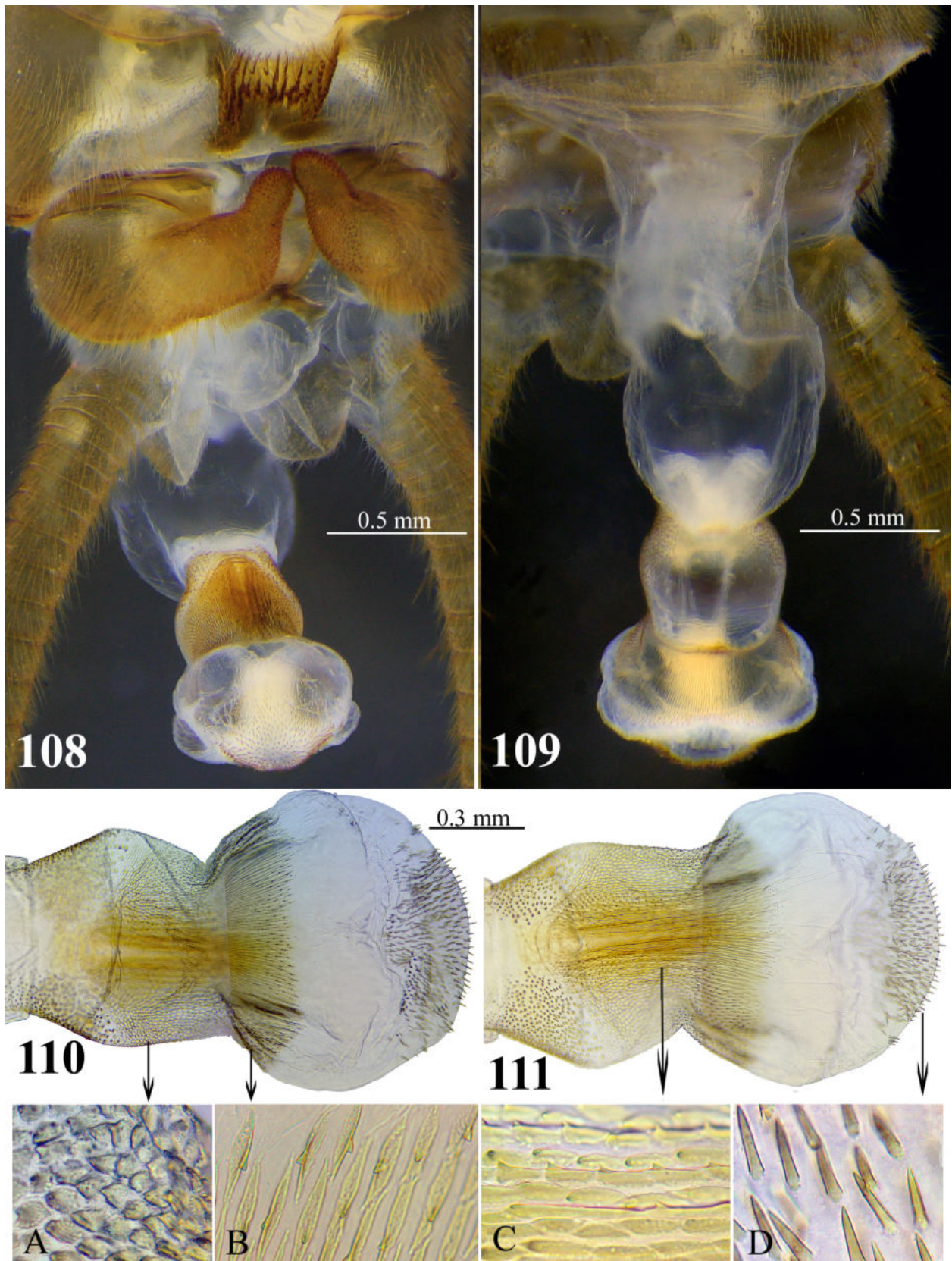
Murányi *et al.*, 2021: 73 (distribution, Azerbaijan)

Perla pallida was originally described by Guérin-Méneville (1843) based on a male from the Caucasus without indicating the type locality. The original description was supplemented by Pictet (1841). Later, the species was redescribed by Klapálek (1923) on Caucasian specimens from Azerbaijan, Georgia, and Turkey. These specimens subsequently became neotypes and are stored in the Natural History Museum of Wien (NHMW) (Murányi *et al.* 2021). The primary types were presumably lost during the 19th century. The current concept of the species is based on these Caucasian specimens (Sivec & Stark 2002). Taking into account differences in egg structure, Sivec & Stark (2002) considered *P. pallida* to be a species complex of three or more species or subspecies distributed in the Caucasus, Anatolia, Balkans, and Carpathians.

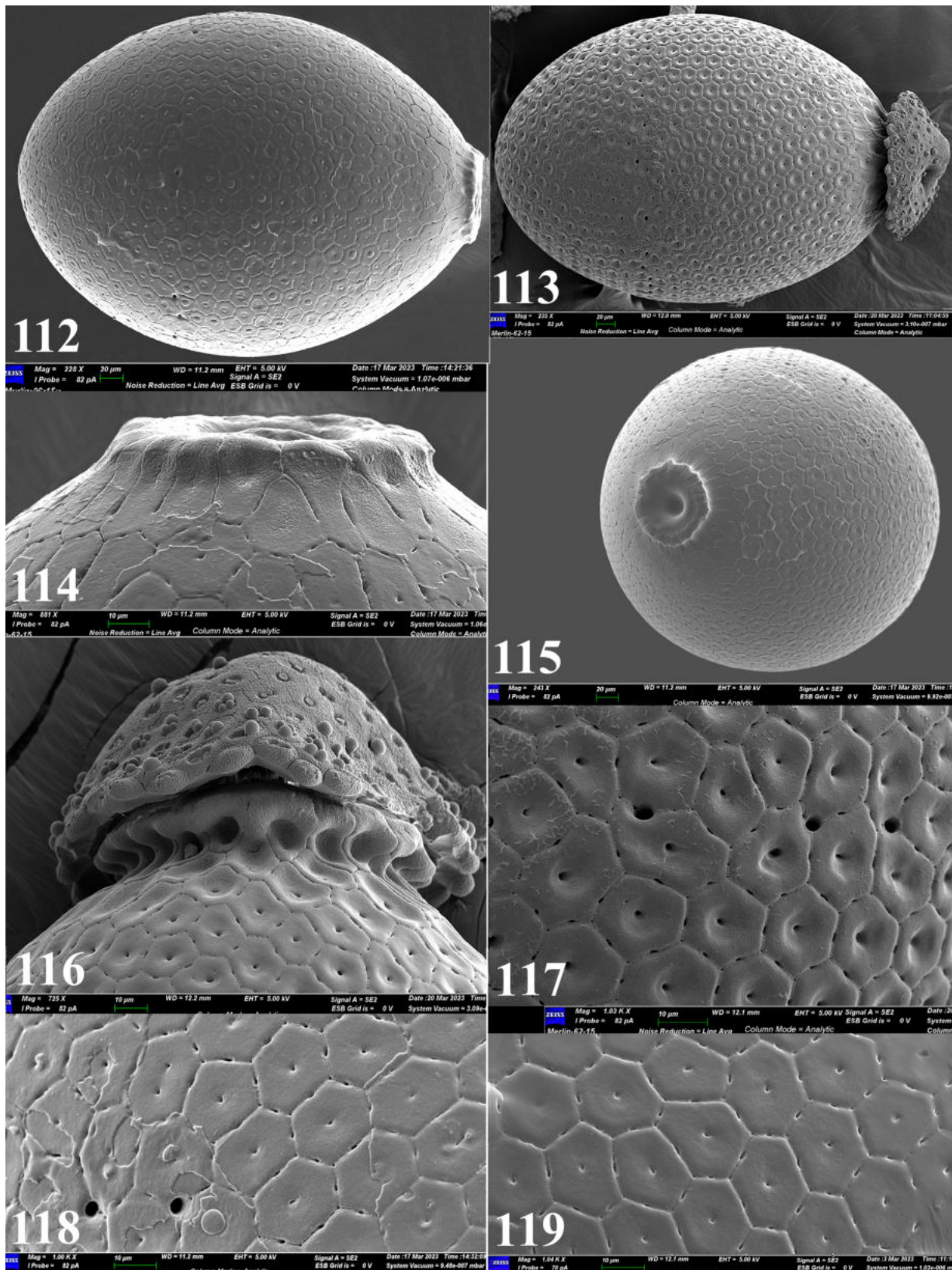
Diagnosis. Mesal field on tergum 9 of male slightly expanded anteriorly and posteriorly, width slightly greater than length; longitudinal serrated ridges (10–12) closer to anterior and lateral margins; posterior margin avoids serrated ridge rows (Figs. 106, 108). Hemitergites are strong, narrowed towards the rounded apex, and hook wide at the base with a weak notch distally (Figs. 104, 106, 108). The tube of the penis is 1.6 times the length of the sac and has a constriction before the sac; the sac is large, wider than the tube, and covered with a patch of coarse



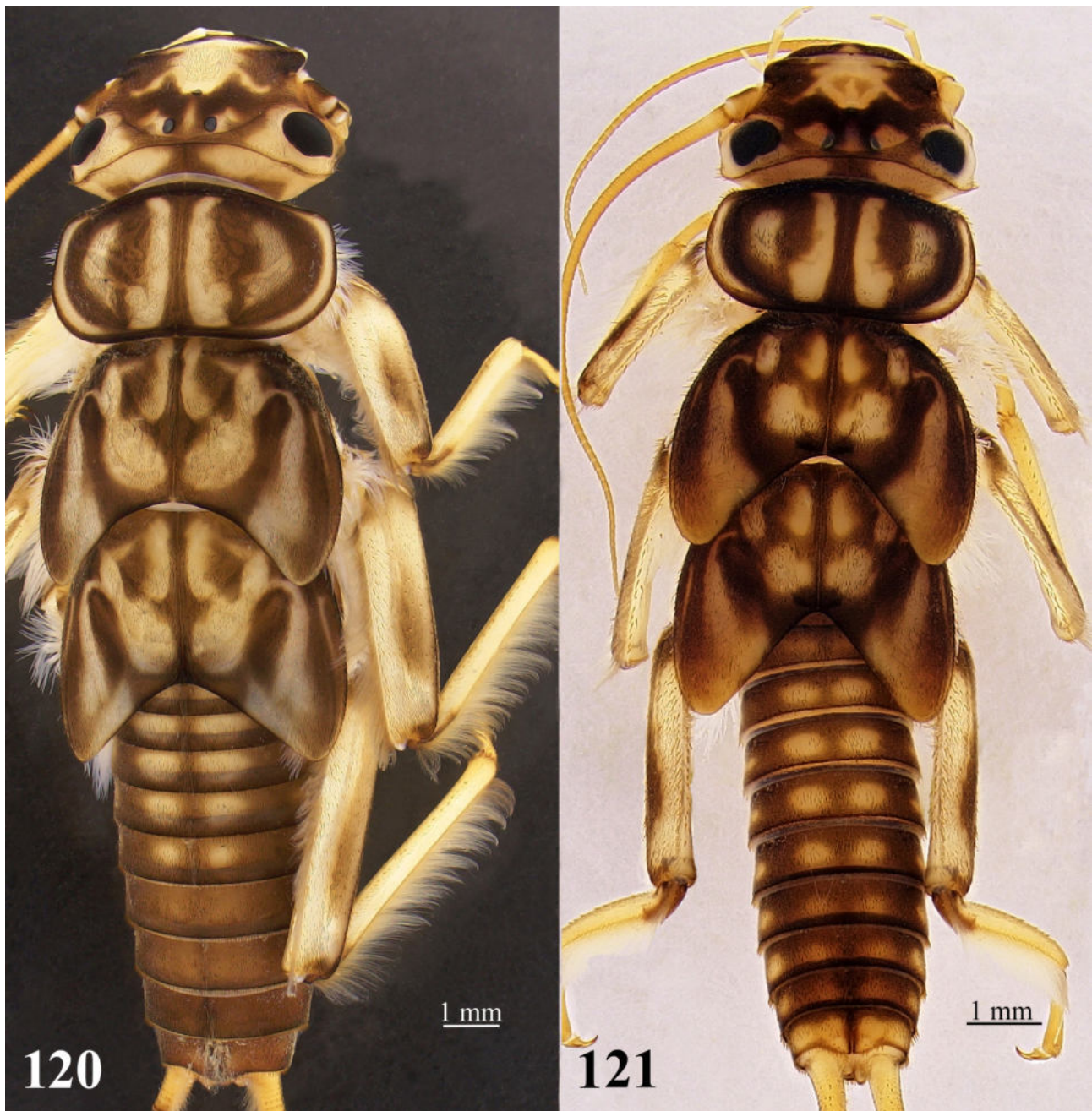
FIGURES 102–107. *Perla pallida* Guérin-Méneville, 1843. Caucasus, Russia, Krasnodar Kray, Papay River, Pshada River Basin; 3rd tributary Kutarka River, Sochi River Basin. 102. Male habitus, dorsal. 103. Male, head and pronotum, dorsal. 104. Male, hemitergal hook, lateral. 105. Female, head and pronotum, dorsolateral. 106. Male, abdominal tip, mesal plate and hemitergites, dorsal. 107. Female, abdominal tip, ventral.



FIGURES 108–111. *Perla pallida* Guérin-Méneville, 1843. Caucasus, Russia, Krasnodar Kray, 3rd tributary Kutarka River, Sochi River Basin. Male. 108. Abdominal tip, mesal plate, hemitergal hooks, and artificially everted penis, dorsal, cleared. 109. Penis, ventral. 110. Chaetotaxy of the penis, dorsal. 111. Chaetotaxy of the penis, ventral. A. Oval scales with small spines. B. Leaf-shaped scales with small spines. C. Densely arranged longitudinal rows of heavy sclerotized serrate sclerites. D. Pointed brown spines in the apical brush.

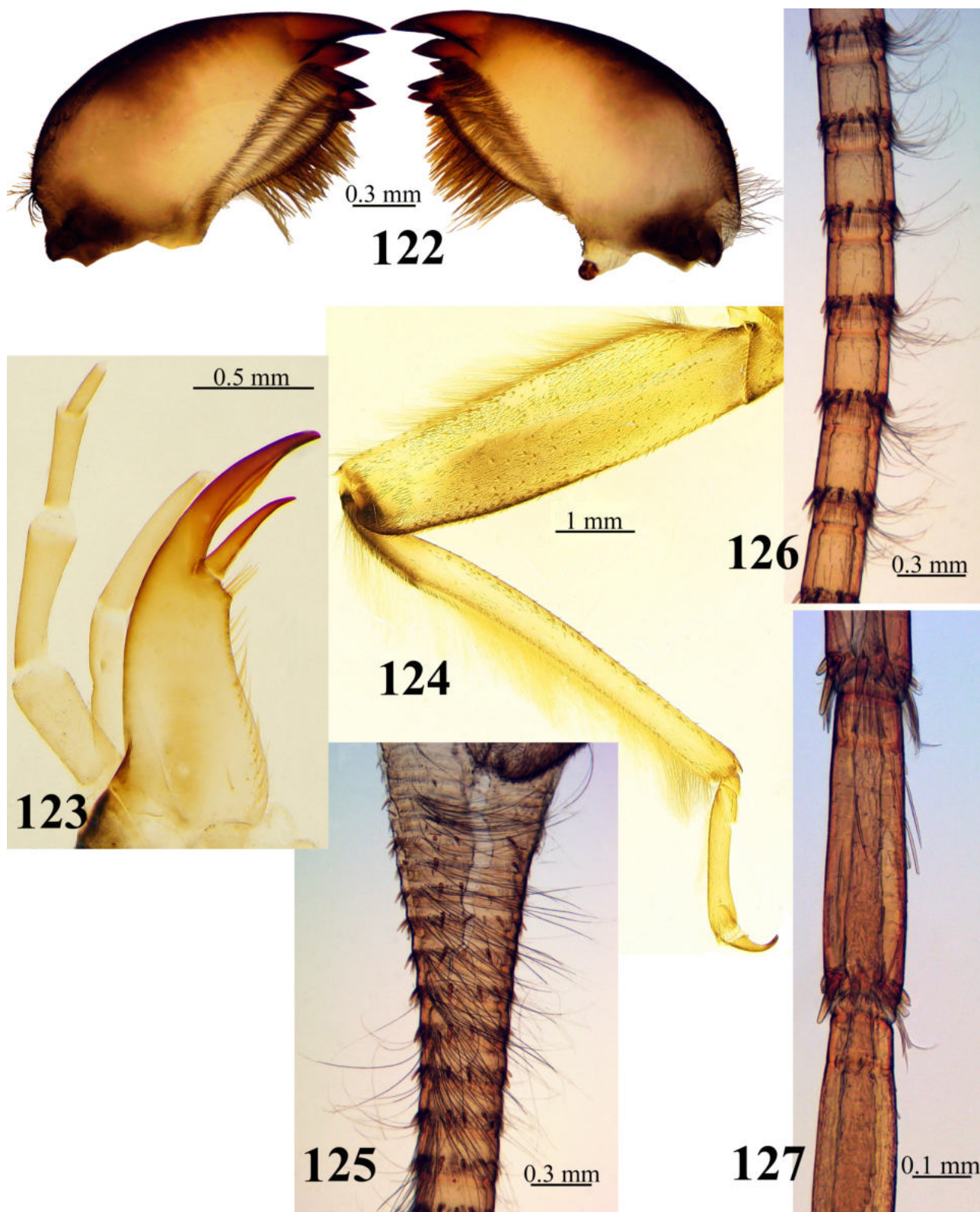


FIGURES 112–119. *Perla pallida* Guérin-Ménéville, 1843. Caucasus, Russia, Krasnodar Kray, 3rd tributary Kutarka River, Sochi River Basin; Republic of North Ossetia-Alania, Prigorodny District, Mairamadag River, Terek River Basin. Armenia, Syunik Marz, Tzav River. Egg. 112. Appearance with micropylar row, lateral. 113. Appearance with mushroom-shaped anchor plate and micropylar row, lateral. 114. Collar with flanged rim and raised ribs, lateral. 115. Collar, dorsal. 116. Collar with anchor, covered with globular bodies, flanged rim and raised ribs, lateral. 117–118. Chorion structure with micropylar row. 119. Chorion structure with follicle hexagonal cell impressions.



FIGURES 120–121. *Perla pallida* Guérin-Ménéville, 1843. Caucasus, Russia, Krasnodar Kray, 3rd tributary Kutarka River, Sochi River Basin; Republic of North Ossetia-Alania, Prigorodny District, Mairamadag River, Terek River Basin. Larva. 120. Habitus, female, dorsal. 121. Habitus, male, dorsal.

triangular spines, forming a wide, loose triangular apical brush; the spines of the brush along the lateral edges of the sac are absent; ventrally, the brush end is triangular; dorsally, the edge of the apical brush is semi-rounded (Figs. 108–111). Egg oval; collar with flanged rim that is incised and distinctly wider than the neck; the collar sides covered ribs; chorion smooth, covered with follicle hexagonal cell impressions, limiting at the corners by six tiny round punctuations and by six small, slit-shaped punctuations located between them; cells have boundaries, a central depression, and one pore on the floor; pore and hexagonal punctuation are different in size (Figs. 112–119). The micropylar orifices lack rims (Figs. 117–118). Head of larvae with a large trapezoidal pale spot expanding from the anterior ocellus to the labrum base; the lateral edges of the spot with two pair pointed projections; paired projections near the labrum wide; a thin pale M-line delimiting the spot from below; the epicranial sutures brown (Figs. 120–121). Anal gills are absent.



FIGURES 122–127. *Perla pallida* Guérin-Ménéville, 1843. Caucasus, Russia, Krasnodar Kray, 3rd tributary Kutarka River, Sochi River Basin; Republic of North Ossetia-Alania, Prigorodny District, Mairamadag River, Terek River Basin. Larva. 122. Left and right mandibles, ventral. 123. Left lacinia, galea, maxillary palpus, ventral. 124. Right hind leg, dorsal. 125–127. Chaetotaxy of the left cercus, lateral. 125. Basal cercal segments. 126. Middle cercal segments. 127. Apical cercal segments.

Complimentary description. The coloration, external structures of the male and female genitalia, eggs, and appearance of larva in our material generally correspond to existing descriptions of *P. pallida* (Guérin-Ménéville 1843; Pictet 1841; Klapálek 1923; Sivec & Stark 2002; Zhiltzova & Cherchesova 2003), although the resemblance with Carpathian populations is also noticeable (Kis 1974, Teslenko & Zhiltzova 2009, their figs. 314–318), with the exception of the distinctive features of the penis described below.

Adult habitus. The main body color is yellow-brown (Fig. 102). The head is mostly yellow; the M-line is yellow and moderately defined (Figs. 102, 105). The interocellar area bears a dark brown spot reaching the M-line and directed to compound eyes above yellow posterior tentorial pits; the posterior edge between the lateral ocelli with a solid pale line (Figs. 105). The female head is darker due to a larger dark brown spot in the interocellar area, with more distinct lateral edges approaching the M-line and the posterior tentorial pits closely but not going beyond them (Fig. 105). A triangular light brown spot, widening towards the anterior margin of the clypeus, is in front of the M-line and anterior ocellus; the antenna is brown (Figs. 102–103, 105). Occiput bears a wide, V-shaped brown spot in the area of the epicranial suture and stem, the spot is darker and more pronounced on females (Figs. 103, 105).

Pronotum is trapezoidal, narrowed, and rounded posteriorly (Figs. 102–103, 105). The anterior and posterior margins arched, the lateral margins straight, the anterior corners almost straight; yellow, with a narrow dark brown stripe along the anterior and posterior margins; the lateral margins with a relatively wide dark sinuous band sometimes the lateral edges bent down, and the dark band is not visible dorsally (Figs. 102–103, 105). The medial pronotal band is brown and relatively narrow, widening more anteriorly than posteriorly; lateral pronotal fields have dark, rounded, patches on which light rugosities are visible (Figs. 103, 105). Legs yellow; femur with a narrow longitudinal grayish band close to the outer edge and a narrow dark brown band distally; tibia with a short, narrow transverse brownish band in the basal third; tarsi brown apically (Fig. 102). The cerci are long, projecting far beyond the end of the wings; they are bicolored, with each segment yellowish at the base and brown distally. The wings are yellow with dark brown veins (Fig. 102).

Male. Tergum 8 medially with a membranous furrow narrowed posteriorly; posterolateral humps and posterior tergal margins covered with dense, relatively long setae (Fig. 106). Tergum 9 with a sclerotized mesal field; width is slightly greater than length; slightly expanded anteriorly and posteriorly; posterior margin with a small membranous notch in the middle (Figs. 106, 108). Longitudinal serrated ridges (10–12) cover the mesal field closer to the anterior and lateral margins; the posterior margin avoids serrated ridge rows (Figs. 106, 108). Hemitergites are strong and slightly narrowed towards the rounded apex (Figs. 104, 106, 108). In dorsal view, the hemitergal hook (not cleared) is wide at the base, with a weak notch on the inner edge in the distal 1/3 (Fig. 104); the top of the hook and inner edge are covered with sensilla basiconica (Figs. 104, 106, 108). The artificially everted penis carries a tube that is 1.6 times the length of the sac, a tube with a noticeable constriction in the distal third before the sac, covered dorsally with densely arranged longitudinal rows of serrate sclerites, changing into scales with small spines or without them (Figs. 108–111). The base of the tube is membranous, with paired patches of round spine bases laterally (Figs. 110–111). Ventrally, the tube is partly membranous and covered with rows of oval-elongated or polygonal sclerites with or without small spines, the same as on the dorsal surface (Figs. 111, A–C). The membranous sac is spherical and large; the sac width exceeds the tube width by 1/3; in dorsal view, the sac bears two rounded lobes at the base and a central tongue-shaped lobe narrowed to the sac base; ventrally, the sac bears two rounded lobes (Figs. 108–111). The apex of the sac is covered with a patch of rather coarse triangular brown spines, forming a relatively wide, loose apical brush, reaching almost to the middle of the tongue-shaped lobe (Figs. 108, 110–111, D); there are no spines along the lateral edges of the sac. Ventrally, the apical brush ends with a triangular protrusion; dorsally, the edge of the brush is semi-rounded (Figs. 108, 110–111). The configuration of the apical brush of the penis in the Caucasian population differs from the pattern of *P. pallida* from the Romanian Carpathians (Kis 1974, Teslenko & Zhiltzova 2009, their fig. 317), which is wide and covers the sac completely.

Female. The subgenital plate is typical of several *Perla* species, occupying $>1/2$ of sternum 8 width and has a small bilobed projection posteromedially. The lobes are small, pointed, and covered with reddish setae; the lateral edges of the lobes are slightly beveled; and the lobes slightly protrude beyond the anterior margin of the sternum 9 (Fig. 107).

Egg. Oval of medium size, with mean dimensions of $452 \times 300 \mu\text{m}$ ($n=8$) (Fig. 111). The anchor plate is mushroom-shaped and covered with globular bodies gathered in small groups (Figs. 113, 116). The collar has a flanged rim, which is incised and distinctly wider than the neck (Figs. 114–116). The sides of the collar have prominent, continuous ribs extending from the shoulders to the rim (Figs. 114, 116). The chorion surface is smooth

and pitted; the chorion is covered throughout with follicle hexagonal cell impressions, limiting at the corners by six tiny round punctuations and six small, slit-shaped punctuations located between them; cells are separated from adjacent ones by expressed boundaries; the cell floor has one pore, and the pore and hexagonal punctuations are different in size (Figs. 118–119). A central depression in the cell floor is well pronounced in eggs from the Armenian population (Figs. 113, 116–117). The ring of micropyles is located ca. 1/3 of the egg length removed from the anterior pole, the micropylar orifices without rims (Figs. 112–113, 117–118).

Larva. The appearance of the larva agrees well with the description by Zhiltzova & Cherchesova (2003). The body is brown with contrasting pale patterning, covered with short dark clothing hairs, and has a dorsomesal band of erect silky white setae that is more pronounced on the last abdominal terga (Figs. 120–121). The head is brown, bearing a large trapezoidal pale spot expanding from the anterior ocellus to the labrum base; the lateral edges of the spot with two pair pointed projections; paired projections near the labrum are wide; a thin pale M-line medially delimiting the spot from below; an interocellar area with a short slit-shaped pale spot between lateral ocelli; and the epicranial sutures are brown (Figs. 120–121). Mandible strongly sclerotized, outer edge rounded, base with tuft of thin setae at outer edge; mandibular teeth strongly pointed; left mandible with 5 teeth; right mandible with 6 teeth; the number and arrangement of rows of short setae on the molar areas of the left and right mandibles is the same as in other species (Fig. 122). Lacinia bidentate, teeth are pointed, terminal tooth strongly curved, subapical tooth less curved, and extending ca. 2/3 of terminal tooth length. Below the subapical tooth, there is a small downward-sloping projection with 3–4 submarginal setae (Fig. 123). The marginal fringe of setae along the inner lacinial margin is complete (Fig. 123). Abdomen brown, each tergum with two transverse pale spots on the sides of the medial line and paired small pale spots laterally; in the female larva, the spots on the last abdominal terga are faintly visible (Figs. 120–121). The anal gills are absent. The legs pale, the femur darkened basally and distally, with a dark spot in the distal half close to the outer edge; the tibia basally has a short brown band on the outer edge (Figs. 120–121, 124). The fine pilosity between dark short spines in the cercal circlet is the same as that of other *Perla* species (Figs. 125–127). A dorsal longitudinal fringe of swimming hairs is tightly pressed to the segments; the length and density of long silky hairs decrease towards the cercal apex (Figs. 125–127). On the middle and apical cercal segments, long and thin intercalary setae are visible; their length exceeds the length of fine circlet hairs (Figs. 126–127).

DNA barcoding. GenBank accession numbers are PP216457–PP216461. Sequences of *P. pallida* from the Caucasus showed deep COI divergence between populations from Macedonia (AEG1356), Croatia (AAL2357), Croatia (AEK2845), and Slovenia, Croatia (AEB9929), whose minimum p-distances were 8.1%, 4.8%, 4.7%, and 2.8%, respectively (Table 2). However, the phylogenetic analysis showed that this species is polyphyletic (Fig. 160). In addition, *P. pallida* under BINs AAL2357 and AEB9929 cannot be distinguished using COI barcodes due to other species related to these BINs. Considering that *P. pallida* was originally described from the Caucasus, this casts doubt on the validity of European populations.

Material examined. Caucasus, Russia, Republic North Ossetia-Alania: 1 larva, Prigorodny District, Mairamadag River, Terek River Basin, altitude 690 m above sea level, 42.993308 N, 44.49815 E, 17.07.2021, coll. D. Palatov; 1♂, Alagirsky District, Komdon River near Upper Tsey village, Terek River Basin, altitude 1832 m above sea level, 42.803514 N, 43.933395 E, 25.07.2021, coll. D. Palatov; Krasnodar Kray: 2♂, Gelendzhik, Papay River, 2.5 km below Novosadovyy farm, Pshada River Basin, altitude 195 m above sea level, 44.569305 N, 38.42889 E, 8.06.2021, coll. D. Palatov; 6♂, 1♀, 3 larvae, District of the Sochi City, Plastunka village, 3rd tributary of the Kutarka River, Sochi River Basin, altitude 143 m above sea level 43.672794 N, 39.772125 E, 21.07.2022, coll. D. Palatov.

Additional material. Armenia, Syunik marz: 4♂, 1♀, Tzav River, about 3 km above the village Tzav, before the fork in the valley, altitude 2500 m above sea level, 39.316400 N 46.251943 E, 20.07.2014, coll. D. Palatov.

Distribution. Widespread in the Caucasus: Russia, North Ossetia-Alania, Krasnodar Kray; Armenia, Georgia, Azerbaijan, Turkey (Anatolia) (Zhiltzova 1956; Zwick 1975; Sivec & Stark 2002; Darilmaz *et al.* 2016; Murányi *et al.* 2021).

Perla palatovi sp. nov. Teslenko & Semchenko

Figs. 128–156

Diagnosis. Tergum 9 of males is distinguished by the arrangement of serrated ridges on the mesal field that are relatively short and do not reach the posterior margin (Figs. 133, 137). The hemitergal hooks are strong, with a weak

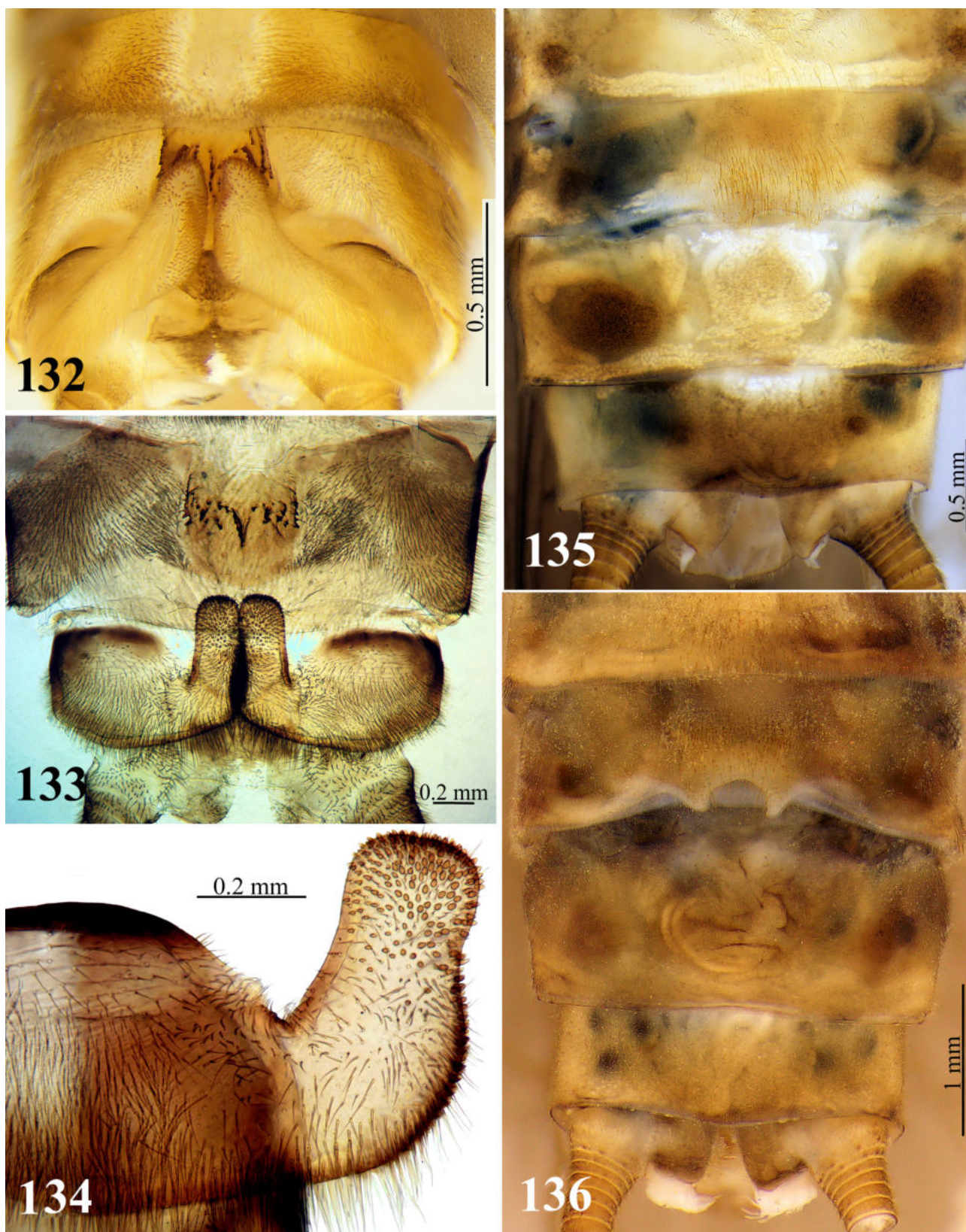
notch in the apical third along the inner edge; the apex is rectangular and rounded (Figs. 132–133, 137). The tube of the penis is 1.8 times longer than the sac. The membranous sac is rough, covered with tufts of tiny setae associated with patches, and arranged in concentric lines following the shape of the lobes (Figs. 139–140, B, D). The apical brush is narrow and pointed ventrally (Figs. 138, 140, D). The egg has a short, slightly ribbed collar (Fig. 144). The chorion surface is rough and pitted with follicle hexagonal cell impressions, weakly separated from each other; the cell floor is without a central depression; and the number of central pores ranges from one to four (Fig. 146). Micropylar orifices lack rims (Fig. 147). The larva is distinguished by pale bands along the lateral margins of the pronotum; the width of the pale bands is wider than the semi-oval dark band; a paired dark S-shaped spot extends from the anterior margin to the middle of the pronotum (Figs. 148–149).

Adult habitus. Body length: males 13.0–14.0 mm (n=6), females 17.3–22.7 mm (n=7); length of forewing: males 12.8–13.7 mm; females 17.4–20.5 mm; wingspan: males 27.4–29.3 mm; females 37.5–43.5 mm. Head and pronotum are dorsally grayish-yellow with dark brown spots; mesonotum and metanotum are dark brown, especially in females; the three small, pale spots on the prescutum and scutum form a triangle; the abdomen is grayish-yellow (Figs. 128–129). The wings are yellowish with dark brown veins (Figs. 128–129). Antennae and palpi are yellow-grey. The M-line on the head is brownish, connected with a triangular brownish spot on the clypeus; the anterior margin and lateral edges of the clypeus are dark brown, clearly contrasting with a pair of transverse small oval pale spots between the clypeal edges and the triangular spot on the clypeus (Figs. 128–131). Frontal tentorial pits are brownish (Fig. 130). The interocellar area has an X-shaped dark brown spot; the upper branches reach the base of the M-line; the lower branches attain the lateral ocelli; and between the lateral ocelli is a triangular yellowish blurred spot limited basally by a brown stripe of the epicranial suture (Figs. 130–131). A pair of drop-shaped, bright yellow spots are located between the posterior ocelli and the compound eyes; the tentorial pits are brownish (Fig. 131). The posterior occipital fold is indicated by a thin light stripe, limited above and below by a narrow-darkened band interrupted in the area of the epicranial stem; the epicranial stem darkened (Figs. 130–131). A pair of transversely oblique dark bands extends from the base of the occiput to the posterior edge of the compound eyes. Pronotum as wide as head with eyes, slightly narrowing posteriorly, posterolateral margins rounded; anterior margin arcuate, darkened; medial stripe dark brown, widened to anterior and posterior margins, wider at the anterior margin than at the posterior one; pronotal posterior margin darkened; lateral pronotal margins bordered by a dark brown stripe, widening posterolaterally; sometimes the lateral edges are bent down and not visible dorsally (Figs. 117–118). Pronotal rugosities are grayish-yellow, darkly contoured, and form an X-shaped pattern (Figs. 130–131); in the posterior third, dark rugosities in the form of narrow paired transverse short stripes reach the lateral pronotal margins (Figs. 130–131). The legs and cerci are grayish-brown. Femur with a dark spot basally and a narrow light stripe dorsally; the distal part darkened; tibia darkened at base with a narrow brownish band in the basal $\frac{1}{5}$ (Figs. 115–117); cowl also darkened. Anal gills are very small, noticeable in newly molted specimens. Cerci are bicolored, each segment with a narrow yellowish ring basally and a thick grayish-yellow band apically (Fig. 128).

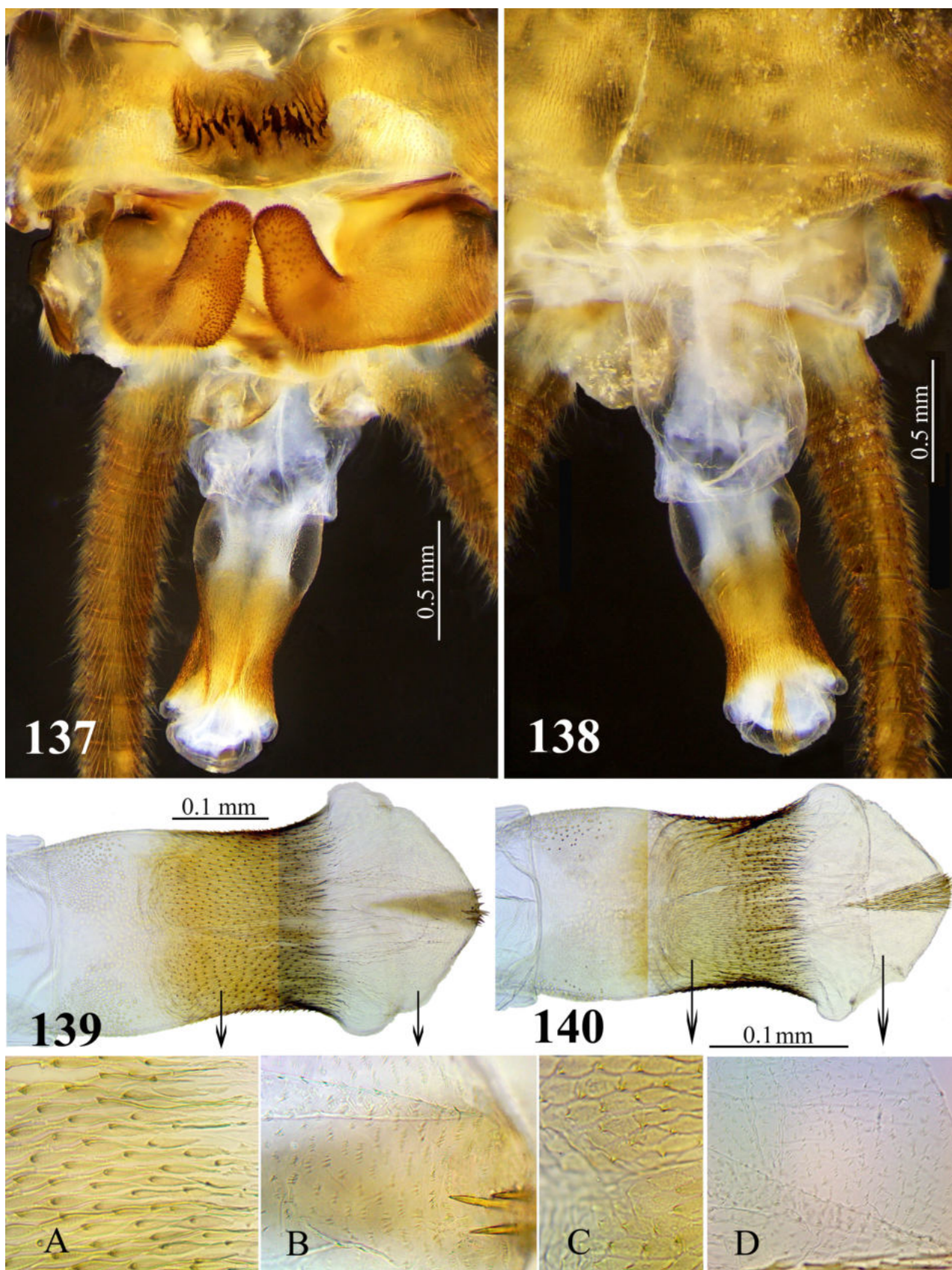
Male. Tergum 8 is medially depressed with a central membranous furrow; posterolateral humps are covered with dense and thick setae; along the posterior margin of the furrow, setae are short and sparse (Fig. 132). Tergum 9 has a sclerotized mesal field; the width is slightly greater than or equal to the length (Figs. 132–133, 137). The mesal field bears sharp, heavy sclerotized teeth that merge into long and short longitudinal serrated ridges (8–14), located in the middle of the mesal field, and do not reach the posterior margin (Figs. 133, 137). Tergum 10 has strong hemitergal hooks (cleared) with a weak notch in the distal third of the inner edge laterally (Figs. 134, 137); in dorsal view, the notch on the hook corresponds to a shallow depression in the side (Fig. 132). The apex of the hook is rectangular and rounded (Fig. 134); in its natural state, dorsally, the tip is slightly slanted (Fig. 132). Sensilla basiconica covers the inner side of the hook from top to outer edge; the base of the hook is rounded and covered with long setae (Figs. 132–134, 137). The artificially everted penis has a tube that is 1.8 times the length of the sac; the dorsal tube is covered with densely arranged longitudinal rows of serrate sclerites, sometimes with small spines; the shape of sclerites in different parts of the tube varies from polygonal to oval elongated; the tube is membranous basally with paired patches of rounded spine bases laterally (Figs. 137–140, A, C). The sac is bulbous and membranous at the base, with two lateral lobes and folds that increase its width (Figs. 139–140); thin pointed brown spines are present, forming a relatively narrow apical brush that is pointed ventrally (Figs. 139–140, B). The membranous sac is rough and covered with tufts of tiny setae arranged in concentric lines following the shape of the lobes (Figs. 139–140, B, D).



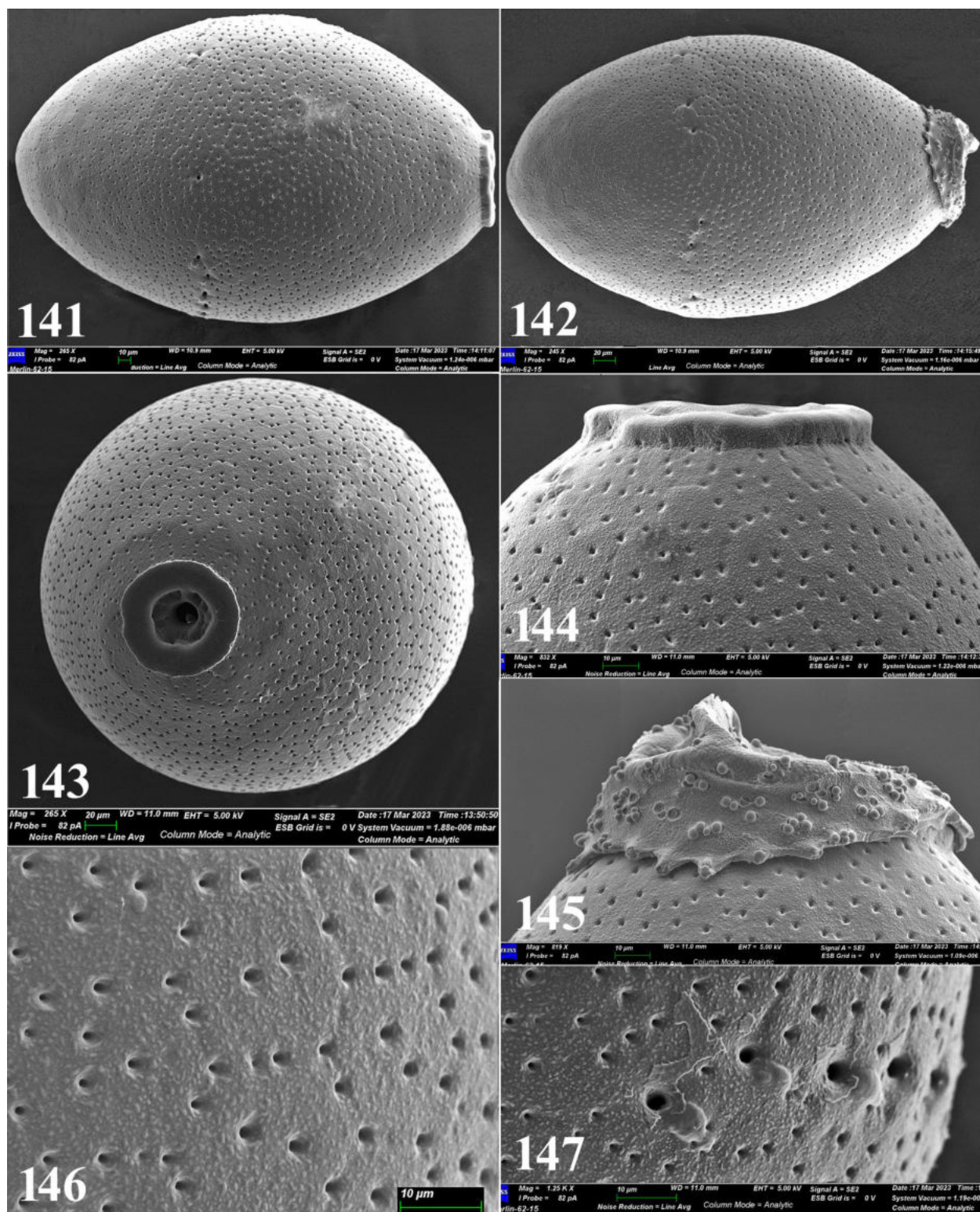
FIGURES 128–131. *Perla palatovi* **sp. nov.** Caucasus, Russia, Krasnodar Kray, Gelendzhik District, Papay River, Pshada River Basin. 128. Paratype. Female habitus, dorsal. 129. Holotype. Male, habitus, dorsal. 130. Holotype, male, head and pronotum, dorsal. 131. Paratype, female, head and pronotum, dorsal.



FIGURES 132–136. *Perla palatovi* sp. nov. Caucasus, Russia, Krasnodar Kray, Gelendzhik District, Papay River, Pshada River Basin; Tuapse District, Shapsukho River. 132. Male, abdominal tip, dorsal. 133. Male, abdominal tip, dorsal, cleared. 134. Male, hemitergal hook, lateral, cleared. 135–136. Female abdominal tip, variations in color.



FIGURES 137–140. *Perla palatovi* **sp. nov.** Caucasus, Russia, Krasnodar Kray, Gelendzhik District, Papay River, Pshada River Basin. Male. 137. Abdominal tip, mesal plate, hemitergal hooks, and artificially everted penis, dorsal, cleared. 138. Penis, ventral. 139. Chaetotaxy of the penis, dorsal. 140. Chaetotaxy of the penis, ventral. A. Leaf-shaped scales with small spines. B, D. Tufts of tiny setae arranged in concentric lines, following the shape of the lobes. C. Oval scales with small spines.



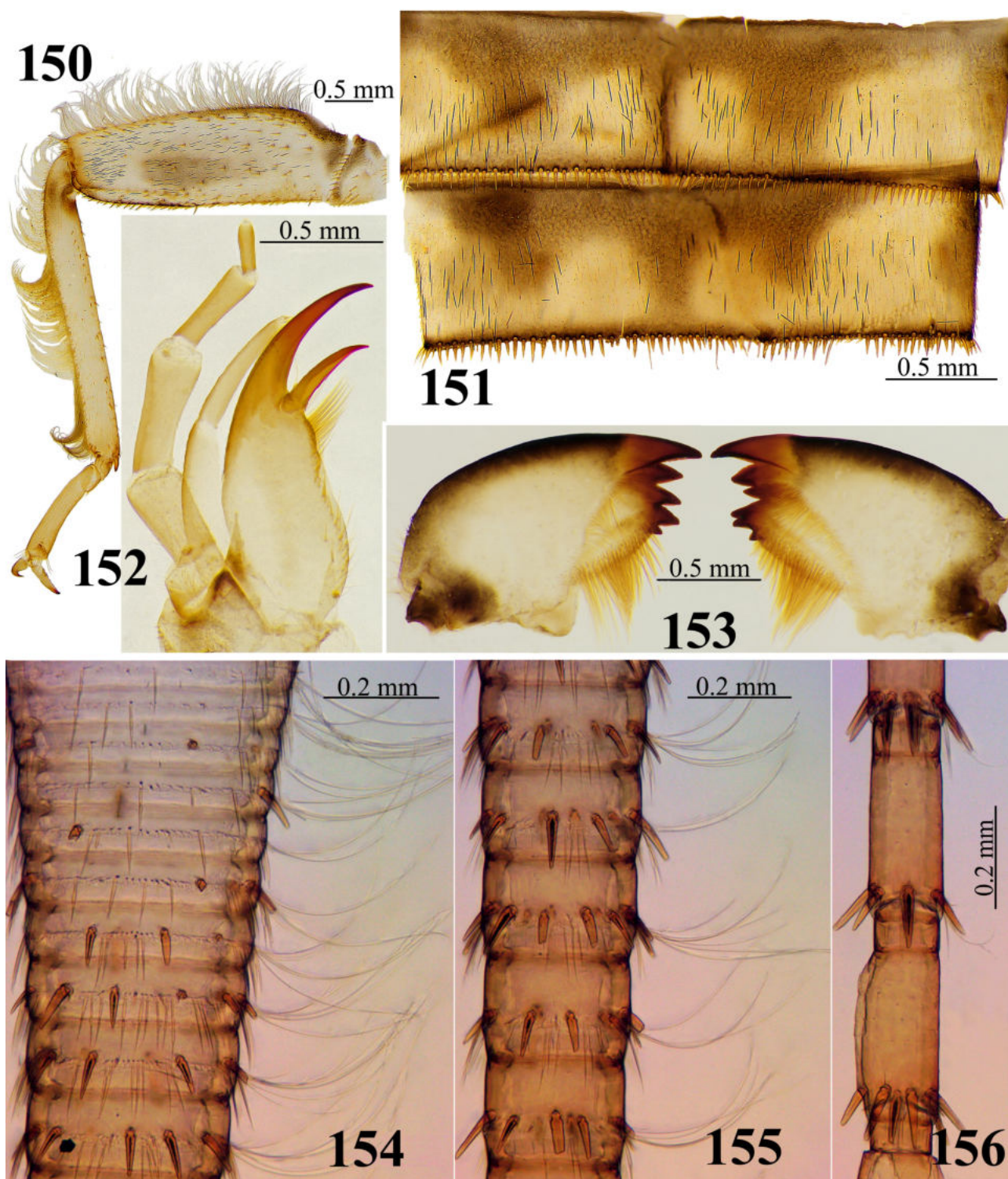
FIGURES 141–147. *Perla palatovi* sp. nov. Caucasus, Russia, Krasnodar Kray, Gelendzhik District, Papay River, Pshada River Basin. Egg. 141. Appearance without mushroom-shaped anchor plate, micropylar row, lateral. 142. Appearance with mushroom-shaped anchor plate, micropylar row, lateral. 143. Appearance, dorsolateral. 144. Collar with weakly ribbed rim, lateral. 145. Mushroom-shaped anchor with globular bodies concentrated in groups, lateral. 146. Chorion structure with follicle hexagonal cell impressions, the cell floor without a central depression with one or four pores. 147. Chorion structure with micropylar row, the micropylar orifices without rims.



FIGURES 148–149. *Perla palatovi* sp. nov. Caucasus, Russia, Krasnodar Kray, Gelendzhik District, Papay River, Pshada River Basin; Tuapse District, Shapsukho River. Larva, males, habitus, dorsal. Variation of the pattern.

Female. Sternum 8 has a subgenital plate, occupying almost half of the sternum width, with two small triangular lobes posteromedially. The lobes projecting slightly beyond the anterior margin of sternum 9 are covered with rufous setae (Figs. 135–136).

Egg. Elongate and oval, with mean dimensions of $435 \times 272 \mu\text{m}$ ($n = 6$), with a short collar with the same diameter at the rim and the base; the rim is weakly ribbed (Figs. 141–144). The neck is not constricted. A mushroom-shaped anchor plate is present on some eggs and covered with globular bodies concentrated in small groups (Figs. 142, 145). The chorion surface is rough and pitted; the chorion is covered throughout with follicle hexagonal cell impressions; hexagonal cells with differences in cell widths; cells separated from adjacent ones by poorly expressed boundaries; the cell floor without a central depression with one or four pores (Figs. 144, 146). A ring of micropyles is located ca. $1/3$ of the egg length from the anterior pole, the micropylar orifices are without rims (Figs. 141–142, 147).



FIGURES 150–156. *Perla palatovi* sp. nov. Caucasus, Russia, Krasnodar Kray, Gelendzhik District, Papay River, Pshada River Basin; Tuapse District, Shapsukho River. Larva. 150. Right middle leg, dorsal. 151. Chaetotaxy of abdominal terga 7 and 8, dorsal, cleared. 152. Left lacinia, galea, maxillary palpus, ventral. 153. Left and right mandibles, ventral. 154–156. Chaetotaxy of the right cercus, lateral. 154. Basal cercal segments. 155. Middle cercal segments. 156. Apical cercal segments.

Larva. Mature males of medium size, length 12.2–12.4 mm (n=3), antennae 9.5 mm, and cerci greater than 8.8 mm contain more than 36 segments. The color is generally pale, yellow-brown in dorsal view (Figs. 148–149), with a distinct dark pattern on the head, pronotum, mesonotum, and metanotum, but with a less distinct pattern

on the abdomen. The ventral body side is yellow-brownish. Body covered with short dark clothing hairs, with a dorsomesal band of erect silky white setae more pronounced on the last abdominal terga (Figs. 148–149). Antennae and cerci are yellow-brown. Clypeus on head basally with paired dark and wide V-shaped spots, outlining branches of yellow M-line from above. Head with a large transverse dark spot, vaguely resembling a pilot's badge with truncated “wings” not extending beyond epicranial arms; the spot limits the pale M-line from below extending from the anterior ocellus to the posterior ocelli; a small triangular spot between the ocelli darkened; epicranial stem and occiput edge also darkened (Figs. 148–149). The occipital ridge is distinct and complete; short spines are arranged in the medial part of the fold; along the postocular crest, spines are noticeably longer and pointed. Mandibles (Fig. 153) are typical for *Perla*: heavily sclerotized, with a rounded outer margin; left mandible with five pointed teeth and two medial rows of setae on the molar area; the marginal row of setae extends from the base of the 4th tooth to the basal third of the mandible; right mandible with six pointed teeth; single medial setal row extends from the base of the first tooth to the base of the mandible; the configuration of the marginal setal row is the same as that of the left mandible. Lacinia bidentate with a large, heavily sclerotized, and strongly curved apical tooth (Fig. 152). The subapical tooth is shorter; the length does not exceed 2/3 of the apical tooth length. The marginal fringe of setae along the inner margin is complete; a tuft of long and dense setae of marginal fringe is clearly visible below the subapical tooth. Galea length reaches 1/2 of subapical tooth length (Fig. 152).

Pronotum transverse, not wider than the head, with obtusely rounded anterior corners; lateral margins and posterior angles are evenly rounded (Figs. 148–149). The pronotal fringe is complete with mixed short and relatively long setae. The pronotum has a thin brown stripe along the edge; paired semi-oval pale bands outline a full (or incomplete, open anterolaterally) oval brown band on the lateral pronotal fields (Figs. 148–149). An oval brown band is narrower than semi-oval pale bands, especially in the anterior 1/3. The central pronotal field is yellow with a brown median band narrowed anteriorly and markedly widened posteriorly; a paired vague S-shaped dark spot extends from the anterior margin to the middle of the pronotum (Figs. 148–149). Mesonotum and metanotum with an identical Ψ-shaped dark pattern medially, posterior margin darkly margined; two wide dark bands limiting the wing pads; a narrow dark stripe runs along the lateral edge of the wing pads. Legs are yellow and covered with dark closing hairs (Figs. 148–149). The femur and tibia bear stout, short, acute bristles along the inner and outer edges and a very dense fringe of long, silky hairs along the outer margins (Fig. 150). The femur is covered with sparse, short, and irregular red bristles; in the distal half closer to the outer edge, with a darkened small and almost oval spot, the distal edge of the femur is also darkened (Fig. 150). Hind femur ca. 3.3–3.6 times as long as wide. Tibia has a diffuse, narrow brownish band basally. The pattern on the abdomen is indistinct; the dark closing hairs are well-marked; the terga are mainly yellowish with a dark median and two lateral longitudinal bands; the lateral dark bands on terga 4–10 are triangular, extending to the anterior margin (Figs. 148–149). The posterior terga margins bear acute bristles that are mostly short, with one or two relatively long setae (Fig. 151). Anal gills are small (Figs. 148–149). Cerci are yellow, and no less than 36 segmented with striking rings of dark spines (Figs. 148–149). Fine pilosity between dark spines is tightly pressed to the segment surface (Figs. 154–156); short fine hairs have the same length as the length of the basal cercal segment; towards the middle of the cerci, fine pilosity length decreases; and on the apical cercal segments, the length of the fine pilosity is slightly >1/3 of the segment length (Fig. 156). Long silky fine colorless hairs are included in the circlet in tufts (no more than 8 in each) and form a dorsal longitudinal fringe, especially on the basal segments (Fig. 154); the length and density of long silky hairs also decrease towards the apex (Figs. 155–156).

DNA barcoding. GenBank accession numbers are PP216454–PP216456 and PP236723.

Material examined. Holotype male (FSC EATB FEB RAS). Caucasus. Russia, Krasnodar Kray: Gelendzhik District, Papay River, 2.5 km below Novosadovy farm, Pshada River Basin, collected by a light trap, 44.569305 N, 38.42889 E, 08.06.2021, coll. D. Palatov; Paratypes: 3♂, 5♀, 2 larvae (FSC EATB FEB RAS), same place and data; 2♂, 2♀, 1 larva, 3 exuvia, Tuapse District, Shapsukho River, downstream, 3 km from the confluence with the Black Sea, near Tenginka village, altitude 22 m above sea level, 44.337647, N 38.786211 E, 22.06.2022, coll. D. Palatov.

Distribution. North Caucasus. North-eastern coast of the Black Sea. Russia. Krasnodar Kray. Gelendzhik and Tuapse Districts. The species was found in small foothill rivers along the Black Sea coast (Figs. 157–158), flowing through low-mountain forest valleys 10–12 m wide with a pebble and rocky bottom and a current up to 0.7 m/s.

Etymology. The species is named in honor of Dr. Dmitry M. Palatov, who collected type material for a new species in the Caucasus as well as other very interesting stonefly material in the Caucasus, Central Asia, and the Middle East.

Remarks. *Perla palatovi* **sp. nov.** bears some similarity to the *P. pallida* species complex. The most noticeable resemblance between the eggs of *P. palatovi* **sp. nov.** was observed with Type 2 and Type 3 in the shape of the collar (Sivec & Stark 2002). The collar is short, with the same diameter at the rim and base; the neck is not constricted but slightly ribbed. The main differences between *P. palatovi* **sp. nov.** and any type of egg consist of punctured hexagonal chorion cells, the boundaries between which are poorly expressed. The *P. palatovi* **sp. nov.** hexagonal floors lack depressions and have four pores; the pores and punctuation of the hexagonal floors are uniform. The larvae of *P. palatovi* **sp. nov.** are very similar to the patterning of *P. caucasica* larvae described by Zhiltzova & Cherchesova (2003). There are differences in the dark closing hairs, which are denser and more pronounced in *P. caucasica*; in *P. palatovi* **sp. nov.**, the pronotal and especially abdominal patterns are lighter and less distinct. For the pronotum of *P. palatovi* **sp. nov.** larvae, the width of the oval dark bands is narrower than the width of the semi-oval pale bands, and vice versa in *P. caucasica*, where a paired S-shaped dark spot extends from the anterior margin to the middle of the pronotum. On *P. caucasica*, the S-shaped dark spot sometimes continues to the posterior margin. The darkish spot on the *P. palatovi* **sp. nov.** femur is fuzzy, small, and almost oval.

Key to Caucasian *Perla* species based on male penial setae patterns

- 1 Sac of the penis dorsomedial bears a tongue-shaped lobe covered with a relatively wide apical brush; the spines of the brush along the lateral edges of the sac are absent (Figs. 77–79, 108–111)2
- Sac bears a narrow apical brush (Figs. 9–10).3
- 2 Tube of the penis with constriction in the distal 1/3 before the sac; the sac is large, 1/3 wider than the tube, and covered with a loose triangular apical brush (Figs. 108–111). North Caucasus. Russia, Krasnodar Kray. Armenia, Georgia, Azerbaijan, and Turkey. Up to 2000 m. Adult presence: May–August *P. pallida* Guérin-Méneville, 1843
- Tube of the penis without constriction; the sac width is the same as the tube width; ventrally, the sac is deeply depressed (Figs. 77–79). Russia, Krasnodar Kray the Black Sea coast of the Caucasus from Tuapse to Sochi. Up to 200 m. Adult presence: July *Perla schapsugica* **sp. nov.**
- 3 Sac is membranous, without tiny setae (Figs. 34–35) 4
- Sac is membranous and covered with tiny setae (Figs. 139–140, B, D).....5
- 4 Sac bears a narrow apical brush; additional ventral brush is absent (Figs. 33–35). Caucasus. Russia, North Ossetia-Alania. Iran, Alborz Mountains. 1770–1900 m. Adult presence: June–July. *P. persica* Zwick, 1975
- Sac bears a narrow apical brush and an additional small ventral brush (Figs. 10, C). North Caucasus. Russia: Adygea, Karachay-Cherkessia, North Ossetia-Alania, Krasnodar Kray. Abkhazia. Georgia. Adult presence: late May–August. *P. caucasica* Guérin-Méneville, 1843
- 5 Sac covered with tufts of tiny setae associated with patches and arranged in concentric lines, following the shape of the lobes (Figs. 139–140, B, D). North Caucasus. Russia, Krasnodar Kray. Up to 1800 m. Adult presence: June *Perla palatovi* **sp. nov.**
- Sac covered with dense, tiny setae spaced relatively evenly (Figs. 58, D). Armenia, Azerbaijan. 1400–1850 m. Adult presence: latter half of May–first half of July *P. kiritshenkoi* Zhiltzova, 1961

Results of DNA barcoding

In this study, 18 barcodes of cytochrome oxidase subunit I (658 bp in length) of *Perla* were obtained: *P. pallida* (5), *P. caucasica* (4), *P. palatovi* **sp. nov.** (4), *P. persica* (4), and *P. schapsugica* **sp. nov.** (1) (Table 1–2). Within this dataset, there were 175 variable sites and 146 parsimony-informative sites; most mutations were synonymous transitions. Sequences were successfully translated into amino acids without stop codons or indels. Intraspecific sequence divergence within this species did not exceed 1% (Table 2).

The mean maximum intraspecific p-distance distribution of the whole data set was 0.9% and did not overlap with distances between distinct BINs except pair *P. caucasica* + *P. persica* (see below). The minimum interspecific p-distance between DNA barcodes of the whole data set in *Perla*, including those obtained from BOLD, was 13.0% (range: 0.0–20.1%). There was no divergence between some specimens of *P. caucasica* and *P. persica*. In contrast, *P. palatovi* **sp. nov.**, *P. schapsugica* **sp. nov.**, and *P. caucasica* + *P. persica* differed from each other and from other DNA barcodes by >12.2%, whereas there was only a modest genetic distance between *P. pallida* and four BINs that were either exclusively *P. pallida* or included *P. pallida* (AEB9929: 2.8%, AEK2845: 4.7%, AAL2357: 4.8%, and AEG1356: 8.1%). The mean minimum interspecific divergence of the remaining sequences was 0.2 – 20.1% (11.3% on average).



FIGURES 157–158. *Perla palatovi* **sp. nov.** Caucasus, Russia, Krasnodar Kray. Type habitat. Gelendzhik District, Papay River, Pshada River Basin.



FIGURE 159. The map of the *Perla* species distribution in Caucasus according to our data. *Perla caucasica*—pink, *P. persica*—green, *P. kiritshenkoi*—blue, *P. schapsugica* **sp. nov.**—white, *P. pallida*—yellow, and *P. palatovi* **sp. nov.**—red.

The Bayesian inference phylogeny using a third dataset (see Material and Methods) and *Kamimuria coreana* as the outgroup revealed four main clades (Fig. 160). The first high-supported clade (Bayesian Posterior Probability, BPP = 1) included four BINs that belonged to *P. marginata* (AAL2358), *P. grandis* (AAL2358 and AFF2910), and

Perla bipunctata Pictet, 1833 (AEG1053). The second clade (BPP = 0.98) united *P. caucasica*, *P. persica*, and *P. schapsugica* **sp. nov.**, while *P. palatovi* **sp. nov.** formed a third clade (BPP = 1), whereas the fourth clade (BPP = 1) united probably conspecific *P. carantana* and *P. abdominalis* (AAN1933), various sequences of *P. pallida* from central Europe, and closely related species *P. marginata*, *P. illiesi* Braasch & Joost, 1973, *P. madritensis* Rambur, 1842, *P. grandis*, and two undescribed species. Thus, the Bayesian tree supports the monophyly of two described species: *Perla schapsugica* **sp. nov.** and *P. palatovi* **sp. nov.**, as well as *P. caucasica*, *P. persica*, and *P. pallida* from the Caucasus. However, *P. caucasica* and *P. persica* were not monophyletic; the branch lengths between them were quite low, consistent with the low genetic distances and results of the three algorithms of species delimitation. At the same time, *P. abdominalis*, *P. grandis*, *P. marginata*, and *P. pallida* were assigned to several BINs, appearing paraphyletic in the BI analysis.

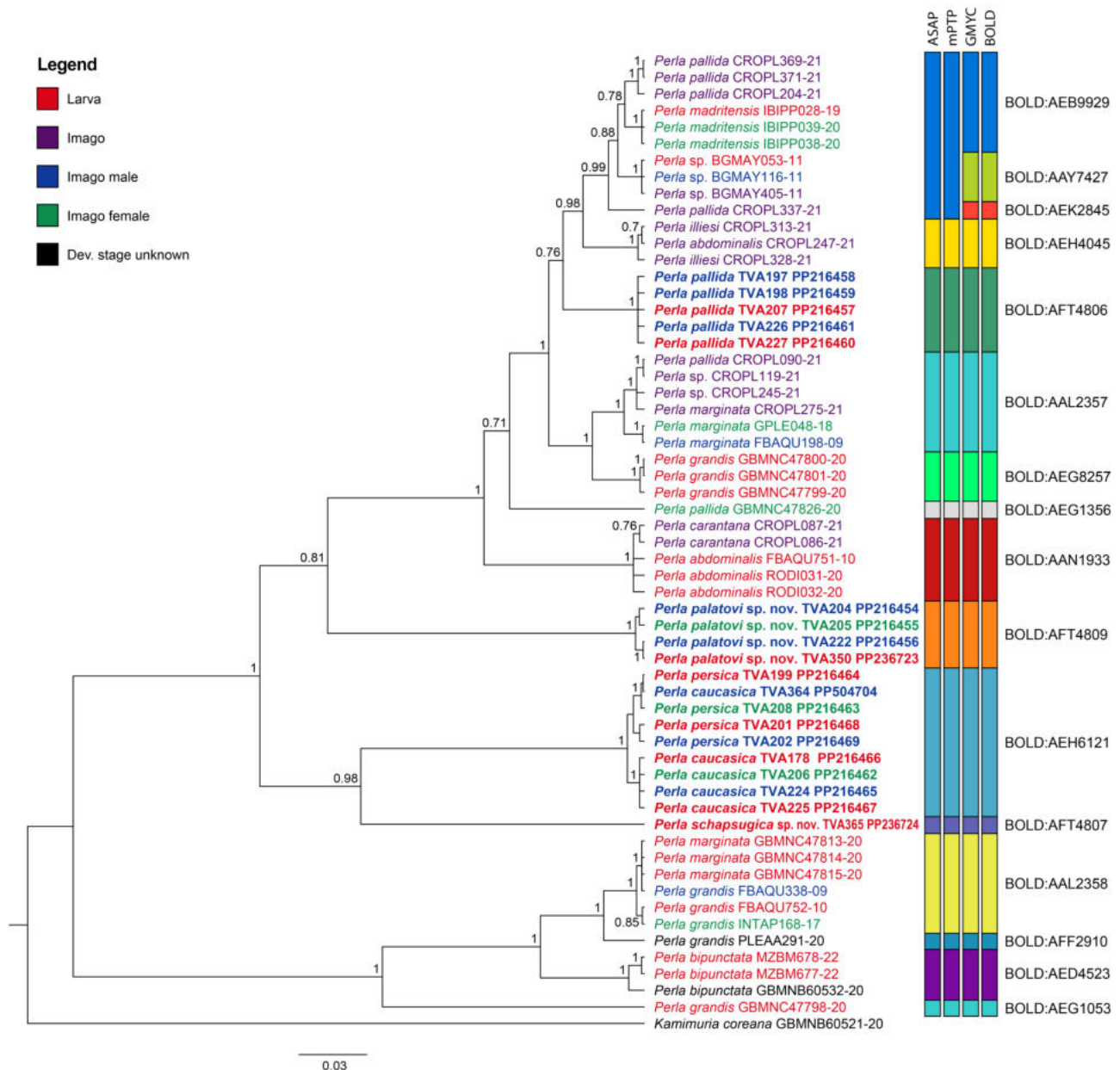


FIGURE 160. Ultrametric Bayesian inference (BI) tree inferred from the cytochrome *c* oxidase I (COI) gene fragment and the results of species delineation of the genus *Perla* Geoffroy, 1762, and out-group *Kamimuria coreana*. Bayesian posterior probabilities (> 0.7) are noted above the tree nodes. Vertical bars correspond to molecular operational taxonomic units by ASAP, mPTP, GMYC, and BINs of BOLD. The color of the specimens indicates the development stage of stoneflies in accordance with the legend, while the sequences obtained in this study are in bold.

TABLE 1. List of taxa, isolate numbers, sex, locations, and GenBank accession numbers.

Species	Isolate	Sex	Country	Coordinates	Accession
<i>P. caucasica</i>	TVA178	Larva	Caucasus, Russia: Krasnodar Kray, District of the City of Sochi, Estosadok, Mzymta River	43.67001 N 40.31990 E	PP216466
<i>P. caucasica</i>	TVA206	Female	Caucasus, Russia: Republic of North Ossetia-Alania, Prigorodny District, Mairamadag River, Terek River Basin	42.99331 N 44.49815 E	PP216462
<i>P. caucasica</i>	TVA224	Male	Caucasus, Georgia: Sukhum District, Kelasuri River	42.97204 N 41.06739 E	PP216465
<i>P. caucasica</i>	TVA225	Larva	Caucasus, Georgia: Sukhum District, Kelasuri River	42.97204 N 41.06739 E	PP216467
<i>P. caucasica</i>	TVA364	Male	Caucasus, Russia, Republic Adygea, Maikop District, Belaya River	43.99514 N 40.13547 E	PP504704
<i>P. palatovi</i> sp. nov.	TVA204	Male	Caucasus, Russia: Krasnodar Kray, Gelendzhik District, Papay River, 2.5 km below Novosadovy farm, Pshada River Basin	44.56931 N 38.42889 E	PP216454
<i>P. palatovi</i> sp. nov.	TVA205	Female	Caucasus, Russia: Krasnodar Kray, Gelendzhik District, Papay River, 2.5 km below Novosadovy farm, Pshada River Basin	44.56931 N 38.42889 E	PP216455
<i>P. palatovi</i> sp. nov.	TVA222	Male	Caucasus, Russia: Krasnodar Kray, Tuapse District, Tenginka village, Shapsukho River	44.33765 N 38.78621 E	PP216456
<i>P. palatovi</i> sp. nov.	TVA350	Larva	Caucasus, Russia: Krasnodar Kray, Tuapse District, Shapsukho River, near Tenginka village	44.33765 N 38.78621 E	PP236723
<i>P. pallida</i>	TVA197	Male	Caucasus, Russia: Krasnodar Kray, Gelendzhik, Papay River, 2.5 km below Novosadovy farm Pshada River Basin	44.56931 N 38.42889 E	PP216458
<i>P. pallida</i>	TVA198	Male	Caucasus, Russia: Republic of North Ossetia-Alania, Alagirsky District, Komdon River near Verhny Tsey village, Terek River Basin	42.80351 N 43.93340 E	PP216459
<i>P. pallida</i>	TVA207	Larva	Caucasus, Russia: Republic of North Ossetia-Alania, Prigorodny District, Mairamadag River, Terek River Basin	42.99331 N 44.49815 E	PP216457
<i>P. pallida</i>	TVA226	Male	Caucasus, Russia: Krasnodar Kray, District of the City of Sochi, Plastunka village, 3rd tributary Kutarka River, Sochi River Basin	43.67279 N 39.77213 E	PP216461
<i>P. pallida</i>	TVA227	Larva	Caucasus, Russia: Krasnodar Kray, District of the City of Sochi, Plastunka village, 3rd tributary Kutarka River, Sochi River Basin	43.67279 N 39.77213 E	PP216460

.....continued on the next page

TABLE 1. (Continued)

Species	Isolate	Sex	Country	Coordinates	Accession
<i>P. persica</i>	TVA199	Larva	Caucasus, Russia: Republic of North Ossetia-Alania, Prigorodny District, Mairamadag River, Terek River Basin	42.99331 N 44.49815 E	PP216464
<i>P. persica</i>	TVA201	Larva	Central Alborz, Iran: Mazandaran province, Zarrin Kamar village, Nurrud (Noor?) River, Haraz River Basin	36.20503 N 51.82055 E	PP216468
<i>P. persica</i>	TVA202	Male	Central Alborz, Iran: Mazandaran province, Zarrin Kamar village, Nurrud (Noor?) River, Haraz River Basin	36.20503 N 51.82055 E	PP216469
<i>P. persica</i>	TVA208	Female	Caucasus, Russia: Republic of North Ossetia-Alania, Alagirsky District, Komdon River near Verhny Tsey village, Terek River Basin	42.80351 N 43.93340 E	PP216463
<i>P. schapsugica</i> sp. nov.	TVA365	Larva	Caucasus, Russia: Krasnodar Kray, District of the City of Sochi, Stream (exit) of the Krasnoaleksandrovskaaya cave (Witches Cave), Ashe River Basin.	44.01536 N 39.36383 E	PP236724

ASAP delimited 14 putative species with the best ASAP score (1.00), which was achieved at a distance threshold of 2.1% (Fig. 160). The results of mPTP were incomplete in concordance with ASAP, whereas BOLD and GMYC turned out to be slightly more sensitive algorithms that delimit individuals into 16 mOTUs (Fig. 160). A comparison of the obtained mOTUs and genetic p-distances (Table 2) revealed that the most closely related species, *Perla* sp. (AAY7427), *P. madritensis* + *P. pallida* (AEB9929), and *P. pallida* (AEK2845), with sequence divergences of 1.1–2.1%, are displayed as distinct BINs, whereas they are merged in a single mOTU with ASAP and mPTP analyses. For the remaining sequences, there was agreement between the different approaches.

Discussion

The present study represents an updated comparison of the morphological and molecular identifications of the genus *Perla*. Several species of this genus could be unambiguously assigned to a single BIN. However, most species cannot be successfully delimited using COI barcodes alone. Two types of errors lead to this ambiguity: (1) when several morphospecies share a single mOTU, and (2) when specimens of one morphological species show deep divergence, leading to their assignment to two or more mOTUs. Both drawbacks often lead to the absence of monophyly and the lack of a barcoding gap and thus cause misidentifications.

The reasons for these drawbacks may be biological, such as potential cryptic species (Vitecek *et al.* 2017), incomplete lineage sorting (Van Velzen *et al.* 2012; Nabholz 2023), or mitochondrial introgression due to hybridization or recent speciation events (Petit & Excoffier 2009, Raupach *et al.* 2014), or artificial, such as incorrect species identification using a limited set of morphological characters, especially for larvae. A high-quality reference database is necessary for practical applications of DNA barcoding, such as metabarcoding (Corse *et al.* 2017, Gauthier *et al.* 2019) and biodiversity assessments (Zhou *et al.* 2009, 2010), in which molecular biologists rely on a database compiled by highly qualified taxonomists.

Only 3 of 16 *Perla* species can be unambiguously delimited using COI barcodes: *P. palatovi* **sp. nov.** (AFT4809), *P. schapsugica* **sp. nov.** (AFT4807), and *P. bipunctata* (AED4523), although the latter species is possibly shared by another BIN (AAL2357, Hlebec *et al.* 2022). To increase this number, it is necessary to perform several taxonomic refinements.

TABLE 2. Maximum intraspecific and minimum interspecific sequence divergence (%) based on p-distances for the cytochrome *c* oxidase subunit 1 (COI) mitochondrial DNA gene of 16 mOTUs of *Perla* according to BINs in BOLD systems.

Species	BIN	BOLD	N	Intra-specific	1	2	3	4	5	6	7	8	9	10	11	12	13	14	15	16
1. <i>P. palatovi</i> sp.nov.	AFT4809		4	0.46																
2. <i>P. schapsugica</i> sp.nov.	AFT4807		1	n/a	15.7															
3. <i>P. caucasica</i>	AEH6121		5	1.52	16.0	14.7														
4. <i>P. persica</i>	AEH6121		4	0.76	16.0	14.9	0.0													
5. <i>P. pallida</i>	AFT4806		5	0.46	13.4	15.4	14.6	14.6												
6. <i>P. marginata</i> , <i>P. pallida</i> , <i>P. sp.</i>	AAL2357		62	1.37	12.9	16.4	14.0	13.8	4.8											
7. <i>P. grandis</i> , <i>P. marginata</i>	AAL2358		33	1.24	17.0	18.8	18.0	18.0	16.2	16.7										
8. <i>P. carantana</i> , <i>P. abdominalis</i>	AAN1933		8	0.95	13.7	17.4	16.3	16.3	9.0	7.6	16.4									
9. <i>P. sp.</i>	AAY7427		10	0.91	12.6	15.4	13.5	13.5	4.0	3.6	16.9	7.0								
10. <i>P. pallida</i> , <i>P. madritensis</i>	AEB9929		11	1.40	12.2	15.7	13.8	13.4	2.8	2.9	16.3	7.2	1.1							
11. <i>P. bipunctata</i>	AED4523		3	1.06	17.1	18.8	18.8	18.8	18.3	17.5	5.8	18.2	18.7	17.5						
12. <i>P. grandis</i>	AEG1053		1	n/a	17.8	19.6	18.5	18.5	14.9	12.7	9.5	15.8	14.4	14.1	11.7					
13. <i>P. pallida</i>	AEG1356		1	n/a	13.3	16.2	14.4	14.4	8.1	7.5	18.0	9.7	6.9	6.9	18.8	16.5				
14. <i>P. grandis</i>	AEG8257		3	0.31	14.9	17.3	15.8	15.8	7.8	0.2	13.8	10.2	6.6	3.8	15.2	9.5	10.7			
15. <i>P. illiesi</i> , <i>P. abdominalis</i>	AEH4045		3	0.61	13.2	17.2	15.8	15.8	6.7	4.7	18.0	8.4	3.8	3.2	20.1	16.1	8.0	8.3		
16. <i>P. pallida</i>	AEK2845		1	n/a	13.1	15.8	14.9	14.7	4.7	4.0	16.9	8.4	2.1	1.2	18.3	14.6	7.8	6.6	4.9	
17. <i>P. grandis</i>	AFF2910		1	n/a	17.6	18.7	19.5	19.5	17.8	17.8	2.3	17.7	18.1	17.6	5.9	11.3	18.7	15.2	19.3	18.2

Perla pallida was originally described from the Caucasus without indicating the type locality and then redescribed from Azerbaijan, Georgia, and Turkey, wherein the holotype is now lost. We obtain sequences of *P. pallida* from the North Caucasus, the Republic of North Ossetia-Alania, and Krasnodar Krai of Russia, which are geographically much closer to descriptions than other sequences from central Europe. Considering the high variability of characteristics of the egg chorion of this species (Sivec & Stark 2002), it is not surprising that we revealed polyphyletic relationships between BINs containing *P. pallida* (Fig. 160, Hlebec *et al.* 2022) and high COI divergence values (Table 2). We propose to narrow the range of this species only to the Caucasus Mountains and consider species beyond its boundaries to be undescribed.

Determinations of *P. marginata* and *P. grandis* larvae and imago, according to several authors, place them at BINs AAL2357 and AAL2358, respectively (Corse *et al.* 2017; Moriniere *et al.* 2017; Gauthier *et al.* 2019; Ferreira *et al.* 2020; Behrens-Chapuis *et al.* 2021; Hlebec *et al.* 2022). Gamboa *et al.* (2023), in contrast, determined the larvae of these species opposite the prior six references, despite significant distances between them (Table 2) and morphological differences, including larvae (Zwick 2004). This misidentification most likely refers to a systematic error rather than cryptic species and confirms the difficulty of identifying stoneflies based only on larvae. Even more perplexing is the situation with *P. abdominalis*, which shares BINs with *P. carantana* and *P. illiesi* (AAN1933 and AEH4045). The species is indistinguishable from the sympatric *P. carantana* except in the characteristic egg stage (Sivec & Graf 2003; Zwick 2004). We believe that the larvae of *P. abdominalis* were misidentified and shared with AAN1933, whereas the imago of this species is currently conspecific with *P. illiesi* using DNA barcoding (AEH4045).

Several pairs of *Perla* species possessed identical or close COI sequences and could not be distinguished by species delimitation methods. Pairs include *P. persica* and *P. caucasica* (AEH6121), *P. illiesi* and *P. abdominalis* (AEH4045), and *P. madritensis* and *P. aff. pallida* (AEB9929). Lack of divergence between the two Caucasian species, *P. persica* and *P. caucasica*, may be the result of recent speciation events and/or mitochondrion introgressions in areas of secondary contact during hybridization. Such an area could be the central Caucasus, while the actual range of both species may be poorly studied or narrowed as a result of local scale extirpations. Although morphological characteristics are usually associated with the characteristics of the egg stage (Sivec & Stark 2002), the structure of the penis and other diagnostic features allow for accurately identifying species. Such results may be due to introgression or hybridization, or perhaps only to recent speciation events.

Acknowledgments

The authors are very grateful to Dávid Murányi (Department of Zoology, Eszterházy Károly Catholic University, Eger, Hungary) and Maribet Gamboa (Department of Ecology, Faculty of Sciences, Universidad Católica de la Santísima Concepción, Concepción, Chile) for useful information about *Perla* species collected in Azerbaijan and the Balkan Mountains. The authors thank Dávid Murányi for constructive suggestions and Scott Grubbs (Department of Biology and Center for Biological Studies, Western Kentucky University, Bowling Green, USA) for editorial recommendations and linguistic revision that improved the manuscript. The research was carried out within the state assignment of the Ministry of Science and Higher Education of the Russian Federation (theme No. 124012400285-7).

References

- Behrens-Chapuis, S., Herder, F. & Geiger, M.F. (2021) Adding DNA barcoding to stream monitoring protocols – What's the additional value and congruence between morphological and molecular identification approaches? *PLoS ONE*, 16 (1), e0244598.
<https://doi.org/10.1371/journal.pone.0244598>
- Burmeister, H.C.C. (1839) Plecoptera. *Handbuch der Entomologie*, Berlin, 2 (2), 863–881.
- Cherchesova, S.K. & Zhiltzova, L.A. (2013) *Opredelitel vesnyanok (Plecoptera) Kavkaza*. RGAU-MI K.A. T, Moskva-Vladikavkaz, 113 pp. [in Russian]
- Cherchesova, S.K., Shapovalov, M.I., Mamaev, V.I. & Palatov, D.M. (2023) Ecology and phenology of stoneflies (Plecoptera) in the northern slopes of the Central Caucasus in winter and spring seasons. *Zoosymposia*, 24 (1), 82–93.
<https://doi.org/10.11646/zoosymposia.24.1.9>

- Corse, E., Megléc, E., Archambaud, G., Ardisson, M., Martin, J.F., Tougard, C., Chappaz, R. & Dubut, V. (2017) A from-benchtop-to-desktop workflow for validating HTS data and for taxonomic identification in diet metabarcoding studies. *Molecular ecology resources*, 17 (6), e146–e159.
<https://doi.org/10.1111/1755-0998.12703>
- Darilmaz, M.C., Salur, A., Murányi, D. & Vinçon, G. (2016) Contribution to the knowledge of Turkish stoneflies with annotated catalogue (Insecta: Plecoptera). *Zootaxa*, 4074 (1), 1–74.
<https://doi.org/10.11646/zootaxa.4074.1.1>
- DeWalt, R.E., Hopkins, H., Neu-Becker, U. & Stueber, G. (2023) Plecoptera Species File. Available from: <http://plecoptera.speciesfile.org> (accessed 5 March 2024)
- Felsenstein, J. (1981) Evolutionary trees from DNA sequences: a maximum likelihood approach. *Journal of Molecular Evolution*, 17, 368–376.
<https://doi.org/10.1007/BF01734359>
- Ferreira, S., Tierno de Figueroa, J.M., Martins, F.M.S., Verissimo, J., Quaglietta, L., Grosso-Silva, J.M., Lopes, P.B., Sousa, P., Pauperio, J., Fonseca, N.A. & Beja, P. (2020) The InBIO barcoding initiative database: contribution to the knowledge on DNA barcodes of Iberian Plecoptera. *Biodiversity Data Journal*, 8, e55137.
<https://doi.org/10.3897/BDJ.8.e55137>
- Fujisawa, T. & Barraclough, T.G. (2013) Delimiting species using single-locus data and the Generalized Mixed Yule Coalescent approach: A revised method and evaluation on simulated data sets. *Systematic Biology*, 62 (5), 707–724.
<https://doi.org/10.1093/sysbio/syt033>
- Gamboa, M., Serrana, J., Takemon, Y., Monaghan, M.T. & Watanabe, K. (2023) Spatial and phylogenetic structure of Alpine stonefly assemblages across seven habitats using DNA-species. *Oecologia*, 201 (2), 513–524.
<https://doi.org/10.1007/s00442-023-05321-0>
- Gauthier, M., Konecny-Dupré, L., Nguyen, A., Elbrecht, V., Datry, T., Douady, C. & Lefébure, T. (2019) Enhancing DNA metabarcoding performance and applicability with bait capture enrichment and DNA from conservative ethanol. *Molecular Ecology Resources*, 20 (1), 79–96. [Epub 2019 Sep 18. PMID: 31484209]
<https://doi.org/10.1111/1755-0998.13088>
- Guérin-Méneville, F.E. (1843) Genre *Perle*. In: Guérin-Méneville, F.E. (Ed.), *Iconographie du Règne Animal de G. Cuvier. Insectes*, 1843, pp. 393–395.
- Hebert, P.D.N., Cywinska, A., Ball, S.L. & DeWaard, J.R. (2003a) Biological identifications through DNA barcodes. Proceedings of the Royal Society B: *Biological Sciences*, 270, 313–321.
<https://doi.org/10.1098/rspb.2002.2218>
- Hebert, P.D.N., Ratnasingham, S. & DeWaard, J.R. (2003b) Barcoding animal life: cytochrome c oxidase subunit 1 divergences among closely related species. Proceedings of the Royal Society B: *Biological Sciences*, 270, 596–599.
<https://doi.org/10.1098/rsbl.2003.0025>
- Hlebec, D., Sivec, I., Podnar, M. & Kučinić, M. (2022) DNA barcoding for biodiversity assessment: Croatian stoneflies (Insecta: Plecoptera). *PeerJ*, 10, e13213.
<https://doi.org/10.7717/peerj.13213>
- Kapli, P., Lutteropp, S., Zhang, J., Kobert, K., Pavlidis, P., Stamatakis, A. & Flouri, T. (2017) Multi-rate Poisson tree processes for singlelocus species delimitation under maximum likelihood and Markov chain Monte Carlo. *Bioinformatic*, 33 (11), 1630–1638.
<https://doi.org/10.1093/bioinformatics/btx025>
- Kasymov, A.G. (1972) *Presnovodnaya fauna Kavkaza*. Elm, Baku, 288 pp.
- Kazanci, N. (1983) Researches on the Plecoptera (Insecta) species of Turkey. *Hacettepe Bulletin of Natural and Engineering*, 12, 85–99.
- Kazanci, N. (2008) *Türkiye Plecoptera (Insecta) Faunasi. Türkiye İç Suları Araştırmaları Dizisi IX*. İmaj Yayınevi, Ankara, 56 pp.
- Kis, B. (1974) Plecoptera. Fauna Republicii Socialiste Romania. *Insecta*, 8 (Fas. 7), 1–271.
- Klapálek, F. (1907a) Japonské druhy podčeledi Perlinae. *Rozpravy České Akademie císaře Františka Jozefa*, 16 (31), 1–28.
- Klapálek, F. (1907b) Die europäischen Arten der Gattung *Perla* Geoffr. *Bulletin international de l'Académie des Sciences de Bohême, Science, Mathematics, Nature*, 12, 117–138.
- Klapálek, F. (1921) Plécoptères nouveaux. *Annales de la Société Entomologique de Belgique*, 61, 57–67 + 146–150 + 320–327.
[<http://www.biodiversitylibrary.org/page/12281956>]
- Klapálek, F. (1923) Plécoptères II. Fam. Perlidae. Collections Zoologiques du Baron Edm. de Selys Longchamps. *Catalogue Systématique et descriptif*, 4, 1–193.
- Kumar, S., Stecher, G. & Tamura, K. (2016) MEGA7: Molecular evolutionary genetics analysis. Version 7.0 for bigger datasets. *Molecular Biology and Evolution*, 33 (7), 1870–1874.
<https://doi.org/10.1093/molbev/msw054>
- Lanfear, R., Calcott, B., Ho, S.Y. & Guindon, S. (2012) Partitionfinder: Combined selection of partitioning schemes and substitution models for phylogenetic analyses. *Molecular Biology and Evolution*, 29 (6), 1695–1701.
<https://doi.org/10.1093/molbev/mss020>

- Morinière, J., Hendrich, L., Balke, M., Beermann, A.J., König, T., Hess, M., Koch, S., Müller, R., Leese, F., Hebert, P.D.N., Hausmann, A., Schubart, C.D. & Haszprunar, G. (2017) A DNA barcode library for Germany's mayflies, stoneflies and caddisflies (Ephemeroptera, Plecoptera, and Trichoptera). *Molecular Ecology Resources*, 17 (6), 1293–1307. <https://doi.org/10.1111/1755-0998.12683>
- Murányi, D., Gamboa, M. & Vera, A. (2016) Lost and found: the Plecoptera types of Blanchard and Mabilbe, with further contributions to the stoneflies of Chile. *Zootaxa*, 4200 (4), 544–560. <https://doi.org/10.11646/zootaxa.4200.4.6>
- Murányi, D., Manko, P., Kovács, T., Vinçon, G., Žiak, M., Kerimova, I.G., Snegovaya, N.Y. & Oboňa, J. (2021) Review and contribution to the stonefly (Insecta: Plecoptera) fauna of Azerbaijan. *Zootaxa*, 4975 (1), 58–80. <https://doi.org/10.11646/zootaxa.4975.1.2>
- Nabholz, B. (2023) Incomplete lineage sorting explains the low performance of DNA barcoding in a radiation of four species of Western European grasshoppers (Orthoptera: Acrididae: *Chorthippus*). *Biological Journal of the Linnean Society*, 141 (1), 33–50. <https://doi.org/10.1093/biolinnean/blad106>
- Panzer, G.W.F. (1799) *Fauna Insectorum Germanicae initia*. Felssecker, Nürnberg, 71 pp.
- Petit, R.J. & Excoffier, L. (2009) Gene flow and species delimitation. *Trends in Ecology & Evolution*, 24 (7), 386–393. <https://doi.org/10.1016/j.tree.2009.02.011>
- Pictet, F.J. (1841) *Histoire naturelle des insectes Névroptères. Famille des Perlides*. Kessmann-Baillière, Genève-Paris, 423 pp
- Puillandre, N., Brouillet, S. & Achaz, G. (2021) ASAP: assemble species by automatic partitioning. *Molecular Ecology Resources*, 21 (2), 609–620. <https://doi.org/10.1111/1755-0998.13281>
- Ra, C.H., Kim, J.S., Kang, Y.W. & Ham, S.A. (1994) Taxonomic study on three families (Peltoperlidae, Perlodidae, Perlidae) of stoneflies (Plecoptera) in Korea. *The Korean Journal of Systematic Zoology*, 10 (1), 1–15.
- Rambaut, A., Drummond, A.J., Xie, D., Baele, G. & Suchard, M.A. (2018) Posterior summarization in Bayesian phylogenetics using Tracer 1.7. *Systematic Biology*, 67 (5), 901–904. <https://doi.org/10.1093/sysbio/syy032>
- Rambur, J.P. (1842) Tribu des Perlides. In: *Histoire naturelle des insectes. Névroptères*. Roret, Paris, pp. 449–462.
- Ratnasingham, S. & Hebert, P.D.N. (2013) A DNA-Based Registry for All Animal Species: The Barcode Index Number (BIN) System. *PLoS ONE*, 8 (7), e66213. <https://doi.org/10.1371/journal.pone.0066213>
- Raupach, M.J., Hendrich, L., Kuchler, S.M., Deister, F., Morinière, J. & Gossner, M.M. (2014) Building-up of a DNA barcode library for true bugs (Insecta: Hemiptera: Heteroptera) of Germany reveals taxonomic uncertainties and surprises. *PLoS ONE*, 9 (9), e106940. <https://doi.org/10.1371/journal.pone.0106940>
- Reding, J.-P.G. (2023) Steps towards a revision of the *Perla bipunctata* Pictet, 1833 species complex (Plecoptera: Perlidae). *Fragmenta entomologica*, 55 (2), 221–262. <https://doi.org/10.13133/2284-4880/1526>
- Ronquist, F.M., Teslenko, M., van der Mark, P., Ayres, D.L., Darling, A., Höhna, S., Larget, B., Liu, L., Suchard, M.A. & Huelsenbeck, J.P. (2012) MRBAYES 3.2: Efficient Bayesian phylogenetic inference and model selection across a large model space. *Systematic Biology*, 61 (3), 539–542. <https://doi.org/10.1093/sysbio/sys029>
- Sivec, I. & Graf, W. (2003) *Perla carantana* - a new species of the genus *Perla* (Plecoptera: Perlidae) from Austria and Slovenia. *Natura Sloveniae*, 4 (1), 31–38. <https://doi.org/10.14720/ns.4.2.31-38>
- Sivec, I. & Stark, B.P. (2002) The species of *Perla* (Plecoptera: Perlidae): evidence from egg morphology. *Scopolia*, 49, 1–33.
- Sivec, I., Stark, B.P. & Uchida, S. (1988) Synopsis of the World Genera of Perlinae (Plecoptera: Perlidae). *Scopolia*, 16, 1–66.
- Stewart, K.W. & Stark, B.P. (2002) *Nymphs of North American Stonefly Genera (Plecoptera)*. 2nd Edition. The Caddis Press, Columbus, Ohio, 510 pp.
- Suchard, M.A., Lemey, P., Baele, G., Ayres, D.L., Drummond, A.J. & Rambaut, A. (2018) Bayesian phylogenetic and phylodynamic data integration using BEAST 1.10. *Virus Evolution*, 4 (1), vey016. [published online] <https://doi.org/10.1093/ve/vey016>
- Tavaré, S. (1986) Some probabilistic and statistical problems in the analysis of DNA sequences. Lectures on Mathematics in the Life Sciences. *American Mathematical Society*, 17, 57–86.
- Teslenko, V.A. & Zhiltzova, L.A. (2009) *Key to the stoneflies (Insecta, Plecoptera) of Russia and adjacent countries. Imagines and nymphs*. Dalnauka, Vladivostok, 382 pp. [in Russian]
- Teslenko, V.A. & Semenchenko, A.A. (2022) Morphological description of a new species of *Capnia* (Plecoptera: Capniidae) with DNA barcoding of genus members from the Russian Far East. *Zootaxa*, 5155 (1), 133–141. <https://doi.org/10.11646/zootaxa.5155.1.7>
- Van Velzen, R., Weitschek, E., Felici, G. & Bakker, F.T. (2012) DNA Barcoding of Recently Diverged Species: Relative Performance of Matching Methods. *PLoS ONE*, 7 (1), e30490.

<https://doi.org/10.1371/journal.pone.0030490>

- Vitecek, S., Vinçon, G., Graf, W. & Paul, S.U. (2017) High cryptic diversity in aquatic insects: an integrative approach to study the enigmatic *Leuctra inermis* species-group (Plecoptera). *Arthropod Systematics & Phylogeny*, 75 (3), 497–521.
<https://doi.org/10.3897/asp.75.e31919>
- Zharkikh, A.J. (1994) Estimation of evolutionary distances between nucleotide sequences. *Molecular Evolution*, 39 (3), 315–329.
<https://doi.org/10.1007/BF00160155>
- Zhiltzova, L.A. (1956) Contribution ‘al’etude des Plecopteres du Caucase. 1. Nouvelles especes de la Fauna des Plecopteres (Taeniopterygidae et Chloroperlidae) des montagnes Trialetzky. *Revue d’entomologie del’ URSS*, 35 (3), 659–670.
- Zhiltzova, L.A. (1961) On the study of the fauna of Plecoptera of the Caucasus V. Plecoptera of Armenia. *Entomologicheskoe obozrenie*, 40 (4), 872–880. [in Russian]
- Zhiltzova, L. A. (1964) Die Plecopteren des europäischen Teils der Sowjetunion und des Kaukasus. *Gewässer und Abwässer*, 34/35, 101–114.
- Zhiltzova, L.A. & Cheresova, S.K. (2003) Description of the larva of genus *Perla* Geoff. (Plecoptera, Perlidae) from the Caucasus. *Entomologicheskoe obozrenie*, 82 (2), 321–326. [in Russian]
- Zhou, X., Adamowicz, S.J., Jacobus, L.M., DeWalt, R.E. & Hebert, P.D.N. (2009) Towards a comprehensive barcode library for arctic life - Ephemeroptera, Plecoptera, and Trichoptera of Churchill, Manitoba, Canada. *Frontiers in Zoology*, 6 (30). [published online]
<https://doi.org/10.1186/1742-9994-6-30>
- Zhou, X., Jacobus, L.M., DeWalt R.E., Adamowicz, S.J. & Hebert, P.D.N. (2010) Ephemeroptera, Plecoptera, and Trichoptera fauna of Churchill (Manitoba, Canada): insights into biodiversity patterns from DNA barcoding. *Journal of the North American Benthological Society*, 29 (3), 814–837.
<https://doi.org/10.1899/09-121.1>
- Zwick, P. (1975) Weitere Plecoptera aus Anatolien. *Mitteilungen der Schweizerischen Entomologischen Gesellschaft*, 48 (3–4), 387–396.
- Zwick, P. (1977) Ergebnisse der Bhutan-Expedition 1972 des Naturhistorischen Museums in Basel. *Entomologica Basiliensia*, 2, 85–134.
- Zwick, P. (1978) Steinfliegen (Plecoptera) aus Griechenland und benachbarten Ländern. *Mitteilungen der Schweizerischen Entomologischen Gesellschaft*, 51, 21–38.
<https://doi.org/10.5169/seals-401866>
- Zwick, P. (2004) Key to the West Palearctic genera of stoneflies (Plecoptera) in the larval stage. *Limnologica*, 34, 315–348.
[https://doi.org/10.1016/S0075-9511\(04\)80004-5](https://doi.org/10.1016/S0075-9511(04)80004-5)